Synthesis and Supramolecular Investigation of Cyclic Naphthalenes and Cyclic Pyrenes

A dissertation

submitted to

Graduate School of Science and Technology,

Nara Institute of Science and Technology

in partial fulfillment of the requirements

for the degree of Doctor of Philosophy

in the subject of Science

Peifeng Mei

September 2021

Contents

Abbreviations

ADF: Amsterdam Density Functional

Bpin: Pinacolato boron

CNB: Carbon nanobelt

CNH: Carbon nanohorn

CNT: Carbon nanotube

CV: Cyclic voltammetry

DCM: Dichloromethane

DFT: Density functional theory

DDQ: 2,3-Dichloro-5,6-dicyano-1,4-benzoquinone

DMF: Dimethylformamide

DPV: Differential pulse voltammetry

Fc/Fc$^+$: Ferrocene/ferrocenium

FET: Field effect transistor

GNR: Graphene nanoribbon

GPC: Gel permeation chromatography

HR: High resolution

HOMO: Highest occupied molecular orbital

HPLC: High performance liquid chromatography

LUMO: Lowest unoccupied molecular orbital

μ_h: Hole mobility

μ_e: Electron mobility

MALDI-TOF-MS: Matrix-assisted-laser-desorption/ionization time-of-flight mass spectrometry

MWCNT: Multi-walled carbon nanotube

NBS: *N*-Bromosuccinimide

NMR: Nuclear magnetic resonance

MO: Molecular orbital

PAH: Polycyclic aromatic hydrocarbon

PEG: Polyethylene glycol

SWCNT: Single-walled carbon nanotubes

$TBAPF_6$: Tetrabutylammonium hexafluorophosphate

TEM: Transmission electron microscopy

THF: Tetrahydrofuran

TIPS: Triisopropylsilyl

TLC: Thin-layer chromatography

TMS: Trimethylsilyl

TRMC: Time resolved microwave conductivity

UV–vis: Ultraviolet–visible

XRD: X-ray diffraction

Chapter 1. General Introduction

1.1 Nanocarbon materials

Nanocarbon materials have piqued interest since the discovery of fullerene C_{60} in 1985 due to its versatile features such as electrical conductivity, absorption, luminescence, and magnetism.[1] For example, according to research published in 2009, conductive carbon nanotube (CNT) thin films produced as a replacement for more brittle indium tin oxide materials have been explored in the visible wavelength range for use in solar cells, solid-state lighting, and displays (**Figure 1a**).[2] On September 29, 2013, a huge plastic balloon (**Figure 1b**) soared high in the skies over New Mexico, carrying devices to collect climate-related test data using CNT chips from the National Institute of Standards and Technology (NIST).[3] In 2017, Jana Zaumseil used a single-walled carbon nanotubes (SWCNT)-based ambipolar light emission field effect transistor (LE-FET) embedded in an optical microcavity to demonstrate electrically pumped near-infrared exciton polariton emission at room temperature.[4] A solar cell based on fullerenes C_{60} was also developed in 2017. It was discovered to be 14% more efficient than conventional materials and architecture (**Figure 1d**).[5] At the same time, it can function as a solar cell and a current inverter. Such a wide range of application prospects has prompted continuous studies on these materials. Continuous research on these materials is necessitated by their wide range of application possibilities. Applications in the field of optoelectronics tend to rely on organic chemistry research, particularly in the fabrication of materials.

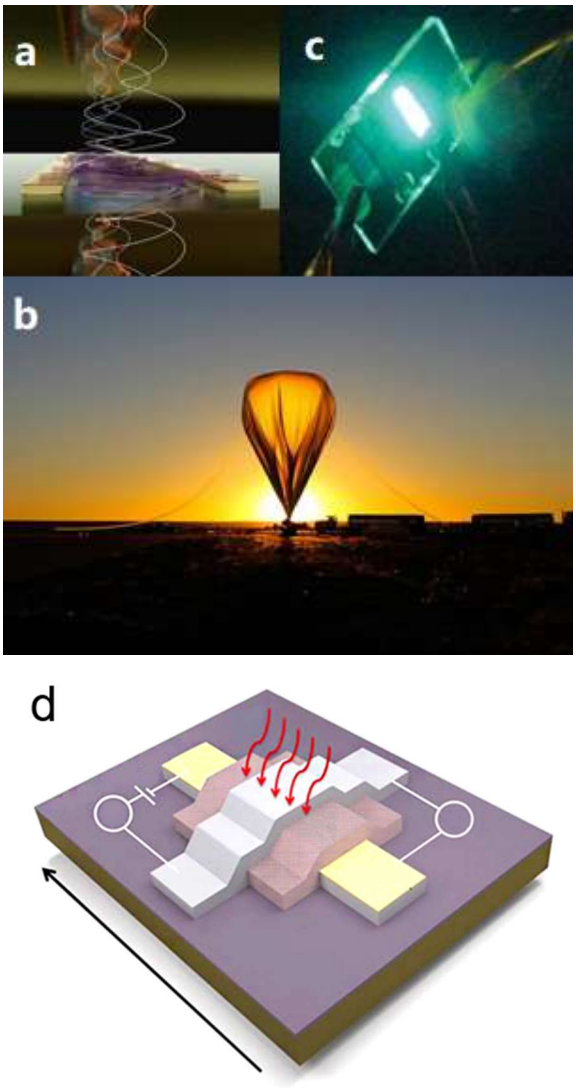

Figure 1. Application of nano-carbon materials[2]-[5]

Fullerenes, graphene, and carbon nanotubes (CNTs) are the most common nano-carbons. As one of the allotropes of carbon, fullerene was discovered by Richard Smalley, Robert Curl, and Harry Kroto through experiments in 1985 (**Figure 2**[6]). It was named Buckminster fullerene after the name of an American architect, Buckminster Fuller. Fullerenes are made up of various numbers of polygons, and their names are determined by the number of carbon atoms in their structure. The empirical formula $\mathbf{C}_{\boldsymbol{n}}$, typically written $\mathbf{C}\boldsymbol{n}$, is used to define fullerenes with a closed mesh topology. $\boldsymbol{n}$ is the number of carbon atoms. However, for some values of $\boldsymbol{n}$, there may be more than one isomer.

Fullerene has high temperature stability, conductivity and can be used in nanocomposites. Graphite laser ablation and arc discharge technology are commonly used to create them. Fullerenes have a huge nonlinear optical response, strong electron affinity, and high charge transfer ability due to the delocalized electrons. Inserting atoms into fullerene molecules can also form embedded fullerene molecules. Accelerated ions or molecules are frequently inserted in fullerene cages. Intensive study has been conducted on their chemical and technical uses, particularly in materials science, electronics, and nanotechnology.

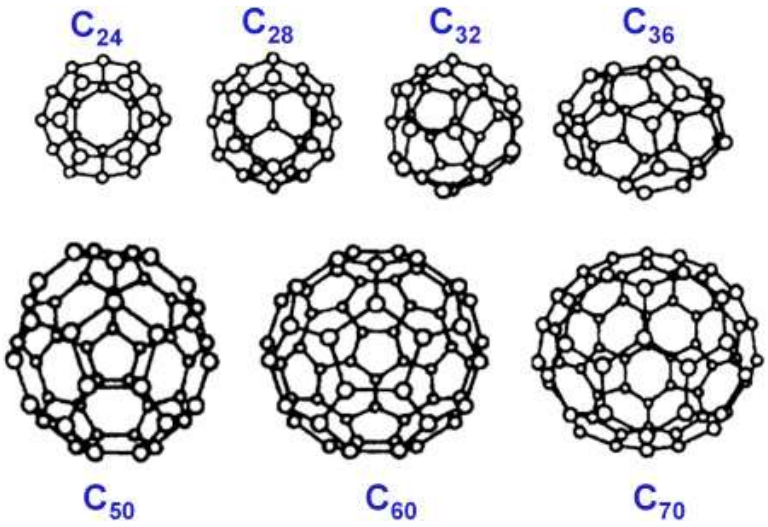

Figure 2. Fullerenes[6]

Graphene is another carbon allotrope. Graphene is made up of a single layer of atoms organized in a honeycomb lattice in two dimensions (**Figure 3**). It can be stacked to make three-dimensional graphite, rolled to make one-dimensional nanotubes, and wrapped to make zero-dimensional fullerenes. Each atom in a graphene sheet has a link with the three atoms closest to it and contributes an electron to the conduction band that runs the length of the sheet. Scientists have been studying the possibility of graphene's existence and manufacture for decades. Andre Geim and Konstantin Novoselov rediscovered, isolated, and described this substance in 2004.[7] The exceptional thermal,

mechanical, and electrical capabilities of graphene are due to its long-range conjugation. The charge carriers in graphene have a linear rather than quadratic energy dependency on momentum, and the material can be used to construct bipolar field-effect transistors. The material shows huge quantum oscillations and large nonlinear diamagnetism, and charge transport is long-distance ballistic transport. Along its plane, graphene conducts heat and electricity very well. Many theoretical studies have focused on these features, and materials science has recently become a hot research subject.

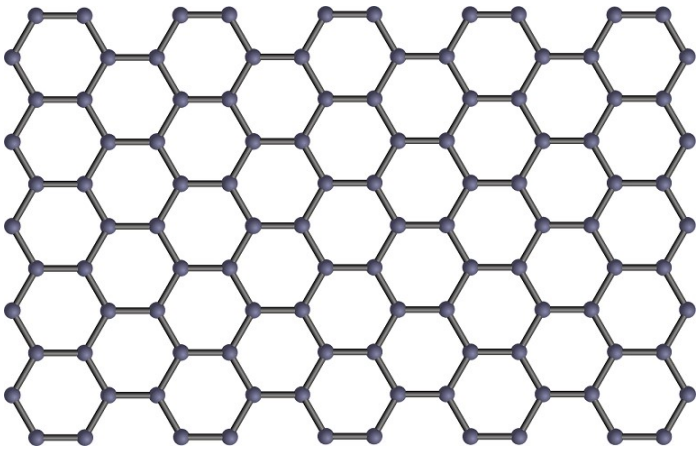

Figure 3. Graphene

The field of CNTs was established by Iijima's early experimental observation of CNTs using a transmission electron microscope (TEM)[8] in 1991 and subsequent studies on a large range of nanotube syntheses conditions. CNTs are carbon tubes with a diameter of roughly 100 nanometers and a length of micrometers.[9] CNTs are generally divided into two types based on the number of layers (**Figure 4**). SWCNTs are made up of a single graphene layer with a diameter of 0.4 to 2 nm range. MWCNTs (multi-walled carbon nanotubes) are made up of two or more cylinders, each of which is made up of graphene sheets. The diameter ranges between 1 and 3 nm. Arc discharge, laser ablation, and chemical vapor deposition are three methods for making CNTs. CNTs have outstanding chemical and physical qualities, including high tensile strength, ultralightweight, a unique

electronic structure, and chemical and thermal stability. Scientists have acquired a strong interest in these nanomaterials as a result of their unique properties. CNTs are the most widely used carbon nanomaterial in a variety of applications. CNTs are used in biomolecules, medicines, and drug delivery to target organs, as well as biosensor diagnosis and analysis.[10]

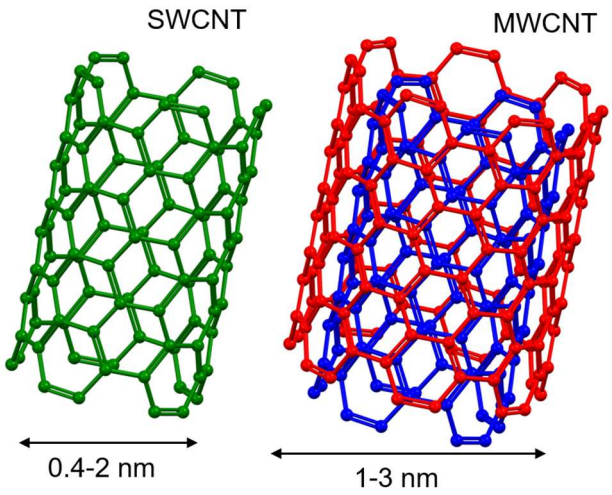

Figure 4. Carbon nanotubes **(**CNTs)

Except for fullerenes, most currently existing nanocarbons such as CNTs and graphene nanoribbon (GNRs) are not regarded as structurally pure molecules. Traditional top-down methods produce a mixture of structures with varying physical properties. They cannot be separated or refined into pure structural forms. Bottom-up organic synthesis is seen as a promising strategy for achieving accurate nanocarbon. A class of molecules that can be utilized as templates for the above forms of synthesis has also been proposed in some previous investigations. As fragments of the three major types of nanocarbons, these small PAH molecules have also been studied in many ways. Representatives are corannulene and sumanene as fragments of the fullerene, acenes as the segments of the GNR and carbon nanorings like cycloparaphenylenes (CPPs), carbon nanobelts (CNBs) as the CNT segments.

For GNRs, in 2010 Klaus Müllen, Roman Fasel and co-workers reported a simple method for the production of atomically precise GNRs of different topologies and widths, which uses surface-assisted coupling of molecular precursors into linear polyphenylenes and their subsequent cyclodehydrogenation.[11] The structure of the precursor monomers, which can be designed to offer access to a wide range of various GNRs, determines the topology, width, and edge periphery of the GNR products (**Figure 5**). This bottom-up method to atomically precise GNR manufacturing should allow for extensive experimental research of the characteristics of this fascinating class of materials. It should also pave the way for GNR structures with tailored chemical and electronic properties, such as intraribbon quantum dots, superlattice structures, and magnetic devices based on specific GNR edge states, as well as the theoretically predicted intraribbon quantum dots, superlattice structures, and magnetic devices based on specific GNR edge states.

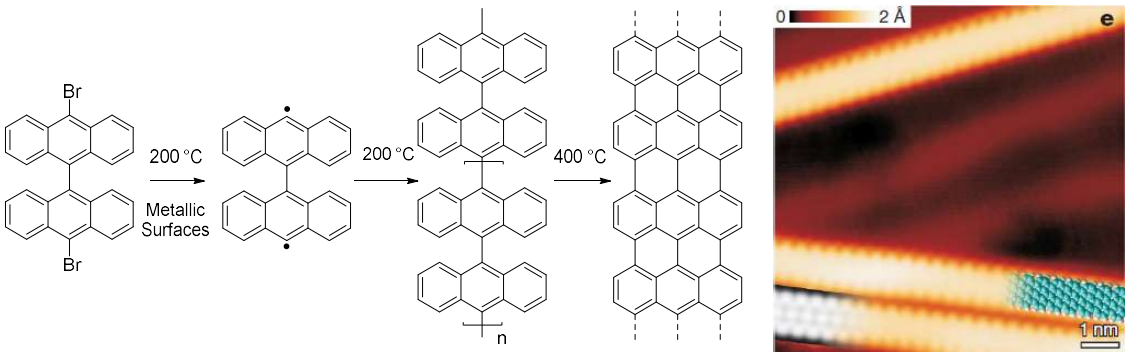

Figure 5. Bottom-up synthesis of GNR[11]

For CNTs, the bottom-up organic synthesis approach was put forward by Jasti in 2010.[12] Small fragments of CNTs that preserve information about chirality and diameter are used as templates for CNT synthesis in this method (**Figure 6**). The growth of armchair CNTs from CPPs was achieved by Itami and coworkers in 2013.[13]

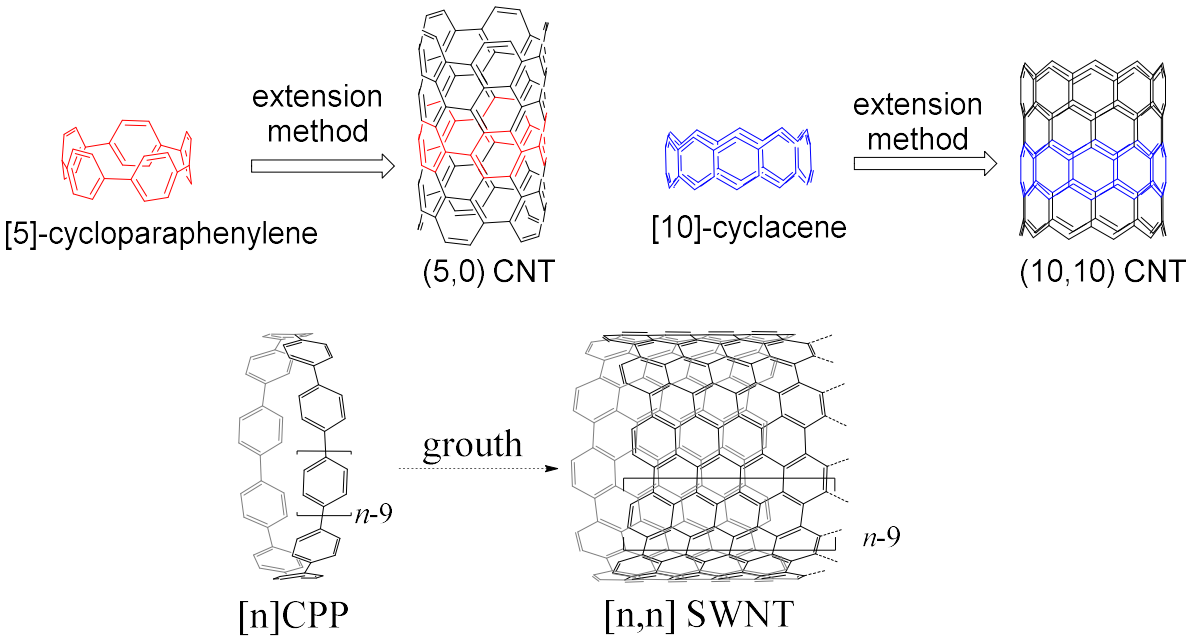

Figure 6. Bottom-up approach towards CNTs[12][13]

In these cases, the template molecules will retain, most of the key information of the target molecule. Therefore, it is critical for the synthesis of small molecules that can be used as templates. Among these template molecules, carbon nanoring compounds and nanobelt compounds are difficult to synthesize, due to the strain of the ring. To prepare these molecules in an easy way, becomes a challenging task for organic chemistry researchers. Therefore, my research focused on these molecules. Moreover, carbon nanorings and CNBs have also received attention because of their special nature and beautiful structure. But due to the synthetic difficulties, the examples are still limited.

1.2 Carbon nanorings and carbon nanobelts (CNBs)

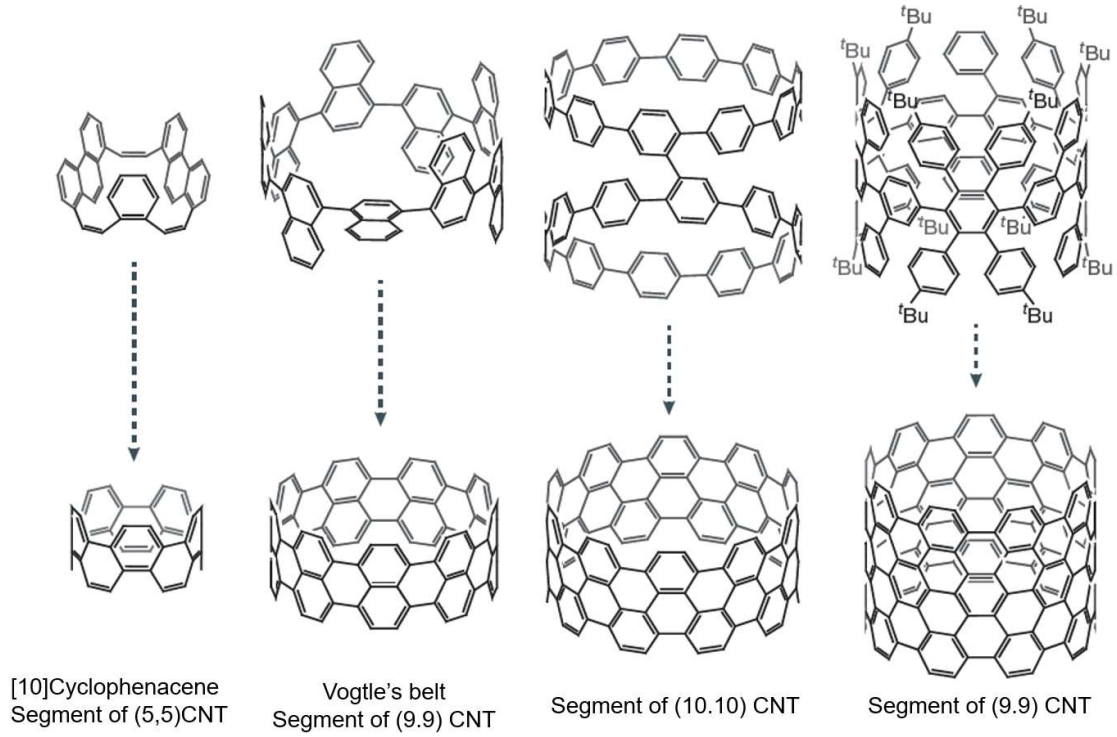

Figure 7. Proposed routes of CNBs[14]

CNBs was listed separately because it is somewhat different from general carbon nanorings. Conjugated nanobelts are belt-shaped fully conjugated molecules with two distinguishing characteristics. One is "the presence of conjugated upper and lower edges that never coincide, that is, they share no atoms in common". The other is radially arranged p-orbitals, which exhibit an in-plane alignment. Easily speaking, the PAH units in carbon nanobelt's main structure are unable to rotate. This is an obvious difference with carbon nanoring. The best-known subgroup of conjugated nanobelts are CNBs that consist of a loop of fully fused benzene rings and represent sidewall segments of SWCNTs. As a result, CNBs can be classified into armchair, zigzag, and chiral nanobelts (**Figure 8**) according to the chiral index, (n, m), of the corresponding SWCNT, which determines the diameter and chirality of an SWCNT.

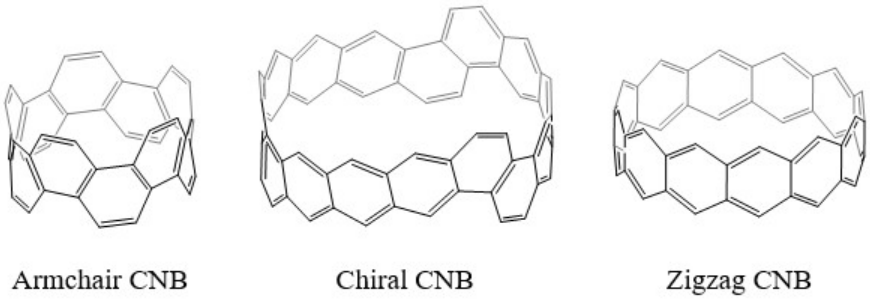

Figure 8. Typical types of CNB

The CNB molecules have been proposed for many years, and the theoretical research precedes the synthesis. Vögtle in 1991 designed armchair nanobelt **CNB1** (**Scheme 1**) which is now known as the Vögtle belt, and synthesized a potential synthetic precursor of **CNB1**, double-stranded cyclophane **1**.[15]

In 2015, the result that is closest to a target CNB is the observation of cyclo[10]phenacene **CNB2** by the mass spectroscopy when all-Z macrocycle **2** was subjected to laser desorption time-of-flight (LD-TOF) conditions as illustrated in **Scheme 1**.[16]

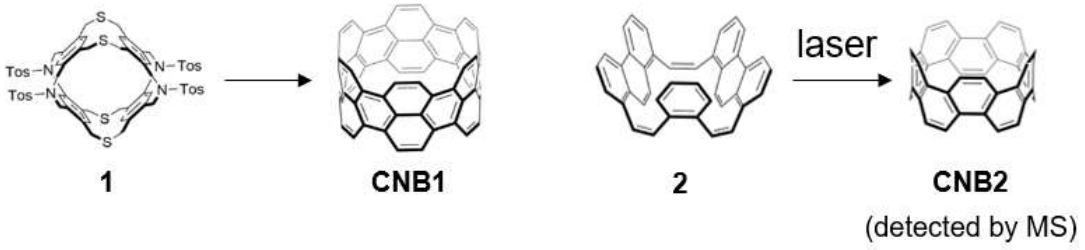

Scheme 1. Vögtle belt and synthesis of CNB **2**[15][16]

Finally, in 2017, Itami and coworkers reported the successful synthesis of the first armchair CNB (**CNB3**), which was inspired by Iyoda's comprehensive research of the all- Z-benzannulenes[16] and the synthesis of strained π-systems reported by Stępien and coworkers.[17] As shown in **Scheme 2**, macrocycle **6** was synthesized from benzylic

bromide **3** and aldehyde **4** through iterative Wittig reactions, which enabled cyclodimerization of **5**. The nickel-mediated aryl-aryl coupling reaction afforded armchair **CNB3** in a yield as low as 1%, which was later improved to 5%.[18]

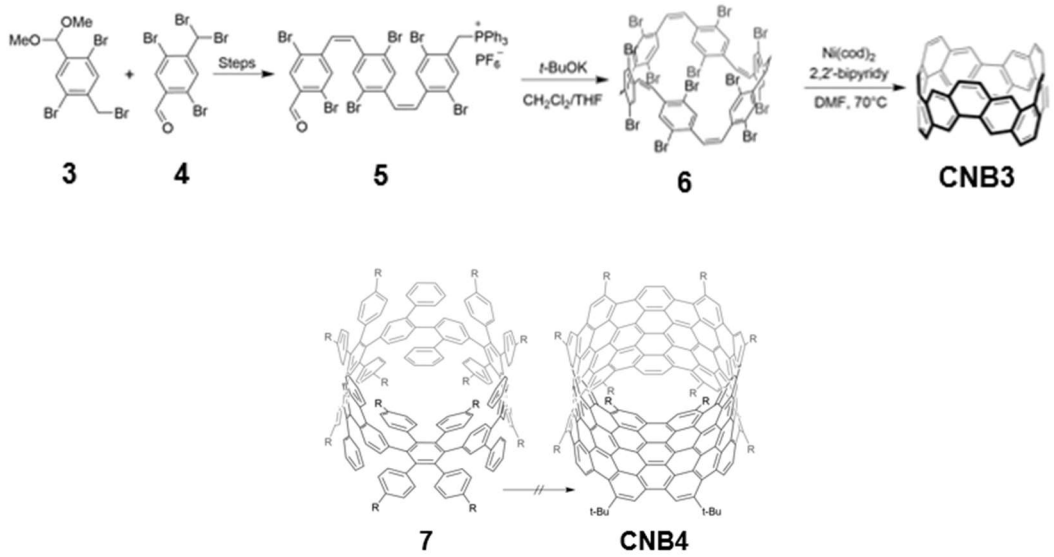

Scheme 2. Synthesis of CNB **3** and **4**[18][20]

The group of Jasti first proposed to synthesize armchair CNBs from phenylated CPPs through the Scholl reaction in 2012,[19] and the group of Müllen reported the first attempts to use this strategy for the synthesis of armchair CNBs.[20] **Scheme 2** shows one example of Müllen's attempts. The cyclodehydrogenation of phenylated CPP **7** under oxidative conditions did not result in **CNB4** but gave mixtures of dehydrogenated products, which indicates the partial formation of cyclic graphenoid structures. They concluded that the failure of complete cyclodehydrogenation for the synthesis of CNBs was caused by an unwanted 1,2-phenyl shift process under Scholl reaction conditions driven by relief of the macrocycle strain, which agreed with Jasti and coworkers' findings.[21]

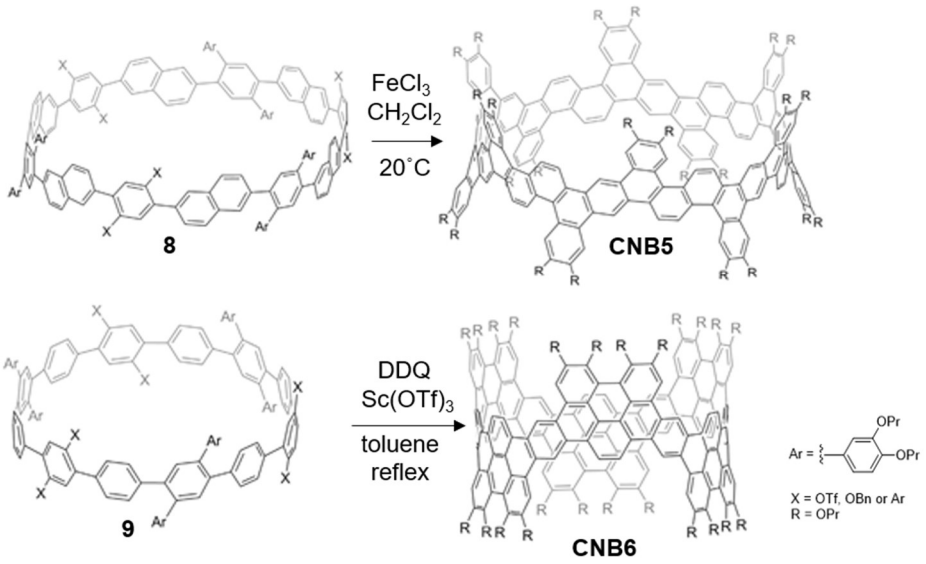

Scheme 3. Synthesis of **CNB5** and **CNB6**[22]

In 2018, Miao's group reported the synthesis of sidewall segments of an armchair (12,12) CNT and a chiral (18,12) CNT through Suzuki coupling, reductive aromatization, followed by Scholl reaction (**Scheme 3**).[22] In 2020, Itami's group attempted to make a CNB with 5-membered ring.[23] In 2021, Itami and Chi reported the synthesis, isolation and structural characterization of the first two zigzag CNBs (**CNB7** and **CNB8, Scheme 4**) respectively.[24][25]

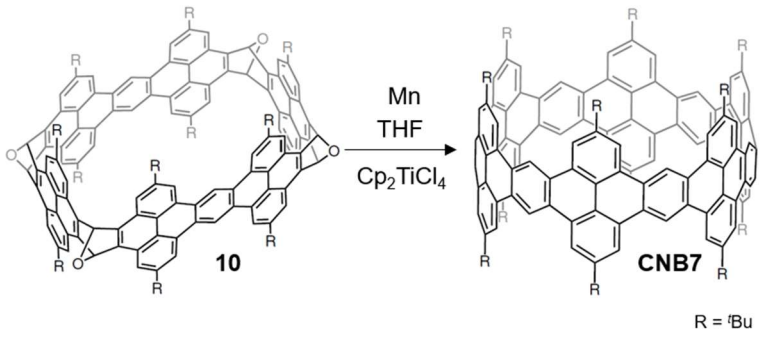

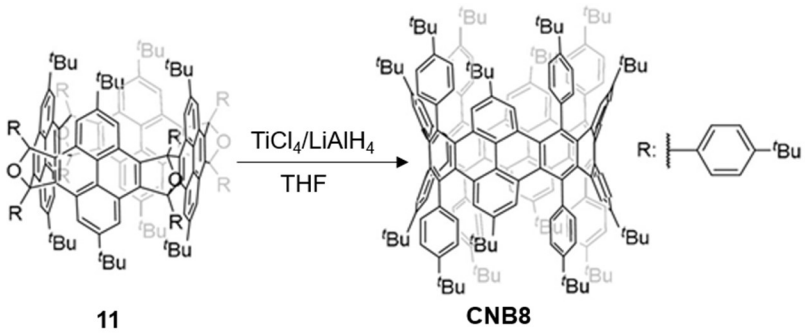

Scheme 4. Synthesis of zigzag CNBs - **CNB7** and **CNB8**[24][25]

Even so, the synthesis is still challenging, the successful cases are still few. Especially that fully fused CNBs with five-membered rings have never been realized. Here, I plan to synthesize a nanobelt with five-membered rings. There are several advantages of introducing five-membered rings. First of all, the five-membered rings in carbon nanobelts (e.g., the Schlüter belt) can induce positive curvature, while the seven- or eight-membered rings in carbon nanobelts can induce negative curvature as demonstrated by Gleiter and coworkers in 2008. They reported the synthesis of $[6.8]_3$cyclacene, an octagon-embedded carbon nanobelt (**Scheme 5**).[26] Therefore, the five-membered rings can share some of structural tension. It's easier for the six-membered rings to keep the planar structure of the normal benzene ring. Therefore, from the view point of ring strain, it will be easier to synthesize than the structure composed of all six-membered rings. Then, for constructing more complex carbon nanostructures, the introduction of non-six-membered rings is necessary. The study of five-membered rings is instructive for the study on introducing non-six-membered rings. Lastly, with the five-membered rings, the two six-membered rings in different direction are connected in one nanobelts. Even though the target CNB will not be used as template for CNT synthesis, it can be used as a bridge or connection between two different carbon nanotubes when constructing an extended structure.

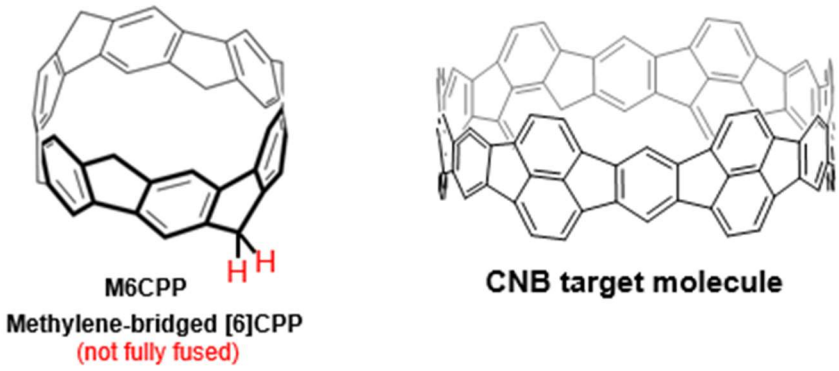

Figure 9. Molecular designs on CNBs including none-six-membered rings

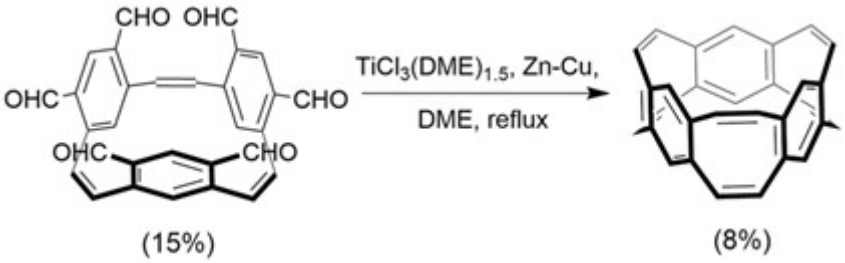

Scheme 5. Introduction of 8-membered rings[26]

To the carbon nanorings and CNBs, apart from their potential as templates for the synthesis of nanotubes, these compounds have their own special characteristics, such as molecular recognition capabilities, especially as acceptors for fullerenes, photoelectric properties like oxygen activation and so on. In terms of theoretical research, they can provide an important model that may reveal the nature of supramolecular interactions. In terms of practical application, they can constitute a light collection and photoelectric conversion system as a key part. One representative is this nano Saturn, which was synthesized in 2018.[27]

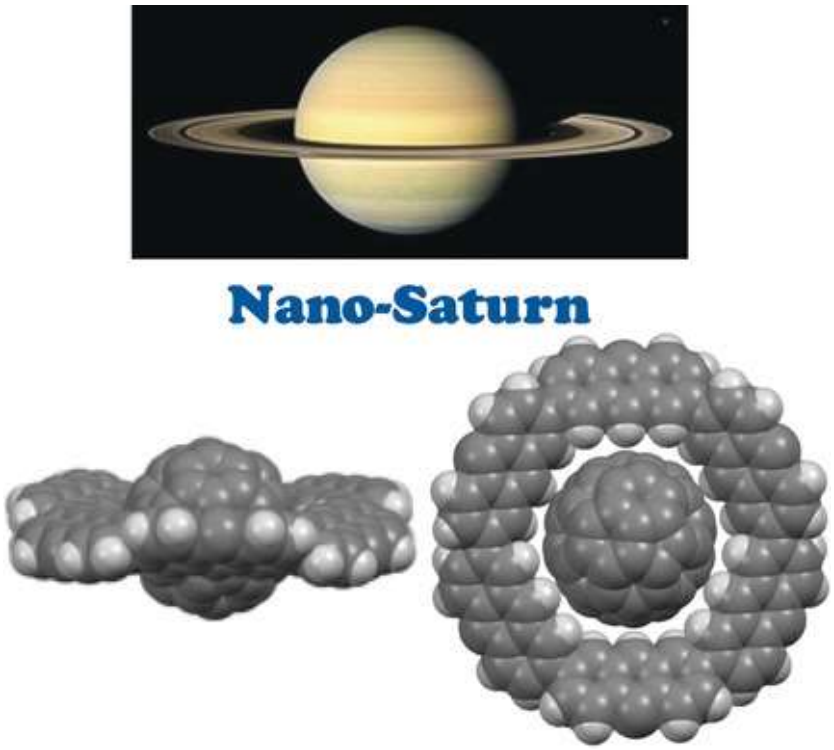

Figure 10. Nano-Saturn[27]

To achieve desirable electronic and photophysical properties, a manipulation of inter-chromophoric interaction is essential. Bottom-up "designed organic synthesis" of benzene-based nanocarbon materials has been extensively attempted since such synthesis will allow for tailored fine-tuning of their structures, properties, and functions.[14] These attempts are also important for cyclic aromatic molecules.[28]-[30] Such cyclic systems are expected to act as host molecules and to display multiple electronic interactions with guest molecules that are not shared with normal linear compounds.

1.3 Aims and methods

1.3.1 Building method of carbon nanorings

Involving synthesis methods of the main skeleton of macrocycles, there has been considerable development in recent years. Such as Itami's cyclohexane aromatization[31], Yamago's square-shaped platinum biphenyl intermediate method[32], Isobe's Yamamoto coupling method[33], branch or direct Suzuki coupling method and so on. Some of the strategies have achieved one-step synthesis. One-pot synthesis eliminates unnecessary halogenation and separation, which is more advantageous in terms of cost and time. With the continuous development of separation instruments such as GPC and HPLC, the difficulty of separation in a one-step method can also be reduced a lot.

As a common method, Suzuki coupling method tolerates wider functional groups (functional group compatibility)[34], which is essential for constructing rich and diverse CNBs, such as CNBs with multiple edges.

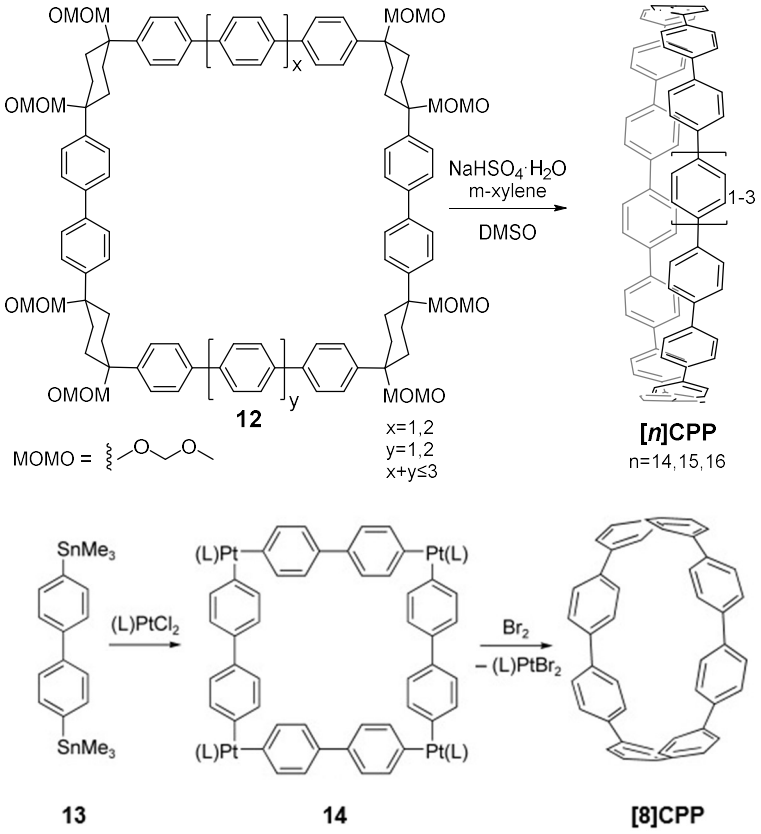

Scheme 6. Synthesis of carbon nanorings[32][33]

1.3.2 Building CNBs

After the skeleton is constructed, to obtain fully fused nanobelt molecules, it is often necessary to further aromatic cyclization. The fusion method usually depends on the structure of precursor molecules.

In early research, Diels-Alder reaction synchronized with the framework and metal-catalyzed dehydrogenation reaction were attempted but not to success. In Itami's case, the Ni catalyzed dehydrobromination worked.[18] The Scholl reaction has been widely used and successful synthesis of CNB compounds. In the following Miao's case, the Scholl reaction with oxidative aromatization was successful.[22] In recent examples of Itami and Chi, reductive aromatization worked well.[24][25] In my work, direct oxidation or dehydrochlorination methods will be flexibly adapted.

1.3.3 Aims and general methods

Cycloarylenes have attracted much attention due to their unique structure, remarkable characteristics and potential applications in materials science.[14] As the building block of the cycloarylenes, the benzene ring is commonly used.[28][32][36] There are not many examples of cycloarylenes based on PAHs that are larger than the benzene ring due to the rapidly increasing difficulty of synthesis. The structure of such macrocyclic compound is often an equilateral triangle[37] or a regular hexagon[38] except for CPPs,[28] due to the requirement that the benzene ring is made up of hexagon.

My research here is to use the one-pot Suzuki reaction to synthesize conjugated aromatic macrocyclic compounds and try to synthesize CNBs via these compounds. The short synthesis route of a one-pot reaction is used to challenge the synthesis of multiple ribbon compounds. In this process, the versatility of the one-pot Suzuki reaction with different reaction substrates will be verified. As well, the possibility of fusion methods other than the Scholl reaction will be explored. The research includes the supramolecular binding properties of the synthesis of belt-shaped compounds and macrocyclic

compounds that can be used as a precursor. The synthesis of CNB containing a five-membered ring or pentacene structure that has never been reported would be achieved by a simple method.

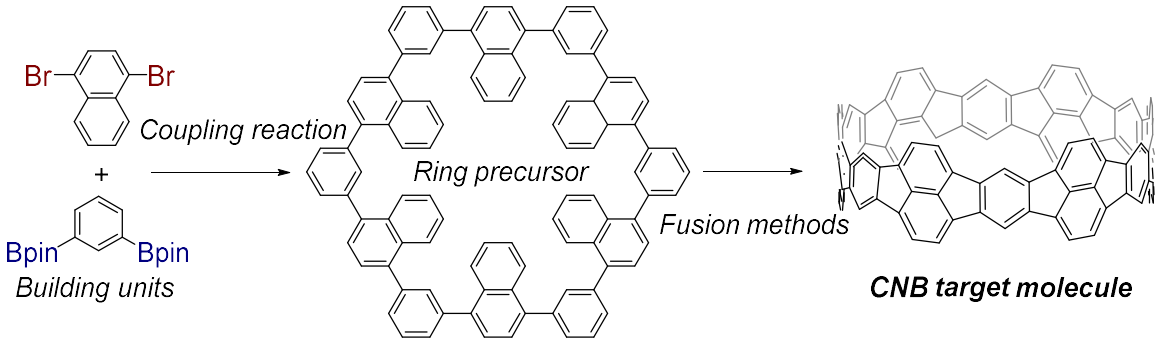

Scheme 7. The general method in this work

References

[1] (a) A. Rahman, I. Ali, S. M. Al Zahrani and R. H. Eleithy, *Nano*, **2011**, *6*(03), 185–203; (b) P. Greil, *Adv. Eng. Mater*, **2015**, *17*(2), 124–137; (c) V. Georgakilas, J. A. Perman, J. Tucek, R. Zboril, *Chem. Rev.* **2015**, *115*, 4744.

[2] https://www.laserfocusworld.com/optics/article/16566592/cnt-thin-films-show-high-infrared-transparency

[3] https://www.nist.gov/news-events/news/2013/10/nist-carbon-nanotube-chips-go-ballooning-climate-science

[4] (a) A. Graf, M. Held, Y. Zakharko, L. Tropf, M. C. Gather and J. Zaumseil, *Nat. mater*, **2017**, 16(9), 911–917; (b) https://news.st-andrews.ac.uk/archive/carbon-nanotubes-turn-electrical-current-into-light-matter-quasi-particles/

[5] (a) X. Sun, S. Vélez, A. Atxabal, A. Bedoya-Pinto, S. Parui, X. Zhu, R. Llopis, F. Casanova and L. E. Hueso, *Science*, **2017**, *357(6352)*, 677-680; (b) http://iresen.majjane.info/2017/08/18/fullerene-device-acts-as-both-solar-cell-and-a-current-inverter/

[6] B. D. Malhotra, and M. A. Ali, *Nanomaterials for Biosensors,* **2018**, 1–74.

[7] A. K. Geim and K. S. Novoselov, *Nat. Nanotechnol,* **2010**, 11–19.

[8] S. Iijima, *Nature*, **1991**, *354*(6348), 56–58.

[9] D. S. Bethune, C. H. Kiang, M. S. De Vries, G. Gorman, R. Savoy, J. Vazquez and R. Beyers, *Nature*, **1993**, *363*(6430), 605–607.

[10] (a) N. Anzar, R. Hasan, M. Tyagi, N. Yadav and J. Narang, *Sensors International*, **2020** *1*, 100003; (b) J. Che, T. Cagin and W. A. Goddard III, *Nanotechnology*, **2000**, *11*(2), 65.

[11] J. Cai, P. Ruffieux, R. Jaafar, M. Bieri, T. Braun, S. Blankenburg, M. Muoth, A. P. Seitsonen, M. Saleh, X. Feng, K. Müllen and R. Fasel, *Nature*, **2010**, *466*(7305), 470–473.

[12] R. Jasti and Carolyn. R Bertozzi, *Chem. Phy. Lett,* **2010**, *494,* 1−7

[13] H. Omachi, T. Nakayama, E. Takahashi, Y. Segawa and K. Itami, *Nat. Chem.* **2013**, *5*, 572–576

[14] (a) Y. Segawa, H. Ito and K. Itami, *Nat. Rev. Mater*, **2016**, *1*, 15002; (b) S. Toyota, E. Tsurumaki, *Chem.–Eur. J.* **2019**, *25*, 6878– 6890.

[15] F. Vögtle, A. Schröder and D. Karbach, *Angew. Chem. Int. Ed*, **1991**, *30*, 575.

[16] T. Nishiuchi, M. Iyoda, *Chem. Rec*. **2015**, *15*, 329.

[17] D. Mysliwiec, M. Stępien, *Angew. Chem. Int. Ed*. **2013**, *52*, 1713.

[18] (a) G. Povie, Y. Segawa, T. Nishihara, Y. Miyauchi, K. Itami, *Science*, **2017**, *356*(6334), 172-175; (b) G. Povie, Y. Segawa, T. Nishihara, Y. Miyauchi, K. Itami, *J. Am. Chem. Soc*. **2018**, *140*, 10054.

[19] T. J. Sisto, X. Tian, R. Jasti, *J. Org. Chem*. **2012**, *77*, 5857.

[20] (a) F. E. Golling, S. Osella, M. Quernheim, M. Wagner, D. Beljonne, K. Müllen, *Chem. Sci*. **2015**, *6*, 7072; (b) M. Quernheim, F. E. Golling, W. Zhang, M. Wagner, H. J. Rader, T. Nishiuchi, K. Müllen, *Angew. Chem. Int. Ed*. **2015**, *54*, 10341.

[21] (a) T. J. Sisto, L. N. Zakharov, B. M. White, R. Jasti, *Chem. Sci*. **2016**, *7*, 3681; (b) M. R. Golder, C. E. Colwell, B. M. Wong, L. N. Zakharov, J. Zhen, R. Jasti, *J. Am. Chem. Soc*. **2016**, *138*, 6577.

[22] (a) K. Y. Cheung, S. Gui, C. Deng, H. Liang, Z. Xia, Z. Liu, L. Chi and Q. Miao. *Chem*, **2019**. *5*(4), 838-847. (b) K. Y. Cheung, S. Gui, C. Deng, H. Liang, Z. Xia, Z. Liu, L. Chi and Q. Miao. *Chem*, **2021**, *5*(4), 838–847.

[23] Y. Li, Y. Segawa, A. Yagi and K. Itami, *J. Am. Chem. Soc*. **2020**, *142(29)*, 12850–12856.

[24] K. Y. Cheung, K. Watanabe, Y. Segawa, and K. Itami, *Nat. Chem*, **2021**, *13*(3), 255–259.

[25] Y. Han, S. Dong, J. Shao, W. Fan and C. Chi, *Angew. Chem*, **2021**, *133*(5), 2690–2694.

[26] B. Esser, F. Rominger and R. Gleiter*, J. Am. Chem. Soc.* **2008***, 130,* 6716.

[27] Y. Yamamoto, E. Tsurumaki, K. Wakamatsu and S. Toyota, *Angew. Chem. Int. Ed*, **2018**, *57*(27), 8199–8202.

[28] K. Yazaki, L. Catti and M. Yoshizawa, *Chem. Commun*, **2018**, *54*, 3195–3206.

[29] D. Lorbach, A. Keerthi, T. M. Figueira-Duarte, M. Baumgarten, M. Wagner and K. Müllen, *Angew. Chem. Int. Ed*, **2016**, *55*, 418–421.

[30] Y. Yamamoto, K. Wakamatsu, T. Iwanaga, H. Sato and S. Toyota, *Chem.–Asian J*, **2016**, *11*, 1370–1375

[31] H. Omachi, S. Matsuura Y. Segawa and K. Itami, *Angew. Chem. Int. Ed*, **2010**, *49*(52), 10202–10205.

[32] S. Yamago, Y. Watanabe and T. Iwamoto, *Angew. Chem. Int. Ed*, **2010**, *49*(4), 757–759.

[33] J. Y. Xue, K. Ikemoto, N. Takahashi, T. Izumi, H. Taka, H. Kita, S. Sato and H. Isobe, *J. Org. Chem*. **2014**, *79*, 9735–9739.

[34] V. Hensel, K. Lützow, J. Jakob, K. Gessler, W. Saenger and A.D. Schlüter, *Angew. Chem. Int. Ed. Engl*, **1997**, *36*, 2654–2656; V. Hensel and A. D. Schlüter, *Chem.–Eur. J*, **1999**, *5*, 421–429.

[35] (a) H. J. S. Winkler, G. Wittig, *J. Org. Chem*. **1963**, *28*, 1733–1740; (b) H. A. Staab, F. Binnig, *Tetrahedron Lett*. **1964**, *5*, 319–321; (c) J. Y. Xue, T. Izumi, A. Yoshii, K. Ikemoto, T. Koretsune, R. Akashi, R. Arita, H. Taka, H. Kita, S. Sato and H. Isobe, *Chem. Sci*. **2016**, *7*, 896–904.

[36] (a) R. Jasti, J. Bhattacharjee, J. B. Neaton C. R. Bertozzi, *J. Am. Chem. Soc*. **2008**, *130*, 17646–17647; (b) H. Takaba, H. Omachi, Y. Yamamoto, J. Bouffard and K. Itami, *Angew. Chem. Int. Ed*. **2009**, *48*, 6112–6116;

[37] (a) J. Zhang, X. Wang, Q. Su, L. Zhi, A. Thomas, X. Feng, D. S. Su, R. Schlögl, and K. Müllen, *J. Am. Chem. Soc.* **2009**, *131*, 11296–11297; (b)R. Kurosaki, H. Hayashi, M. Suzuki, J. Jiang, M. Hatanaka, N. Aratani and H. Yamada, *Chem. Sci*. **2019**, *10*, 6785–6790.

[38] (a) P. Mei, A. Matsumoto, H. Hayashi, M. Suzuki, N. Aratani and H. Yamada, *RSC Adv.* **2018**, *8*, 20872–20876; (b) H. W. Jiang, S. Ham, N. Aratani, D. Kim and A. Osuka, *Chem.–Eur. J.* **2013**, *19*, 13328–13336.

Chapter 2. Facile synthesis and supramolecular investigation of *m*-phenylene bridged cyclic naphthalene oligomers

2.1 Introduction

Pd-catalyzed cross coupling reactions were demonstrated to be quite powerful in the synthesis of a variety of oligomers of PAHs. Despite these signs of progress, 1,3-phenylene bridged cyclic PAH hexamers that can be regarded as benchmark wheels in terms of their simple hexagonal structure were rarely synthesized.[39]-[42] Cyclic heptamers and higher analogs are rather scarcer. Schlüter *et al.* made a cyclotetraicosaphenylene by using a repetitive Suzuki-Miyaura cross coupling protocol.[39] The first [6]cyclo-*m*-phenylene was prepared by Staab and co-workers.[40] and recently a series of [*n*]cyclo-*m*-phenylenes were synthesized by a one-pot Ni-mediated Yamamoto coupling.[41] The cyclic porphyrin hexamer is interesting not only as an artificial light-harvesting photosynthetic antenna but also as a shape-persistent organic molecule.[42] The conformationally rather restricted cyclic structure is amenable for studies on the structure-optical property relationship but likely poses a synthetic challenge. In my research, the first synthesis of 1,3-phenylene bridged hexameric and heptameric naphthalene wheels via one-step cross-coupling at multiple sites starting from simple monomers was attempted, and their complexation with fullerenes was investigated.

After that, similar coupling reactions with a wider range of wheel-shaped PAHs were challenged. Then those compounds would be set as precursors for further curved PAHs like CNBs.

2.2 Synthesis

2.2.1 Synthesis of *m*-phenylene bridged cyclic naphthalene hexamer N6

At the very beginning, I followed the synthetic route in **Scheme 8**. It was a step-wise route but quite close to the one-pot synthesis. Fortunately, the target ring compound can be successfully synthesized. The *m*-phenylene bridged naphthalene hexamer was obtained in a yield of 1%. In the ^{1}H NMR spectrum, the numbers of proton peaks were limited. Only highly a symmetric structure or small molecules can lead to this result. And the MALDI-TOF-MS confirmed it to be hexamer instead of a small molecule. Based on these two points, the cyclic hexameric conformation of this product was confirmed. And it has a highly symmetric structure in solution. It's exciting to obtain the cyclic compound. But can it be obtained with even simpler ways or higher yield?

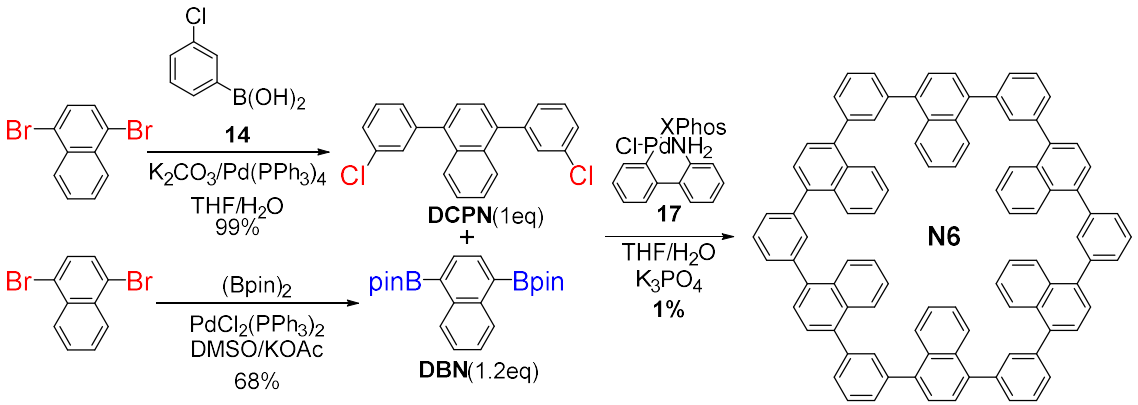

Scheme 8. Synthesis of **N6**.

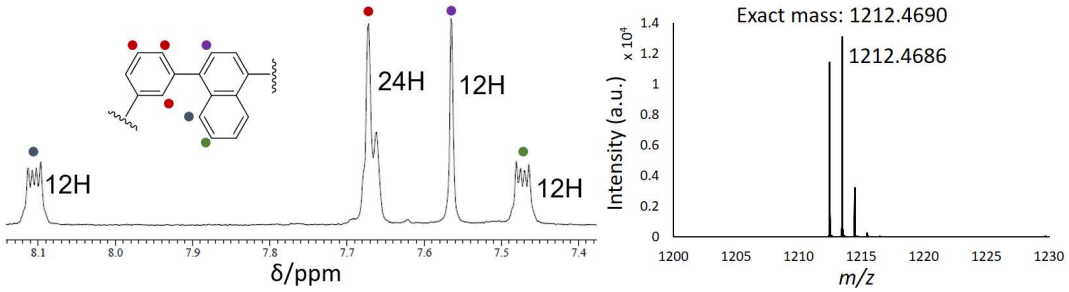

Figure 11. ^{1}H NMR spectrum (600 MHz) in $C_2D_2Cl_4$ at 60 ºC (left) and HR-MALDI-TOF-MS (right) of **N6**.

2.2.2 Optimization of the reactions

Therefore, reactions to optimize the synthetic route as well as the yield were attempted. Fortunately, the optimization worked well. First, I succeeded in making it by one-pot reaction from the monomers. And in this case, the reaction selectively produced cyclic hexamer. Later, I succeeded in improving the yield. In this case, three kinds of cyclic compounds were obtained with better yields. And I could finally obtain the cyclic compounds in a larger 100 mg scale.

I noticed that the temperature seemed to affect the reaction result much. It looks like lower temperature will benefit the cyclization and formation of larger cycles. The two starting materials (dibromide: diboride = 1: 1) in DMF/ toluene with CsF at 80°C temperature gave **N6** in 6% yield with a trace amount of **N7**. However, the two starting materials (dibromide: diboride = 1: 1.3) in THF/H_2O with Cs_2CO_3 and 18-crown-6 gave 13% **N7** and 4% **N6**. The condition was reported during my research by Yokozawa and co-workers.[43] The distribution of **N6** and **N7** could be controlled by changing reaction conditions. One possible reason might be that the rotation rate of the linear intermediates slows down at low temperature increasing the chance of large wheels' forming.

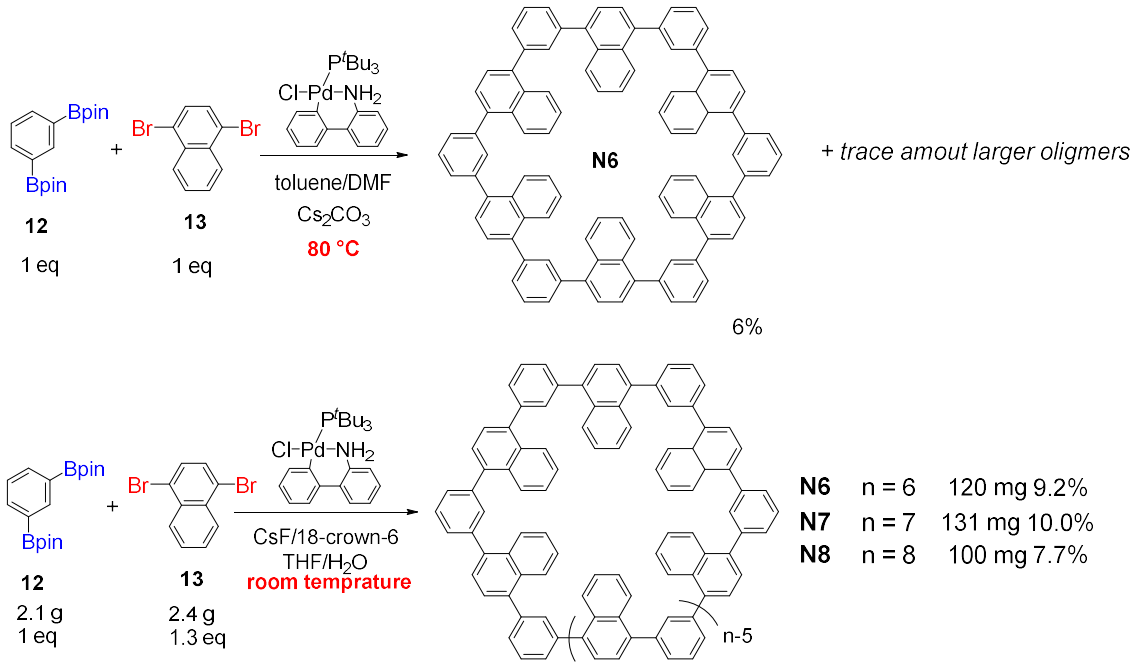

Scheme 9. One-pot synthesis of **N6** (and **N7**)

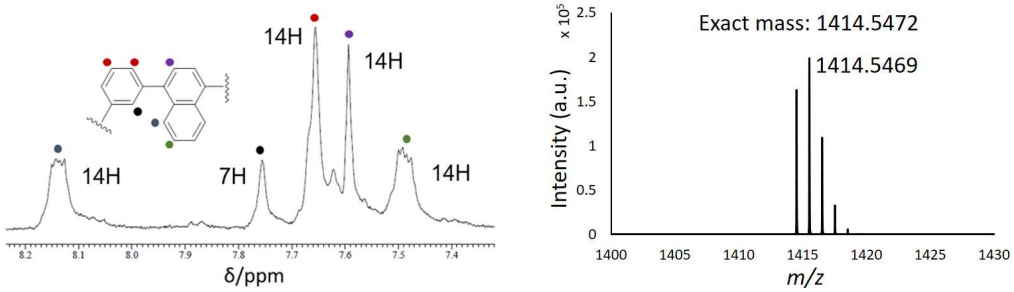

Figure 12. ^{1}H NMR spectrum (400 MHz) in $C_2D_2Cl_4$ at 120 ºC (left) and HR-MALDI-TOF-MS (right) of **N7**.

2.3 General investigation

2.3.1 Single crystal X-ray analysis of N6

Definitive structural assignment of **N6** was accomplished through a single crystal X-ray diffraction analysis, which unveiled a distinct hexagonal conformation (**Figure 13**). The inside cavity was determined by the distance of naphthalene plane, which is nearly 15 Å. The phenylene-bridges are on the co-plane, suggesting less structural strain. The dihedral angles between the naphthalene mean-plane and phenylene groups are in the range of 58°-64°. Interestingly, the hexagons are interconnected through phenylene C–H and naphthalene π-plane interactions in the crystal, forming infinite one-dimensional tubular packing structure along the *c*-axis structure of **N6**.

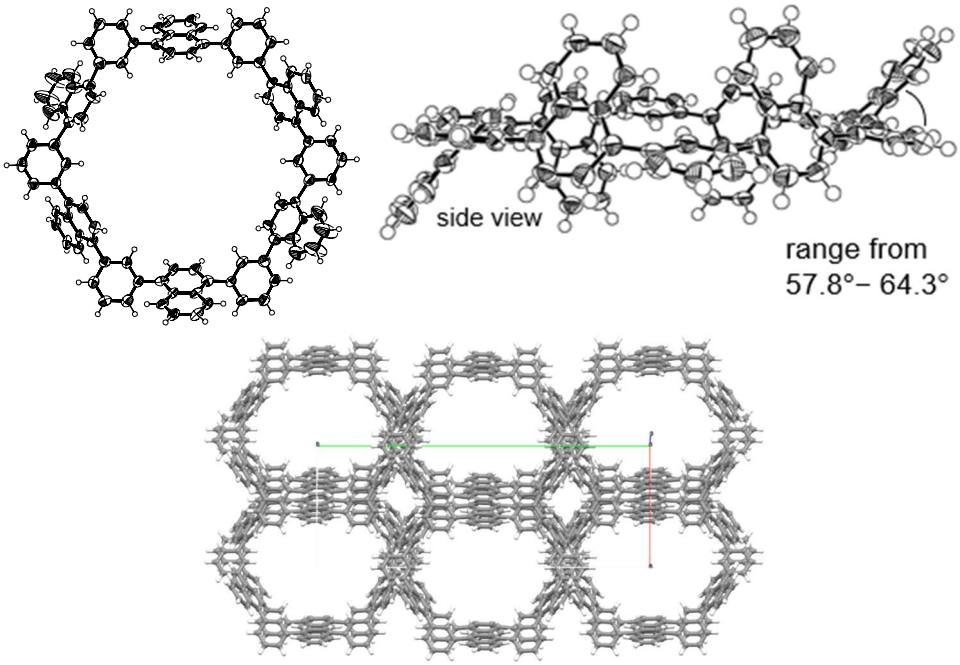

Figure 13. Single crystal X-ray structure of **N6** with packing structure. Thermal ellipsoids are scaled at 50% probability. Solvent molecules are omitted for clarity.

2.3.2 UV-vis absorption spectra of N6 and N7

Figure 14 shows the UV-vis absorption and fluorescence spectra of **N6** and **N7** in CH_2Cl_2. Cyclic hexamer **N6** shows a single absorption band at 306 nm and a blue emission at 383 nm. This broad single band can be qualitatively understood in terms of the weak π-conjugation and the exciton coupling,[44] as similarly to previously reported 1,3-phenylene naphthalene dimer.[45] Given the rigid hexagonal conformation for the wheel, J-type exciton coupling of transition dipoles is effective. The interacting components lead to red-shifted absorption band compared with the naphthalene monomer (275 nm in CH_2Cl_2). The steady-state fluorescence spectrum in toluene is also displayed in **Figure 14**. Cyclic heptamer **N7** exhibits a slightly red-shifted absorption band at 308 nm and a blue-shifted emission at 382 nm. These are presumably because the conformational deformation from **N6** to **N7** makes the forbidden S_1 transition just a little allowed.

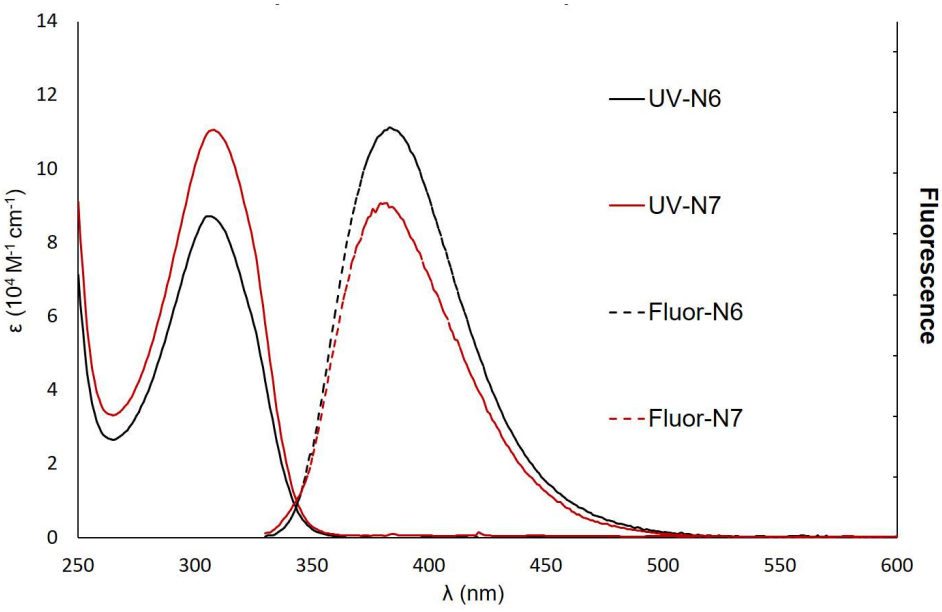

Figure 14. UV-vis absorption and fluorescence spectra of **N6** and **N7** in CH_2Cl_2

2.3.3 CV and DPV plots of N6

Figure 15 shows the cyclic voltammetry - differential pulse voltammetry (CV-DPV) plots of **N6** in CH_2Cl_2. A single step irreversible oxidation wave was observed. With the high oxidation potential E_{ox} 1.11 V, **N6** is supposed to be oxidatively stable under normal conditions. The oxidative modification of **N6** may require some strong conditions.

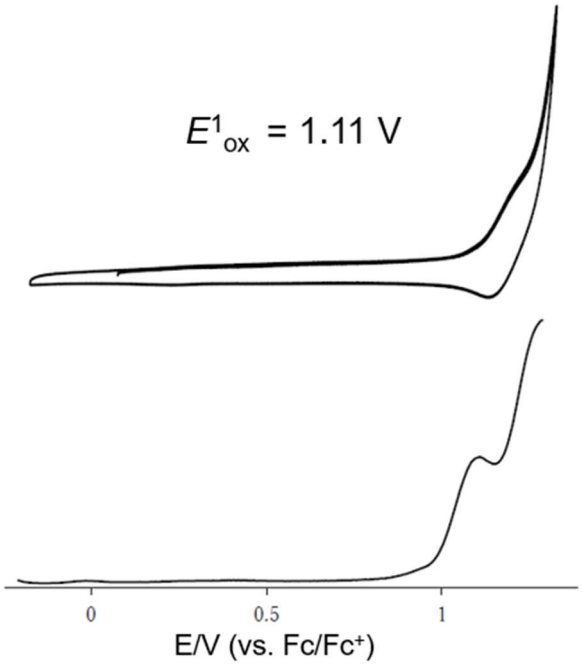

Figure 15. CV and DPV of **N6. (**In 0.1 M $TBAPF_6$/ CH_2Cl_2; Scan rate: 100 mVs^{-1}; Solvent: CH_2Cl_2; **N6** = 0.1 mM; W. E.: glassy carbon; C. E.: Pt; R. E.:$Ag/AgNO_3$)

2.3.4 DFT calculations of N6

To further understand the electronic features of **N6**, the density functional theory (DFT) and the time-dependent (TD)-DFT calculations both at the B3LYP/6-31G(d) level using the Gaussian 09 software package were carried out (**Figure 15**). [45][46] It is revealed that the frontier orbitals are degenerated. The coefficients of HOMO and LUMO of **N6** localize on the six naphthalene units. The main absorption band of **N6** at 306 nm predominantly comprises the S_2 and S_3 transitions (oscillator strength, f = 1.03 and f = 1.02), whereas the long wavelength S_1 absorption is forbidden (f = 0.00). The transition

energies and oscillator strengths simulated by TD-DFT calculations showed a good agreement with the observed absorption spectrum of **N6**.

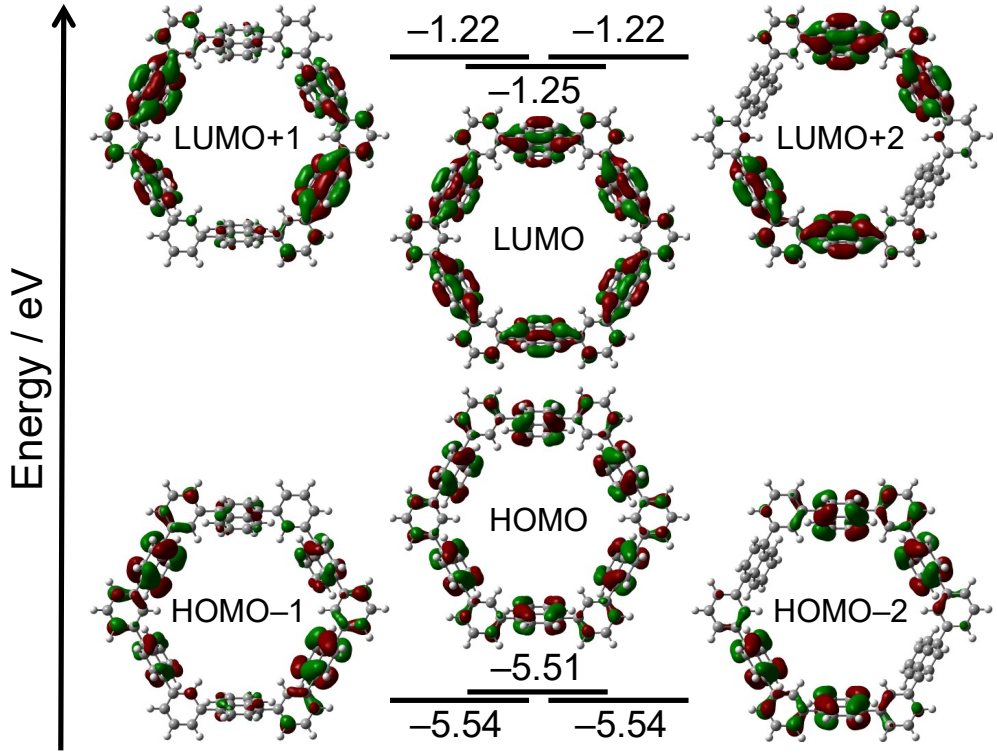

Figure 16. MO diagrams of **N6** calculated at the B3LYP/6-31G(d) level.

2.4. Supramolecular investigation

2.4.1 Complexation of N6 with C_{60}

In the next step, the encapsulation of C_{60} into **N6** and was examined, since the diameter of the interior cavity of **N6** is ca. 15 Å, being possibly fit the diameter of C_{60}.[47]

2.4.1.1 NMR titration of N6 with C_{60}

The encapsulation was also confirmed by NMR spectroscopy. The experiment started with a 0.400 mL deuterated toluene solution of **N6** at a concentration of 3.98×10^{-4} M. In the case of adding C_{60}, for each one equivalence, 20 μL deuterated toluene solution

of C_{60} at a concentration of 7.99×10^{-3} M was added. Each time of adding was followed by one measurement of ^{1}H NMR after mixing well. The experiment ended at a 0.600 mL mixed solution with 10 equivalents of C_{60}. The association constant $K_{1[C60]}$ was calculated through the tools on the website: http://supramolecular.org/ based on the data gathered in this experiment.[48]

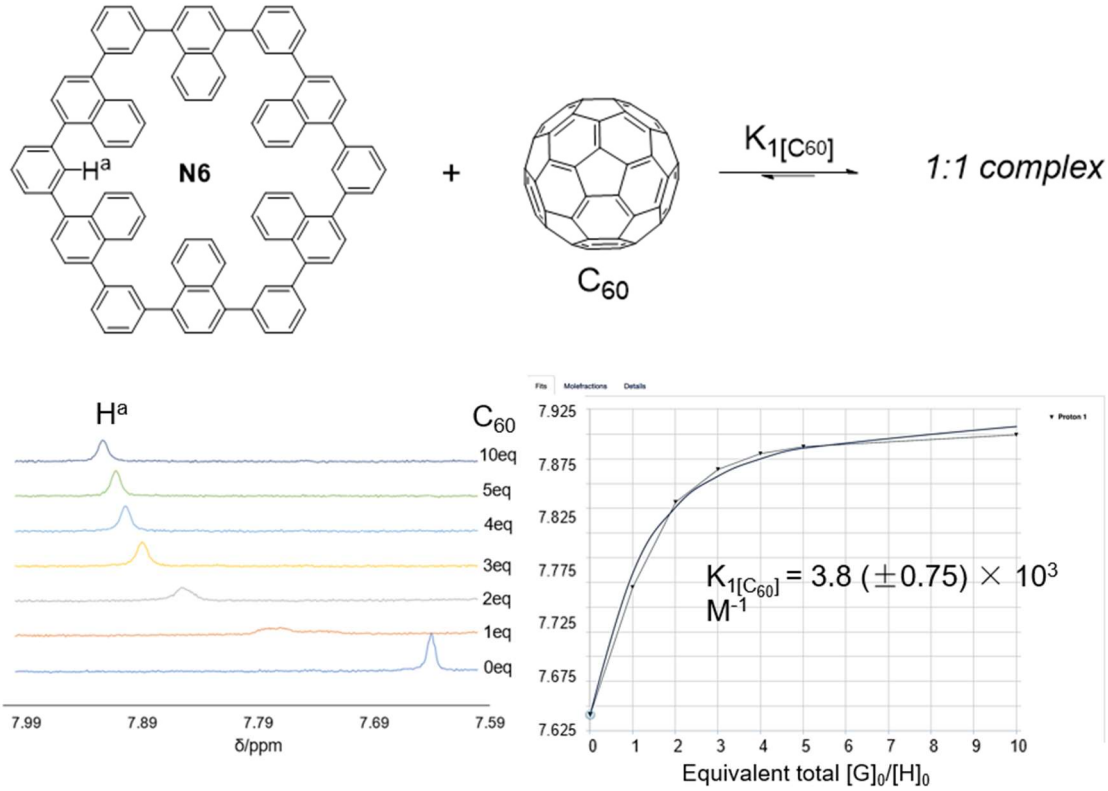

Figure 17. NMR titration of C_{60}-**N6**

2.4.1.2 Co-crystallization of N6 with C_{60}

The attempts towards co-crystals of **N6** with C_{60} were carried out. The host-guest binding structure was unambiguously confirmed by the single-crystal X-ray diffraction analysis (**Figure 18**). A higher concentration on the crystallization process could give the encapsulation complex. In the solid state, the naphthalene units of C_{60}@**N6** take a similar structure to those of **N6** which respects to dihedral angles of phenylene toward naphthalene (51~72°), and an inside space (15 Å diameter). The positions of C_{60} are

disordered in two parts (66: 34), which again proved the weak interactions between the two components. As shown in **Figure 18**, a C_{60} molecule is nicely captured within the cavity. Closer inspection of the crystal structure reveals that the naphthalene planes are protruding their planar face toward the interior space, which interacts with C_{60}. Interestingly, the C_{60} molecules in the crystal are aligned with the aid of **N6** agent to form a 1D structure along the *a*-axis (**Figure 18**).

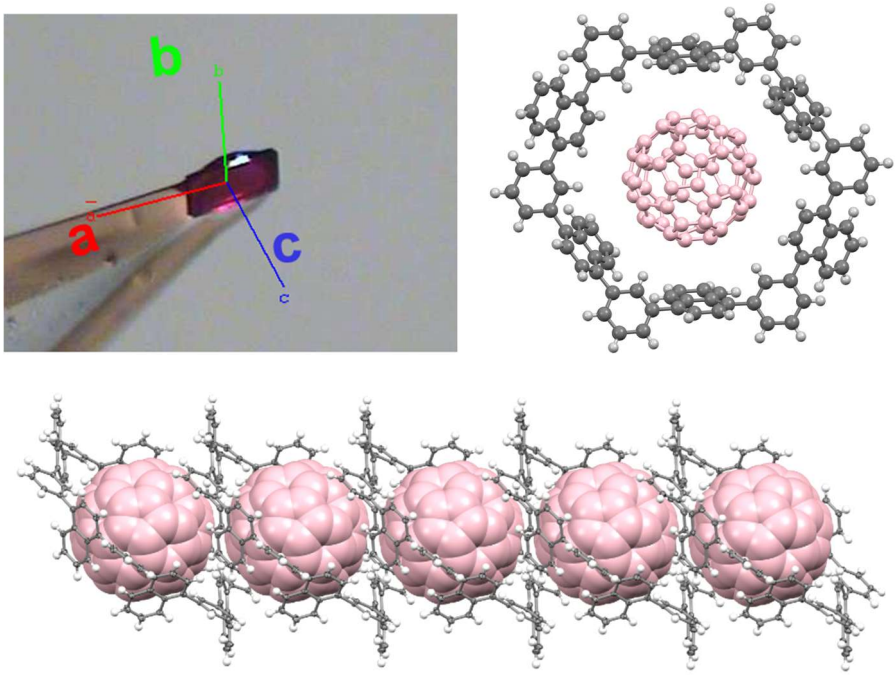

Figure 18. Single crystal X-ray structure and packing structure of C_{60}@**N6**.

2.4.2 Complexation of N6 with C_{70}

In the next step, the encapsulation of C_{70} into **N6** and was examined, since the diameter of the interior cavity of **N6** is ca. 15 Å, being also possibly fit the diameter of C_{70}.[49]

2.4.2.1 NMR titration of N6 with C_{70}

The encapsulation was also confirmed by NMR spectroscopy. The experiment started with a 0.400 mL deuterated toluene solution of **N6** at a concentration of 3.98×10^{-4} M. In the case of adding C_{70}, for each one equivalence, 30 μL deuterated toluene solution of C_{70} at a concentration of 7.99×10^{-3} M was added. Each time of adding followed by one measurement of ^{1}H NMR after mixing well. The experiment ended at a 0.700 mL mixed solution with 10 equivalents of C_{70}. The association constant $K_{1[C70]}$ was calculated through the tools on the website: http://supramolecular.org/ based on the data gathered in this experiment.[48]

The value of $K_{1[C70]}$ is 30 times that of $K_{1[C60]}$, indicating that the combination with C_{70} is much stronger than C_{60}. For this reason, first is the shape, the C_{60} is spherical. But C_{70} is a narrow ellipsoid in the middle.

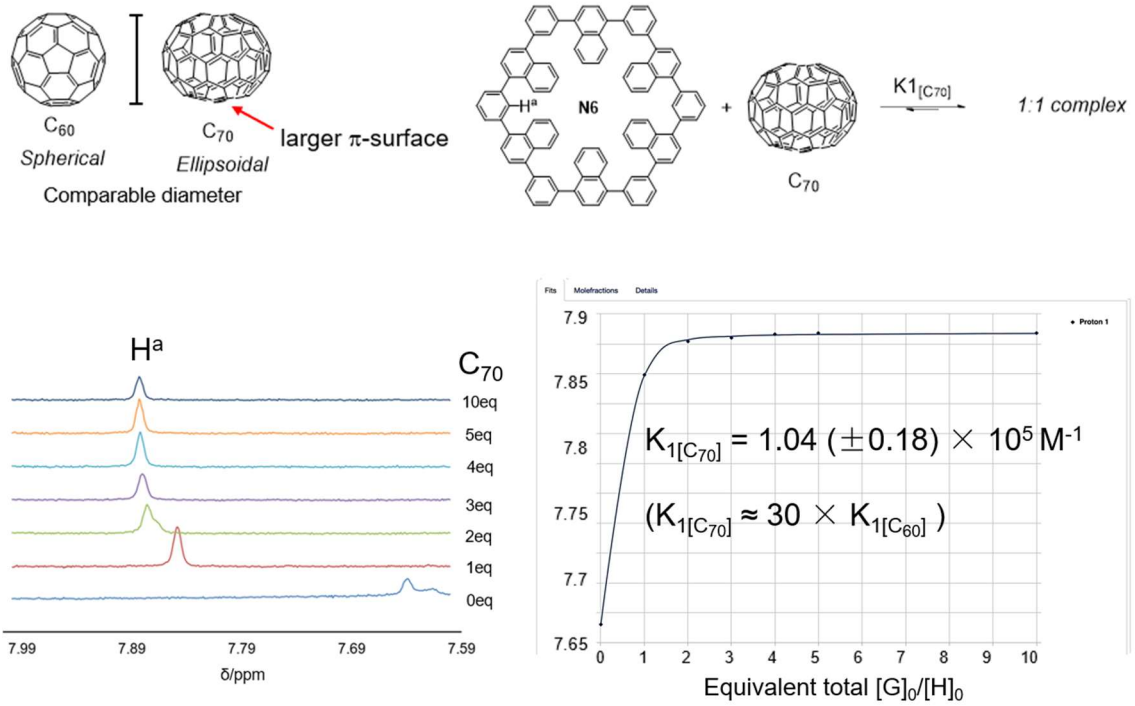

Figure 19. NMR titration of C_{70}-**N6**

2.4.2.2 Co-crystallization of N6 with C_{70}

The attempts towards co-crystals of **N6** with C_{70} were carried out. The host-guest binding structure was unambiguously confirmed by the single-crystal X-ray diffraction analysis (**Figure 20**). A higher concentration on the crystallization process could give the encapsulation complex. In the solid state, the naphthalene units of C_{70}@**N6** take a similar structure to those of **N6** which respects to dihedral angles of phenylene toward naphthalene (51~72°), and an inside space (15 Å diameter). As shown in **Figure 20**, a C_{70} molecule is nicely captured within the cavity. Closer inspection of the crystal structure reveals that the naphthalene planes are protruding their planar face toward the interior space, which interacts with C_{70}. Interestingly, the C_{70} molecules in the crystal are aligned with the aid of **N6** agent to form a 1D structure along the *a*-axis (**Figure 20**).

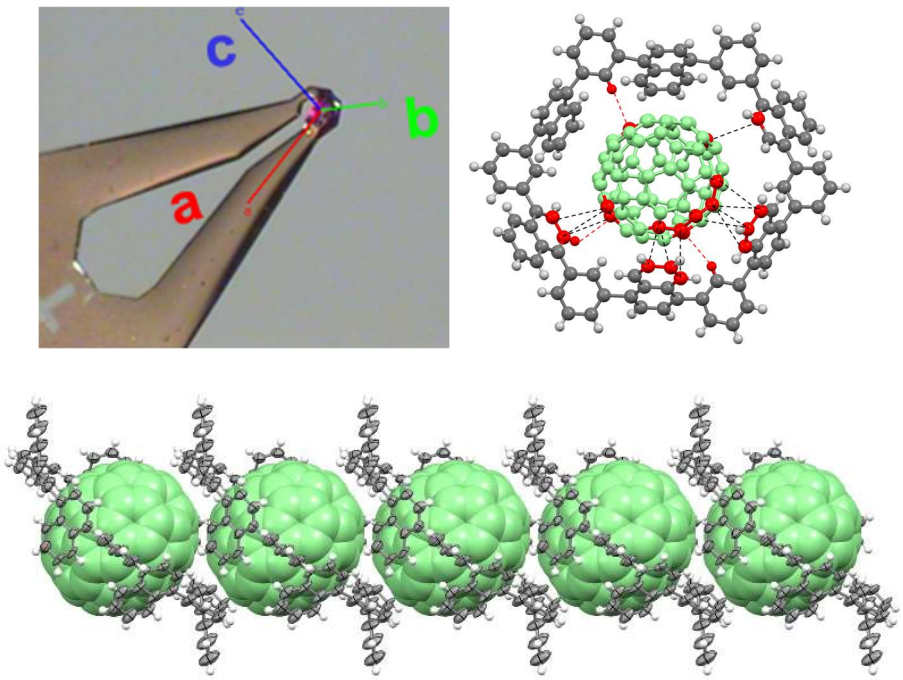

Figure 20. Single crystal X-ray structure of C_{70}@**N6** and packing structure

Through the addition of C_{70} into a toluene solution of **N6** the change the absorption spectrum was hard to observe because of the severe overlap on the absorption peaks of **N6** and C_{70}.

2.4.3 Conductivity investigation on co-crystals via DFT calculations

2.4.3.1 Charge transfer properties and charge transfer integrals.

As we know, there are two theories on conductivity. One is hopping theory and another is band theory. The hopping theory is widely used in semi-conductive materials. According to this theory, the charge transfer probability κ_{ET} between two adjacent molecules is expressed by the following first equation:

$$\kappa_{ET} = \frac{V^2}{h}\left(\frac{\pi}{\lambda \kappa_B T}\right)^{1/2} exp\left(-\frac{\pi}{4\kappa_B T}\right) \qquad (1)$$

V is the charge transfer integral, λ the rearrangement energy, the κ_B the Boltzmann constant, T the temperature and h the Plank constant.

And the mobility between them can be expressed by the second equation:

$$\mu = \frac{ed^2}{\kappa_B T}\kappa_{ET} \qquad (2)$$

d is the distance between two molecules and e is the elementary charge.

If we combine the two equations, we can get that:

$$\mu \propto V^2$$

The charge carrier mobility is proportional to the square of charge transfer integral V. In this case, when HOMO level was considered, for the hole transfer, there is the V_{hole} value. While LUMO levels were considered, for the electron transfer, there is the $V_{electron}$.

Here is of example for pentacene. Simply speaking, a high V value can indicate the possibility of high mobility. [50]

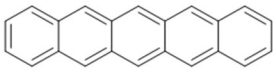

Pentacene
Charge carrier mobility
5 cm^2/Vs reached

Base-set	a	b
V_{hole}/meV	91	92
$V_{electron}$/meV	130	140

Figure 21. DFT calculation [(B3LYP/6-31G(d,p)] result of Vs of pentacene crystal[50]

The π-stacking structure can maximize the intermolecular orbital overlap and thus, the structures of **N6**-C_{60} and **N6**-C_{70} are expected to have large intermolecular orbital couplings. Intermolecular transfer integrals Vs (meV) between the HOMOs and between LUMOs of neighboring fullerenes were calculated with the Amsterdam Density Functional (ADF) program package (GGA:pw91/T2P).[51]

2.4.3.2 Charge transfer properties of C_{60}@N6 and C_{70}@N6

The obtained Vs between C_{60} molecules are 3.1 mV for V_{hole} and 3.0 mV for $V_{electron}$. The prediction from the 1D arrangement basically agrees that carriers can move only along the a-axis. The obtained Vs between C_{60} molecules are 10.4 mV for V_{hole} and 15.8 mV for $V_{electron}$. The prediction from the 1D arrangement basically also agrees that charges can move only along the a-axis. The value of C_{70}-C_{70} (10.4 mV, 15.8 mV) is larger than that of C_{60}-C_{60} (3.1 mV, 3.0 mV). For the interaction of a single 1:1 complex, the value of **N6**-C_{70} (87.3 mV, 93.1 mV) is also much higher than that of **N6**-C_{60} (45.6 mV,

33.4 mV). This is also consistent with the result of the binding constant measured by titration. It can be speculated that a stronger bond is beneficial to strengthen the interaction between fullerenes.

2.4.3.3 One dimensional conductivity and FET properties

Figure 22 highlighted the V values of the two co-crystals along the 1D alignment of fullerenes. Although the distance between fullerenes is not short enough for them to have a comparable value as pentacene. But this value still shows the possibility for electrons or holes to easily move from one fullerene to nearby fullerene and forms the 1D conductivity. Comparing that of C_{60}, the C_{70}'s co-crystal has a 3 times larger V value. The closer distance of C_{70} should be the main reason for the higher V values. And base on this result, it can be predicted that the co-crystal of C_{70} will exhibit better mobility.

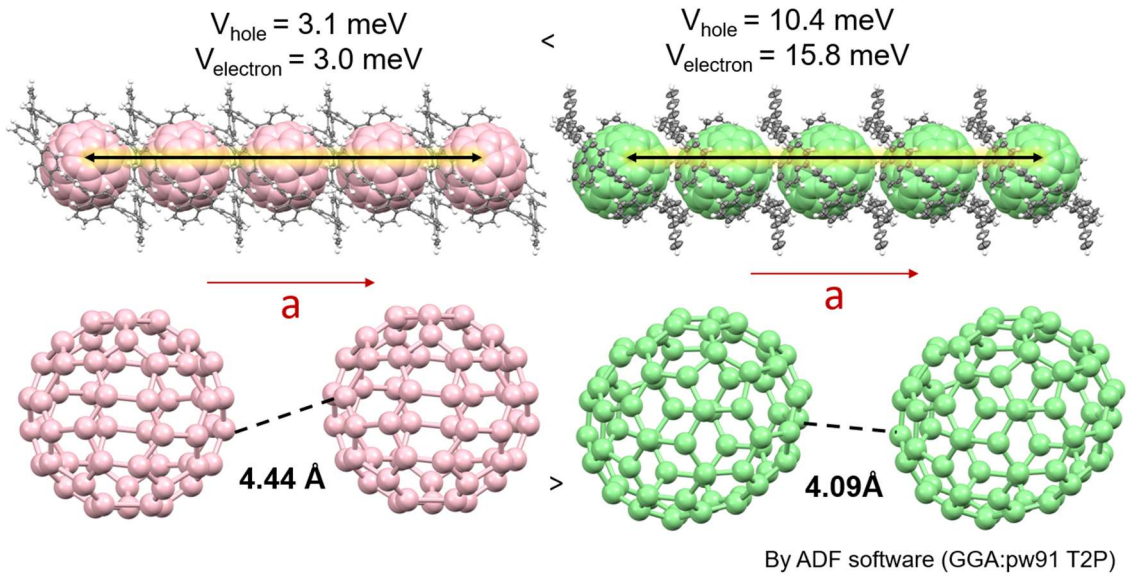

Figure 22. *V* values of the two co-crystals along the 1D alignment of fullerenes

To further check it, the preparation of crystal on the substrate was carried out. The 1:1 complex solution was dropped to cover the silicon substrate, then the solvent was allowed to be evaporated naturally under normal pressure and temperature. This way, the crystals grow on the surface of the substrate. During this process, only C_{70} with **N6** was found to form needle-shaped crystals. Those of C_{60} show short stick-shaped which are not sui in this case. Therefore, only the co-crystal of C_{70} was investigated here.

After getting the co-crystals, the gold electrodes were installed by vacuum evaporation. After Scrape off the silica coating on the surface. The Filed effect transistor structure was built. Unfortunately, the following measurement didn't determine the FET property. But the reason may be that the quality of the FET device was not good enough. Since this method may not be suitable for the two co-crystals.

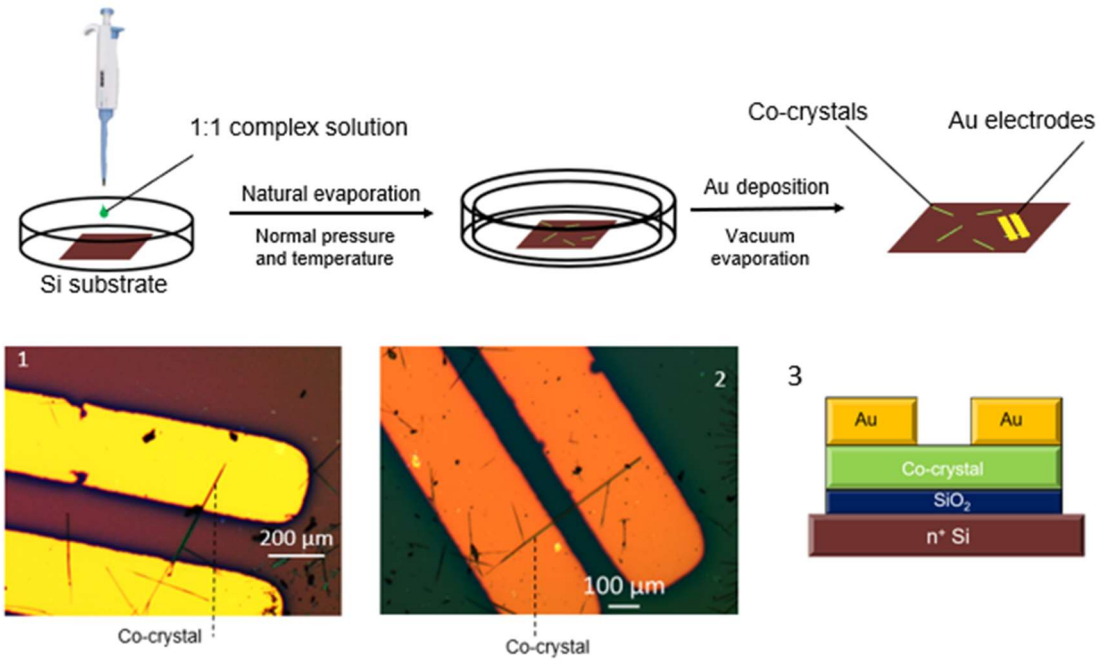

Figure 23. FET preparation of co-crystals

(**Sample 1 and 2: N6**+C_{70},1 mg/mL (**N6**), *o*-DCB/iPrOH, bare Si substrate; **3**: the structure of FET device)

The time resolved microwave conductivity measurement (TRMC) was then carried out. A TRMC signal similar to that of $PC_{61}BM$ was obtained, which means that this material exiting photoconductivity. In the case of $PC_{61}BM$, the value is 2 $\times 10^{-5}$ cm^2/Vs.[52] The value is not that high as that of $PC_{61}BM$. But after combining with other materials to form the heterojunction structure, this can be improved a lot just like that of $PC_{61}BM$. The preparation on that of C_{70} is on the way.

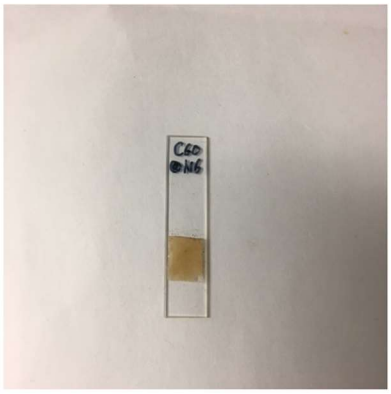

Stick on double-sided tape

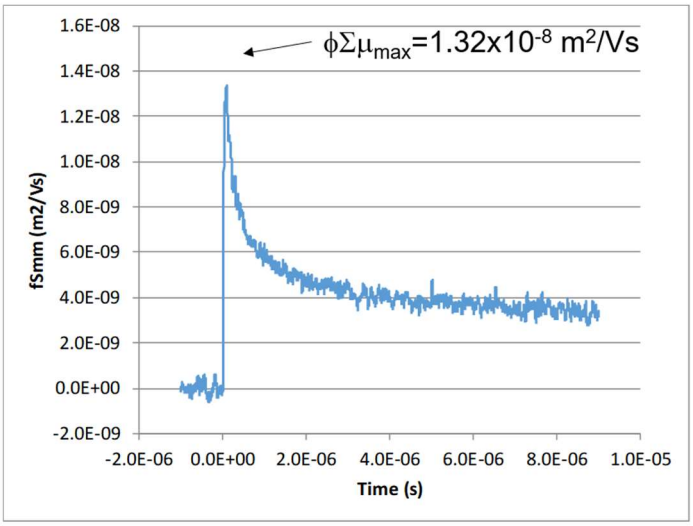

2021/7/27 TRMC (ex355nm, I_0=9.1x10^{15} photons/cm^2)

Figure 24. TRMC measurement on C_{60}@**N6**

2.5 Synthesis towards CNBs via *m*-phenalene bridged carbon nanorings

2.5.1 Methods

The **N6** and other carbon nanorings being successfully synthesized, which can be also treated as the precursors for CNB synthesis. The next step is the fusion of these carbon nanorings to afford double-stranded CNBs. The first fusion method (**Scheme 11**) is the Scholl reactions with oxidative cyclodehydrogenation, which have been reported in fusing molecules with naphthalene structures. [53][54] In the case of making **CNB5** and **CNB6** of Miao's works[22], the reaction worked well in making belt molecules (**Scheme 3**). Therefore, my work started with the oxidative cyclodehydrogenation in making CNBs.

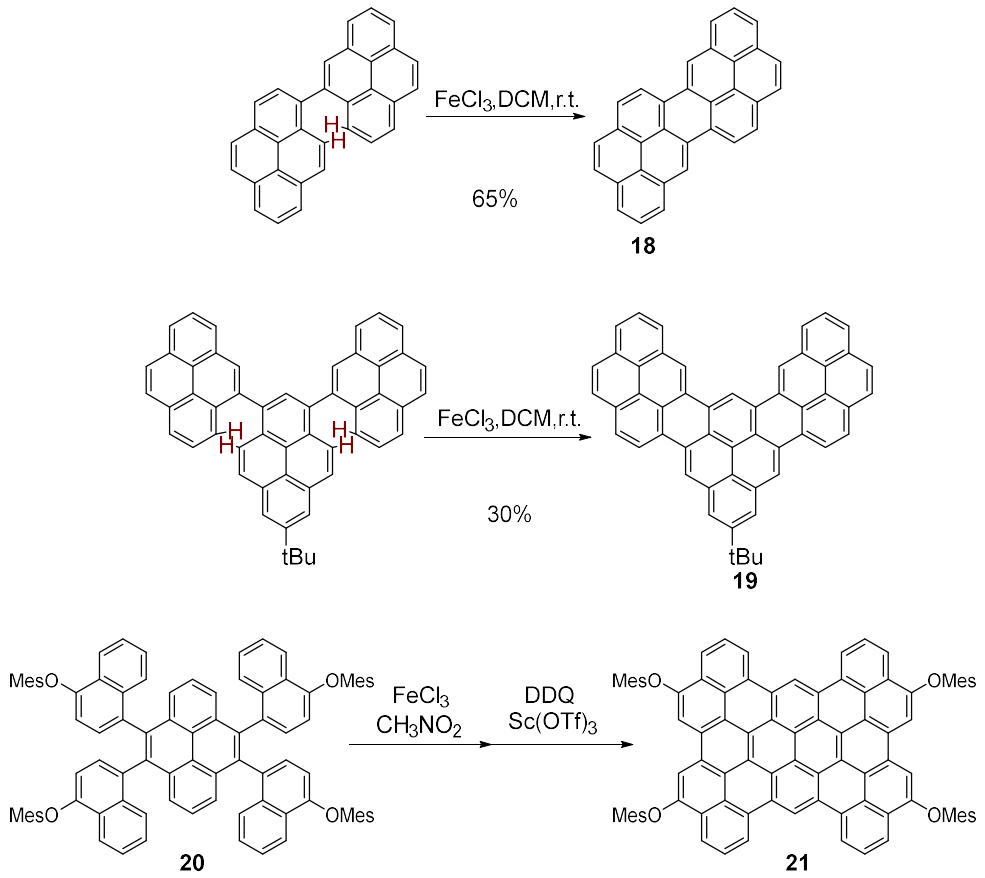

Scheme 11. Oxidative cyclodehydrogenation reactions on substrates with naphthalene structure[53][54]

2.5.2 Oxidation of N6 towards CNB9

To try to make **CNB9**, several reactions with a general procedure as below were carried out. **N6** (~0.5 mg, 4.1×10^{-4} mmol) and DDQ (4 mg, 0.017 mmol) were dissolved in 1 mL toluene. After that, TfOH (0.5 mg, 0.03 mmol) in 0.1 mL toluene was slowly added. The mixture was stirred at 100 ℃ for 11 h. Then the organic layer was separated and the water layer was extracted with DCM. The organic layer was evaporated and checked by MS and TLC. **CNB9** was not detected. The main products were the decomposed species and one compound with m.w 598 which may be assigned as compound **F3.** GPC separation gave a crude product of **F3** which can be detected by APCI MS. The main reason for the results might be that the oxidation potential of **N6** is too high.

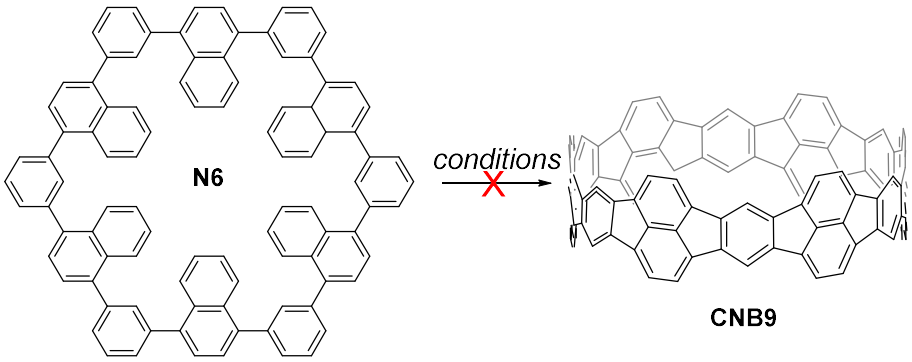

Scheme 10. Oxidation of **N6** towards **CNB9**

Entry	Starting material	Modification	Result	Other
1		DDQ/$Sc(OTf)_3$	×	Starting material
2		DDQ/TfOH	×	Starting material
3	5 mg	$FeCl_3/MeNO_2$	×	Starting material
4		DDQ/TfOH (5 ×)	×	Linear Products (**F3** etc.)

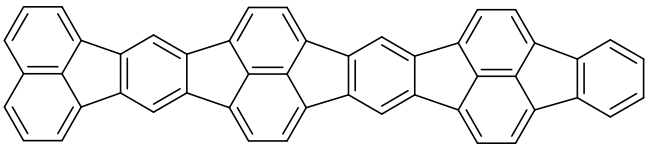

F3
(Speculated structure)

Table 1. Results of oxidation reactions of **N6**

2.6 Synthesis of other *m*-phenalene bridged molecules

2.6.1 Modification of molecular design

The *m*-phenylene bridged cyclic naphthalene hexamer **N6** was designed as a prototype of wheel compounds. Compared with cycloparaphenylenes (CPPs), the *m*-phenylene bridged wheels may have lower intramolecular strain which will make the synthesis much easier.

Based on **N6**, several kinds of derivative wheels could be designed and to be synthesized by similar one-pot coupling reactions (**Figure 25**). The introduction of halogen groups can create the fusion ways through dehydrofluorination or dehydrochlorination, which were explored on making fused oligophenylenes.[55][56]

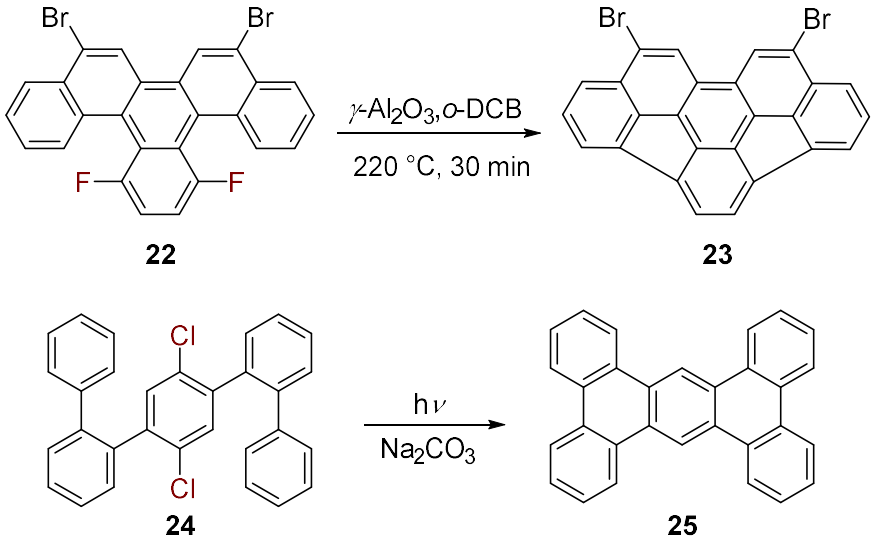

Scheme 12. Dehydrohalogenation reactions[55][56]

F6 is the fluorinated version of **N6** to explore the effects of substituents and also for the next reaction. **A6** is a *m*-phenylene bridged anthracene hexamer. **A6** was designed for strong association with C_{60} in solution with the lager π-planes from anthrylene groups which may have stronger interaction with C_{60}.

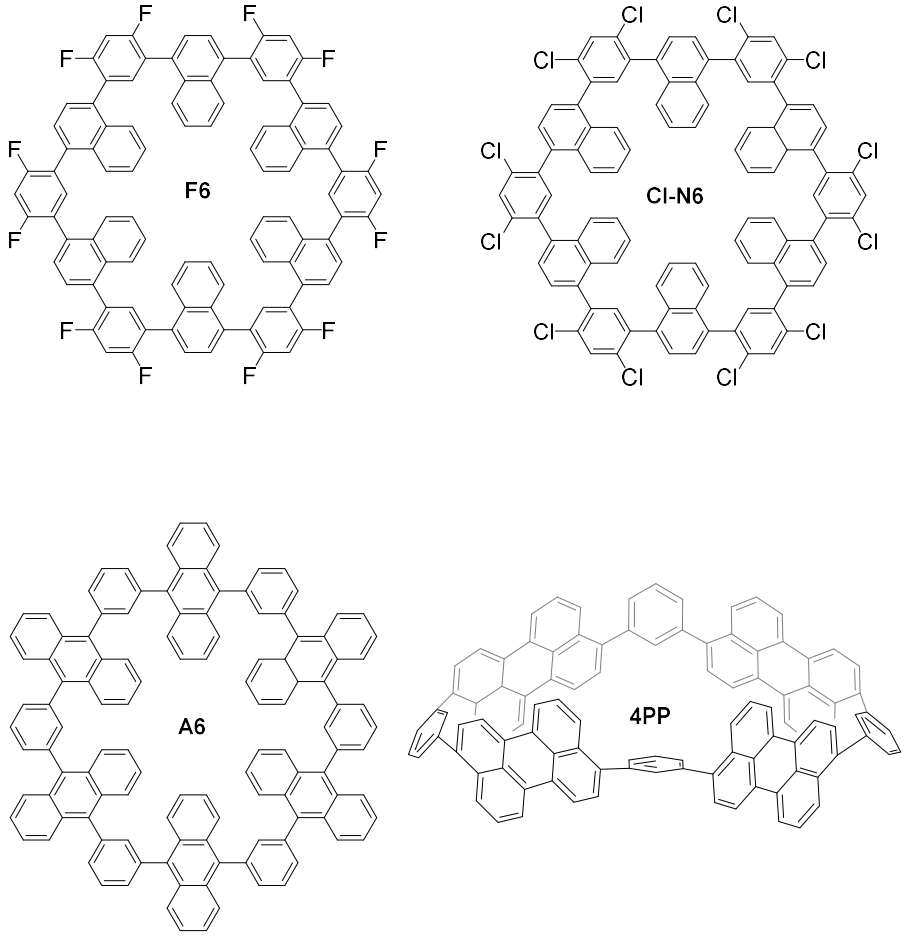

Figure 25. Modified molecular design

2.6.2 Synthesis of fluorinated *m*-phenylene bridged cyclic naphthalene hexamer F6

I ran several one-pot reactions to make **F6** with even exchanging the boryl and bromine groups on the two building units. The one-pot reactions didn't work in this case. The reason might be that the electron withdrawing effect of fluorine groups decreased the reactivity of the diboronicacid ester. Then I checked 4 different combinations on dimer and monomer. The best case is as below. So, it took one more step to prepare the dimer with bromine ends.

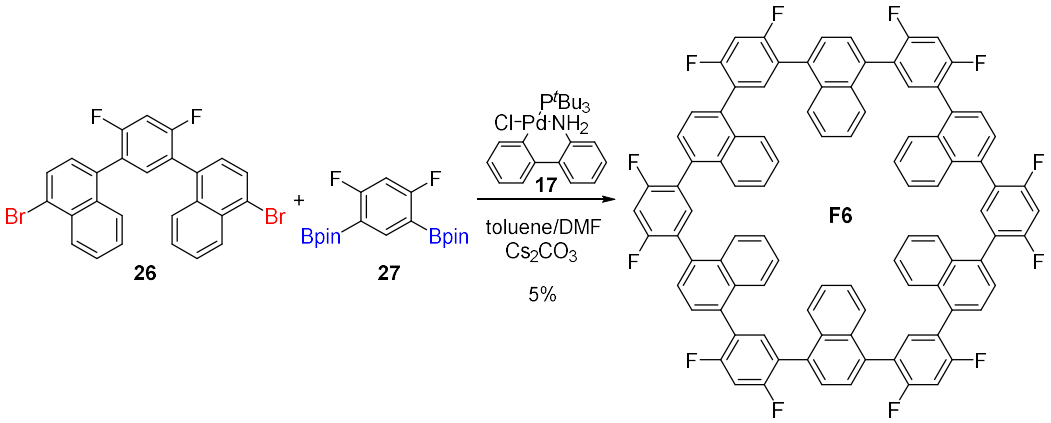

Scheme 13. Synthesis of **F6**.

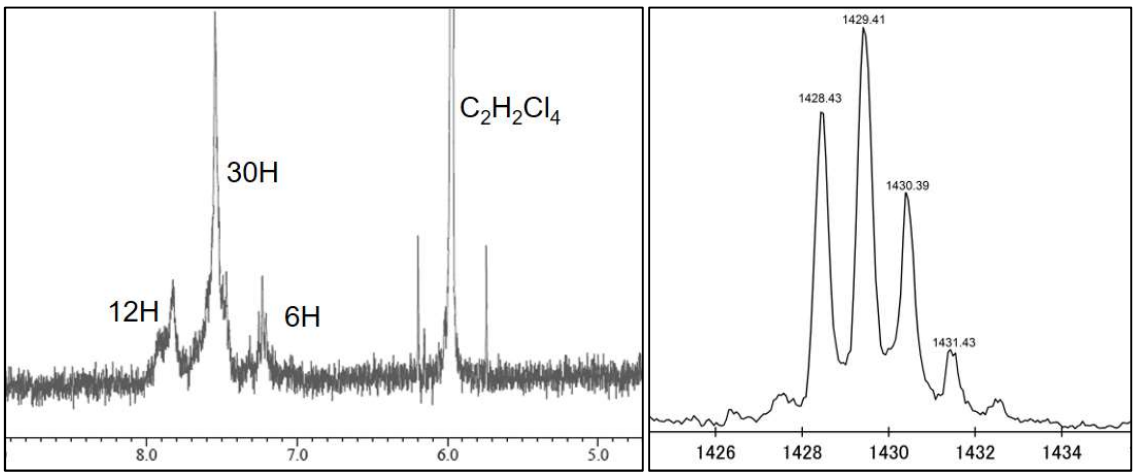

Figure 26. ^{1}H NMR spectrum (400 MHz) in $C_2D_2Cl_4$ at 90 ºC (left) and MALDI-TOF-MS (right) of **F6**.

Limited to experimental conditions, we could not repeat the similar dehydrofluorination reaction in **Scheme 12**, so CNB synthesis from this molecule was suspended.

2.6.3 Synthesis of chlorinated *m*-phenylene bridged cyclic naphthalene hexamer Cl-N6

For the synthesis of chlorinated carbon nanorings, we have proposed the synthesis routes as shown in **Scheme 13**. Unfortunately, none of these routes can successfully give **Cl-N6**. One of the important reasons may be that after introducing two chlorines on the same benzene ring, due to the electron withdrawing effect, the reactivity of the further reaction of this structure is greatly reduced a lot. Especially when introducing the group in the fourth position, it is usually very difficult.

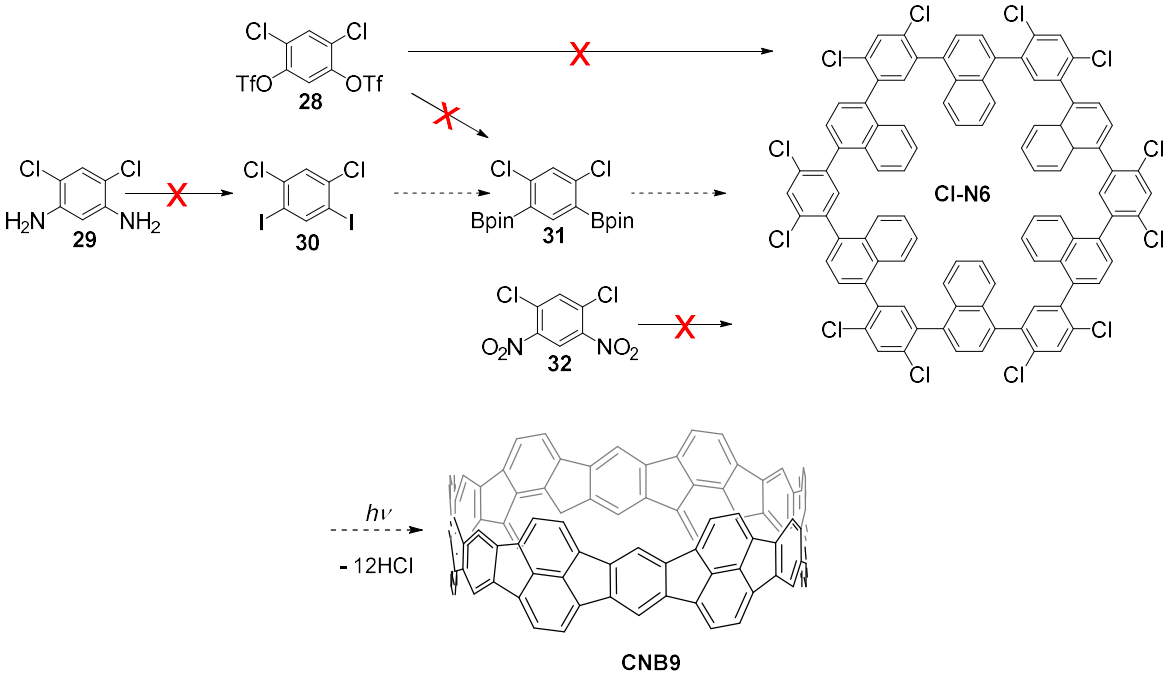

Scheme 13. Proposed synthetic routes of **CNB9** through **Cl-N6**

2.6.4 Synthesis of *m*-phenylene bridged cyclic anthracene hexamer A6

Similar one-pot coupling reaction was carried out between 9,10-dibromoanthracene and 1,3-Benzenediboronic acid bis(pinacol) ester. The signal of target molecule could be detected on MS but the amount of product was too little to be separated. Compared with 1,4-dibromonaphthalene, 9,10-dibromoanthracne has one more benzene ring. This benzene ring may stop the Pd center from moving between the 9 and 10 positions during the reaction. This kind of movement should be better for 1,4-dibromonaphthalene. That should be the reason why it is harder to obtain **A6** than that of **N6**.

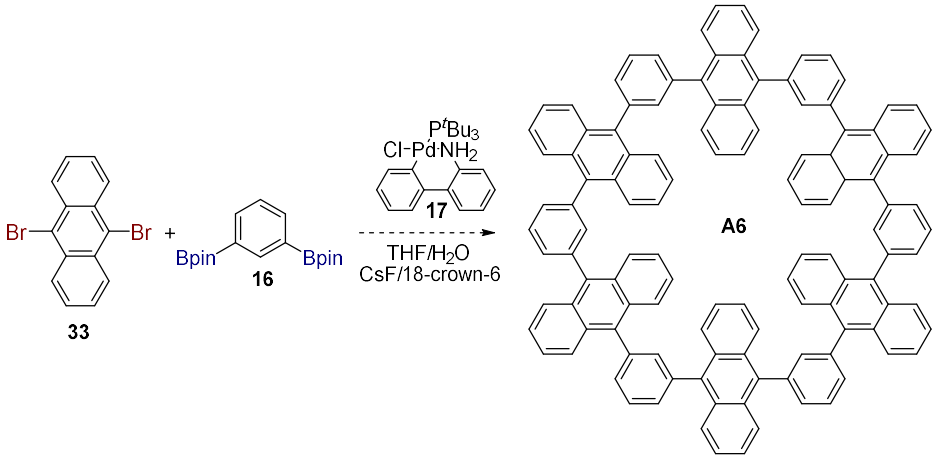

Scheme 14. Synthesis of **A6**.

2.6.5 Synthesis of *m*-phenylene bridged cyclic perylene tetramer

Perylene is an PAH unit which can be treated as one benzene fused two naphthalenes. I've also tried this synthetic route as the beginning of the attempts towards carbon nanorings.

The formation of dimmer could be achieved with 8 equivalent compound **16**. The further cyclization did not work mainly due to the low solubility of the intermediates. Even though the carbon nanoring **4PP** was not obtained, the new compound **35** is possible to be used to make other curved PAH molecules.

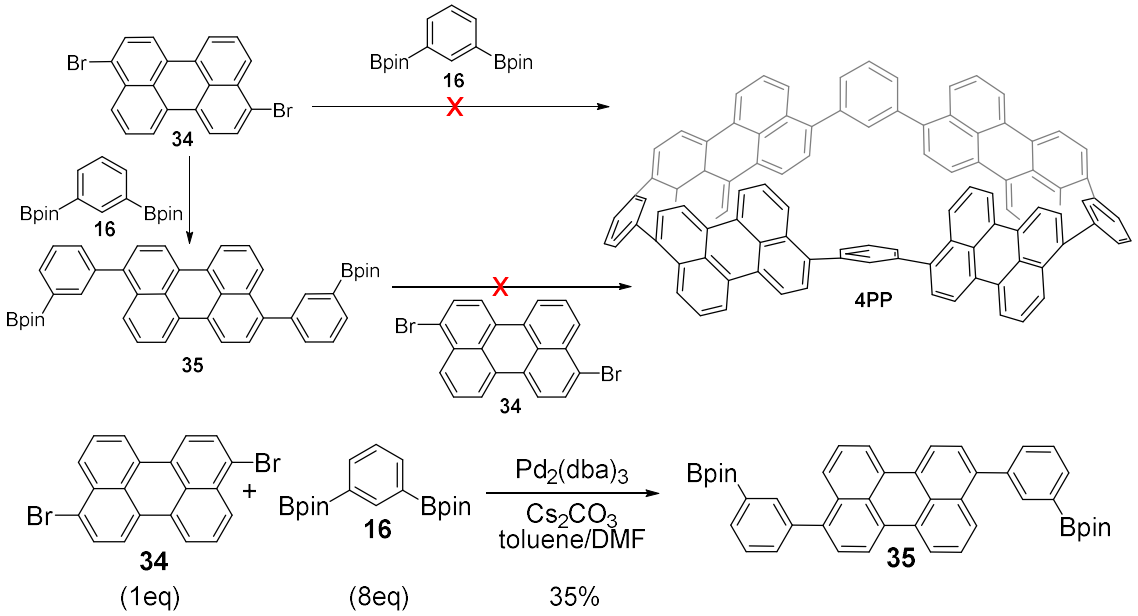

Scheme 15. Synthesis of compounds **35** and **4PP**.

2.7 Conclusions

In summary, 1,3-phenylene-linked cyclic naphthalene hexamer and heptamer were simply constructed by Suzuki–Miyaura cross-coupling reaction via a one-pot route and the hexagonal structure of **N6** was confirmed by X-ray structural analysis. The hexameric wheel **N6** formed co-crystal with C_{60}, C_{70} and was acted as an alignment agent in the solid state. This alignment is promising to lead to good FET properties. The fluorinated wheel **F6** was also achieved by a modified route. The attempts towards anthracene hexamer **A6** were carried out but the low yield made it impossible to be separated. The redox properties of **N6** and optical properties of **N6** and **N7** were explored. This kind of synthetic method of similar wheel molecular was prepared for some more attractive molecules with unique photoelectronic or supramolecular properties as well as precursor molecules of CNB molecules. Synthetic attempts towards 4 other *m*-phenalene bridged cyclic molecules have been made.

Supporting Information

Materials and instrumentation

^{1}H NMR (400 MHz and 600 MHz) and ^{13}C NMR (151 MHz) spectra were recorded with a JEOL JNM-ECX 400, a JEOL JNMECP 400 and a JEOL JNM-ECA 600 spectrometers by using tetramethylsilane as an internal standard. The HR-MALDI-TOF-MS were measured by a Bruker Autoflex II spectrometer using positive ion mode.

UV/Vis absorption spectra were measured with a JASCO UV/Vis/NIR spectrophotometer V-570.

TLC and gravity column chromatography were performed on Art. 5554 (Merck KGaA) plates and silica gel 60N (Kanto Chemical), respectively. All other solvents and chemicals were reagent-grade quality, obtained commercially, and used without further purification. For spectral measurements, spectral-grade solvents were purchased from Nacalai Tesque.

X-ray crystallographic data were recorded at 90 K on a Bruker APEX II X-ray diffractometer equipped with a large area CCD detector by using graphite monochromated Mo-Ka radiation. The structure was solved by using direct methods (SHELXT program).[57] Structure refinements were carried out by using SHELXL-2014/7 program.[58]

DFT calculations (except that using ADF) were performed with a Gaussian 09 program package. The geometries were fully optimized at Becke's three-parameter hybrid functional combined with Lee–Yang–Parr correlation functional abbreviated as B3LYP level of density functional theory. 6-31G(d) bases set implemented was used for structure optimizations and frequency analyses.

Experimental Section

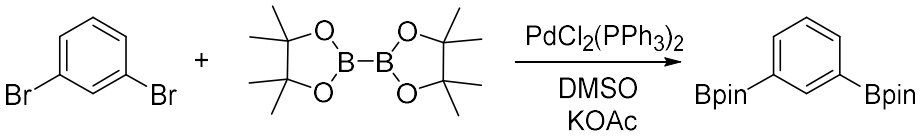

Compound 16:[60] To a 20 mL DMSO solution of 1,3-dibromobenzene (1.0 g, 4.24 mmol) was added bispinacolatodiboron (2.4 g, 9.33 mmol), KOAc (2.1 g, 21.19 mmol) and $PdCl_2(PPh_3)_2$ (149 mg, 0.21 mmol), and the solution was stirred at 80 ℃ for 24 h. After the reaction mixture was cooled to room temperature, the mixture was extracted with ether (100 mL in total) for three times and washed with de-ionized water for twice. The organic layer was dried over Na_2SO_4, concentrated and purified by column chromatography (hexane: EtOAc = 19:1) on silica gel to give benzene-1,3-diboronate (1.2 g, 83%). ^{1}H NMR (400 MHz, $CDCl_3$) δ = 8.27 (s, 1 H), 7.89 (dd, J1 = 7.2 Hz, J2 = 1.2 Hz, 2 H), 7.36 (dt, J1 = 7.2 Hz, J2 = 1.2 Hz 1 H,) 1.34 (s, 24 H).

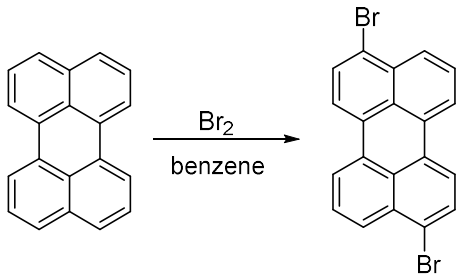

Compound 34:[61] Perylene (2.0 g, 7.49 mmol) was dissolved in benzene (330 mL) at 80℃, then Br_2 (1 mL, 19.3 mmol) was slowly added for 30 min. The mixture was kept at 50℃ and stirred overnight. The mixture was cooled and precipitates were separated. Then the crude products were being recrystallized using aniline-nitrobenzene (v: v = 1:1) for five time. 573 mg purified compound **34** was gained with yield 17.6%.^{1}H NMR (400

MHz, $CDCl_3$) δ = 8.25 (d, J = 7.4 Hz, 2H), 8.14 (d, J = 8.0 Hz, 2H), 8.05 (d, J = 8.0 Hz, 2H), 7.80 (d, J = 8.0 Hz, 2H), 7.61 ppm (t, J = 8.0 Hz, 2H).

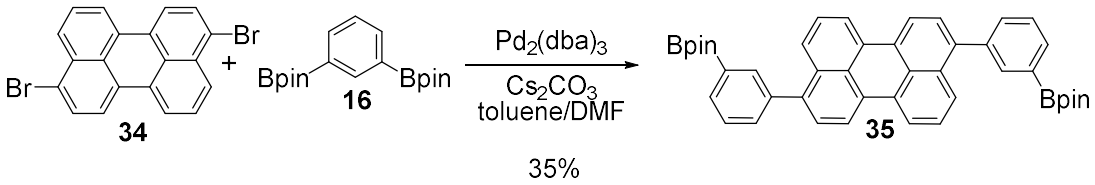

Compound 35: 3,9-Dibromoperylene (50 mg, 0.122 mmol), 1,3-phenyldiboronic acid bis(pinacol) ester (322 mg 0.975 mmol) and Cs_2CO_3 (119 mg, 0.366 mmol) were added to 15 mL mixture solvent (toluene/DMF=2:1). After freezing degassing, $Pd_2(dba)_3$ (22 mg, 0.0244 mmol) was added. Then the mixture was heated at 100℃ overnight. Then after extracted with $CHCl_3$ and washed with water, the organic layer was concentrated. The mixture was purified first by chromatography on silica gel (Hexane: chloroform = 3:1, 1:3 and chloroform: EtOAc = 1:1). After purified by GPC, 28 mg compound **35** was gained with a yield 35%.^{1}H NMR (500 MHz, $CDCl_3$): δ = 8.25 (d, J = 7.8 Hz, 4H), 7.98 (s, 2H), 7.90 (d, J = 7.4 Hz, 2H), 7.74 (d, J = 8.2 Hz, 2H), 7.64 (d, J = 7.4 Hz, 2H), 7.52 (t, J = 7.3 Hz, 2H), 7.46 (d, J = 7.8 Hz, 2H), 7.46 (t, J = 8.2 Hz, 2H), 1.25 (s, 24H) ppm

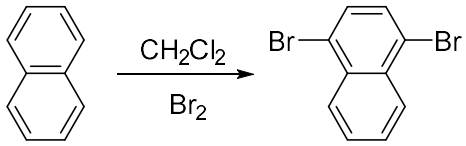

1,4- dibromonaphthalene: A stirred solution of naphthalene (8.97 g, 69.7 mmol) in dichloromethane (70 mL) was cooled to −30 ℃, and then bromine (33.6 g, 10.8 mL, 210

mmol) which had been dissolved in 30 mL dichloromethane was added drop-wise over 10 min in the dark while maintaining the temperature at −30 ℃ with constant magnetic stirring. The mixture was then stirred for 20 h in the dark at −25 ℃. At this point, the excess of bromine was quenched with an aqueous solution of $NaHSO_3$. The organic layer was separated and further washed with aqueous solutions of $NaHSO_3$, water and brine. The organic layer was dried over anhydrous Na_2SO_4 and concentrated to dryness to afford the crude compound, which was further purified by silica gel chromatography using hexane as eluent. Finally, it was purified by recrystallization with MeOH as solvent. 10.1 g 1,4-dibromonaphthatlene was gained with yield 51%. ^{1}H NMR (400 MHz, $CDCl_3$): δ 8.25 (dd, J = 6.5, 3.3 Hz, 2H), 7.65 (dd, J = 6.4, 3.3 Hz, 2H), 7.63 (s, 2H) ppm

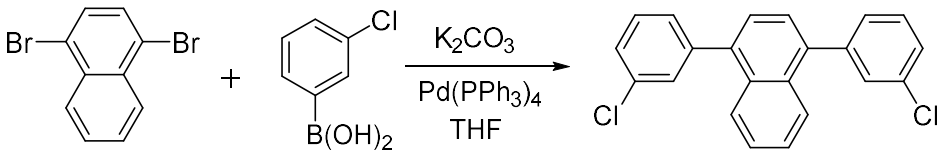

DCPN: A mixture of 1,4-dibromonaphthalene (286 mg, 1.00 mmol), 3-chlorophenylboronic acid (352 mg, 2.24 mmol), potassium carbonate (346 mg, 2.50 mmol), water (2 mL) and THF (16 mL) in a 50 mL two-necked round bottom flask was sealed with septa and deoxygen by bubbling with nitrogen gas for 40 minutes. Afterwards tetrakis(triphenylphosphine)- palladium (30 mg, 0.022 mmol) was quickly added into the mixture by opening the septum, and the mixture was deoxygen for additional 10 minutes. The reaction was kept at 80 ℃ under a nitrogen atmosphere for 22 hours. After cooled down to room temperature, the reaction was extracted with ethylacetate and water for three times. The organic layer was collected, and the solvent was removed by a rotary evaporator. The residue was purified by silica gel chromatography with hexane and

dichloromethane (15:1) as the elute to afford a ropy white solid. 346 mg compound **DCPN** was gained with yield 99%. ^{1}H NMR (400 MHz, $CDCl_3$): δ = 7.98 (dd, J = 6.6, 3.3 Hz, 2H), 7.57 (s, 2H), 7.51 (dd, J = 6.7, 3.3 Hz, 2H), 7.48-7.43 (8H). ^{13}C NMR (400 MHz, $CDCl_3$): δ = 142.57, 138.96, 134.40, 131.82, 130.26, 129.75, 128.48, 127.70, 126.58, 126.50 and 126.27 ppm.

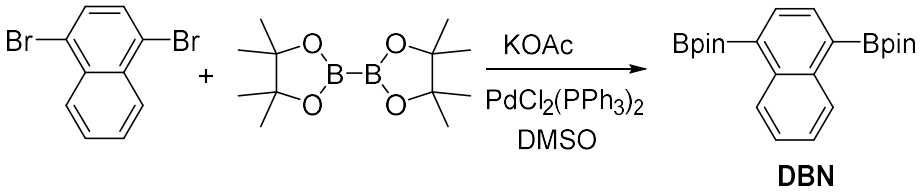

DBN

Synthesis of compound DBN:[64] To a 20 mL DMSO solution of 1,4-dibromonaphthalene (300 mg, 1.06 mmol) was added bispinacolatodiboron (600 mg, 2.36 mmol), potassium acetate (500 mg, 1.06 mmol) and $PdCl_2(PPh_3)_2$ (37 mg, 0.11 mmol), and the solution was stirred at 85 ℃ for 24 h. After the reaction mixture was cooled to room temperature, the mixture was extracted with diethyl ether (100 mL in total) for three times and washed with de-ionized water for twice. The mixture was then separated by recrystallization. After filtration, 273 mg **compound DBN** gained with yield 68%.^{1}H NMR (400 MHz, $CDCl_3$) δ = 8.76-8.74 (m, 2H), 8.02 (s, 2H), 7.53-7.50 (m, 2H), 1.43 (s, 24H).

1,3-Phenylene-bridged cyclic naphthalene hexamer N6:

Step-wise from compound **DCPN**. Compound **DCPN** (158 mg, 0.452 mmol), 1,4-dibromonaphthalene (206 mg, 0.543 mmol), K_3PO_4 (385 mg, 1.81 mmol) dissolved in H_2O (4 mL) and dried THF (6 mL) was added to a 30 mL 3-neck flask. After degassed, chloro[(tri-*tert*-butylphosphine)-2-(2-aminobiphenyl)] palladium (II) (12 mg, 0.013 mmol) was quickly added. After degassing again, the solution was stirred at room temperature for 20 h. Then the mixture was extracted with dichloromethane and washed with water and brine. The organic layer was dried over Na_2SO_4 and concentrated. Then chromatography on silica gel (hexane:CH_2Cl_2 = 3:1) was used to get a crude product which was further separated on GPC. 1 mg **N6** was gained with yield 1%.

One-pot, toluene system: 1,3-Benzenediboronic acid bis(pinacol) ester (115 mg, 0.350 mmol), 1,4-dibromonaphthalene (100 mg, 0.350 mmol), Cs_2CO_3 (325 mg, 1.40 mmol), toluene (5 mL) and DMF (2 mL) were added into a 25 mL 2-neck flask. After degassing, chloro[(tri-*tert*-butylphosphine)-2-(2-aminobiphenyl)] palladium (II) (36 mg, 0.070 mmol) was quickly added under flowing argon. After degassing again, the solution was stirred at 80°C for 24 h. The mixture was extracted with dichloromethane and washed with water and brine. Then it was purified by chromatography on silica gel (hexane: dichloromethane = 3:1). After being purified by a preparative GPC, 4.0 mg of **N6** was gained in 6% yield as a white solid. ^{1}H NMR ($C_2D_2Cl_4$, 600 MHz, ppm, 60 ˚C) δ = 7.47 (q, J = 9.6 Hz, 12H), 7.56 (s, 12H), 7.66–7.67 (m, 24H) and 8.10 (q, J = 9.6 Hz, 12H). ^{13}C NMR ($C_2D_2Cl_4$, 151 MHz, ppm, 60 ˚C) δ 126.14, 126.60, 126.71, 128.31, 129.09, 132.05, 132.22, 139.83 and 141.01.

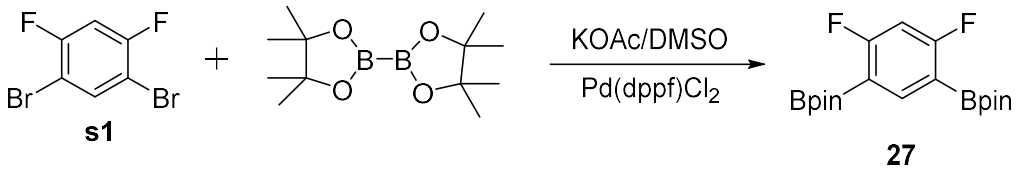

Compound 27:[63] To a 10 mL DMSO solution of compound **s1** (300 mg, 1.10 mmol) was added bispinacolatodiboron(618 mg, 3.42 mmol), KOAc (540 mg, 5.52 mmol) and $Pd(dppf)Cl_2$ (60 mg, 0.056 mmol), and the solution was stirred at 80 ℃ for 5 h. After the reaction mixture was cooled to room temperature, the mixture was extracted with EtOAc for three times and washed with deionized water for twice. The organic layer was dried over Na_2SO_4, concentrated and purified by column chromatography on silica gel. 298 mg of compound **27** was gained with yield 74%.^{1}H NMR ($CDCl_3$, 400MHz) δ = 8.35 (d, J = 8.7, 2H), 7.86 (dd, J = 7.8, 2.3, 2H), 7.77 (dd, J = 11.4, 3.2, 2H), 7.66 (td, J = 6.8, 3.2, 2H), 7.57 (td, J = 7.3, 5.5, 2H), 7.42 (t, J = 7.8, 1H) , 7.34 (d, J = 7.8, 2H) , 7.15 (t, J = 9.1, 1H) ppm.

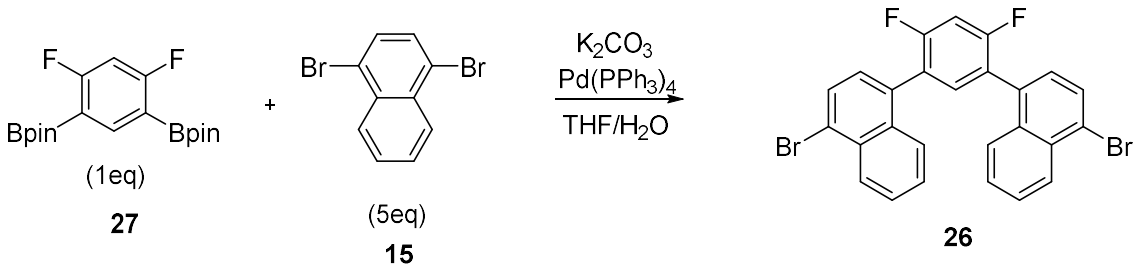

Compound 26: Compound **27** (184 mg, 0.500 mmol) compound **15** (858 mg, 3.00 mmol), K_2CO_3 (346 mg, 2.50 mmol), dry THF (30 mL) and H_2O (2 mL) was added to a 50 mL 3-neck flask. After being degassed, $Pd(PPh_3)_4$ (29 mg, 2.50×10^{-2} mmol) was quickly added. After being degassed again, the solution was stirred at 85 ºC for 8 h. The mixture was extracted with CH_2Cl_2 and washed with H_2O and brine. Chromatography on silica gel (from hexane to hexane: CH_2Cl_2=7:1) gave 96 mg compound **26** with yield 36.4%. ^{1}H NMR ($CDCl_3$, 400MHz) δ = 1.33 (s, 24H), 6.71 (t, J = 9.9, 1H), 8.11 (t, J = 7.7, 1H) ppm.

1,3-Phenylene-bridged naphthalene heptamer N7:

1,3-Benzenediboronic acid bis(pinacol) ester (90 mg, 0.269 mmol), 1,4-dibromonaphthalene (100 mg, 0.350 mmol), CsF (184 mg, 1.21 mmol), 18-crown-6 (310 mg, 2.42 mmol), THF (10 mL) and deionized water (0.3 mL) was added to a 30 mL Schlenk flask. After degassing, chloro[(tri-*tert*-butylphosphine)-2-(2-aminobiphenyl)] palladium (II) (14 mg, 0.027 mmol) was quickly added. After degassing again, the solution was stirred at r.t. for 24 h. The mixture was extracted with dichloromethane and washed with water and brine. Then it was purified by chromatography on silica gel (hexane: CH_2Cl_2 = 3:1). After being purified by GPC, 7.0 mg of **N7** was gained in 13% yield and 2.0 mg of **N6** in 4% yield.

^{1}H NMR ($C_2D_2Cl_4$, 400 MHz, 120 ˚C) δ = 7.49 (m, 14H), 7.59 (s, 7H), 7.61 (d, 7H), 7.66 (d, 21H), 7.75 (d, 7H) and 8.13 (m, 14H) ppm. ^{13}C NMR ($C^2D^2Cl^4$, 151 MHz, 120 ˚C) δ

120.46, 125.92, 125.93, 126.50, 126.66, 128.24, 129.28, 131.60, 132.30, 139.85 and 141.08 ppm.

F6: Compound **26** (130 mg, 0.248 mmol), compound **27** (91 mg, 0.248 mmol), Cs_2CO_3 (404 mg, 1.24 mmol), toluene (5 mL) and DMF (2 mL) was added to a 25 mL Schlenk flask. After degassing, chloro[(tri-*tert*-butylphosphine)-2-(2-aminobiphenyl)] palladium (II) (25 mg, 0.050 mmol) was quickly added. After degassing again, the solution was stirred at r.t. for 24 h. The mixture was extracted with dichloromethane and washed with water and brine. Then it was purified by chromatography on silica gel (hexane: CH_2Cl_2 = 4:5). After being purified by GPC, 6.0 mg of **F6** was gained in a 5% yield. Finally, **F6** was confirmed by the ^{1}H NMR spectrum and HR-MALDI-TOF-MS. The ^{1}H NMR showed broad and complicated peaks until being heated to 90 ºC and hard to be assigned clearly.

A6: 1,3-Benzenediboronic acid bis(pinacol) ester (115 mg, 0.350 mmol), 9,10-dibromoanthracene (100 mg, 0.350 mmol), CsF (184 mg, 1.21 mmol), 18-crown-6 (310 mg, 2.42 mmol), THF (10 mL) and deionized water (0.3 mL) was added to a 30 mL Schlenk flask. After degassing, chloro[(tri-*tert*-butylphosphine)-2-(2-aminobiphenyl)] palladium (II) (14 mg, 0.027 mmol) was quickly added. After degassing again, the solution was stirred at r.t. for 24 h. The mixture was extracted with dichloromethane and washed with water and brine. **A6** was detected by MALDI-TOF-MS in the mixture but was not separated successfully.

NMR

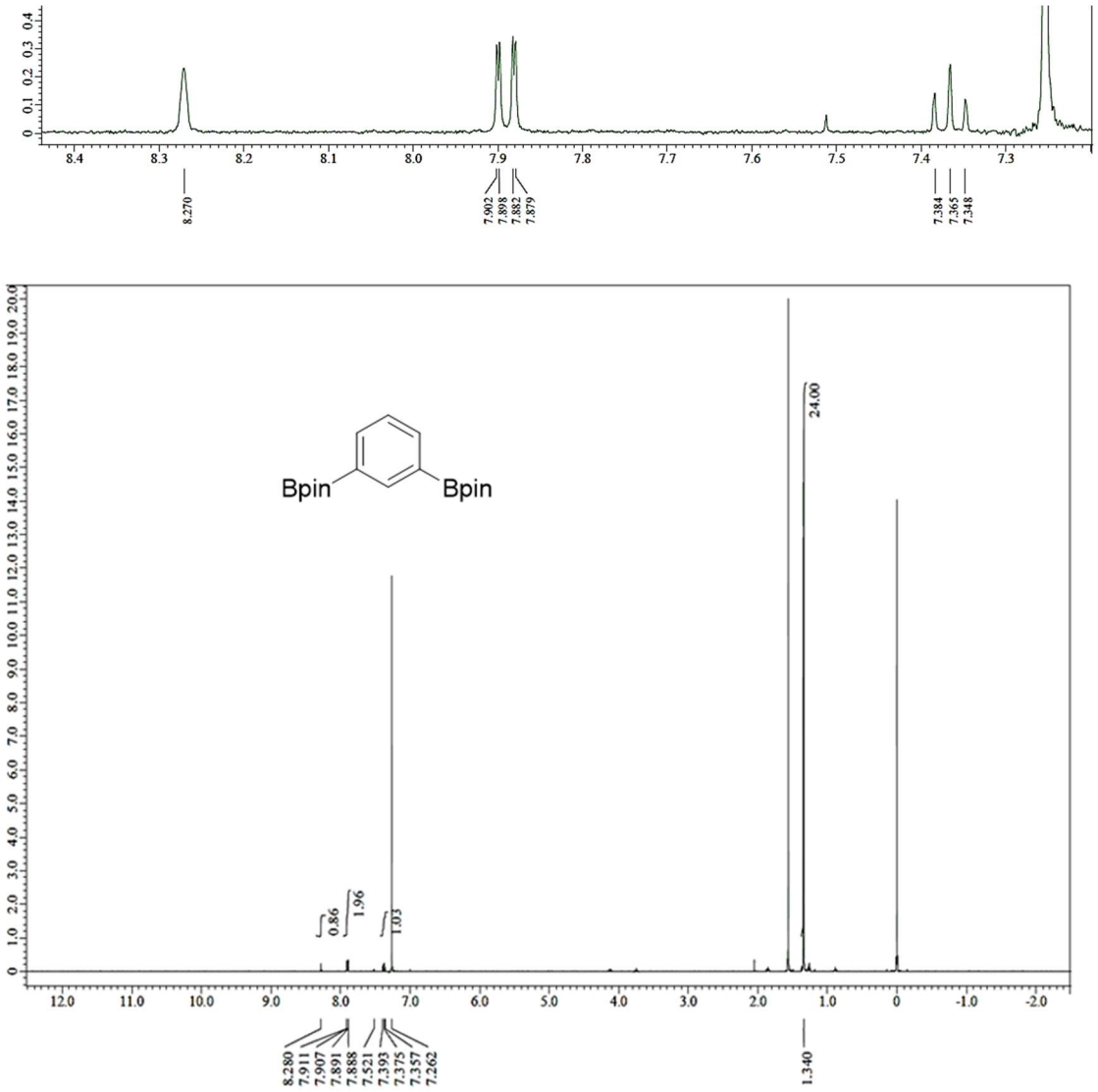

S2.1 ^{1}H NMR (400 MHz) of compound **16** in $CDCl_3$

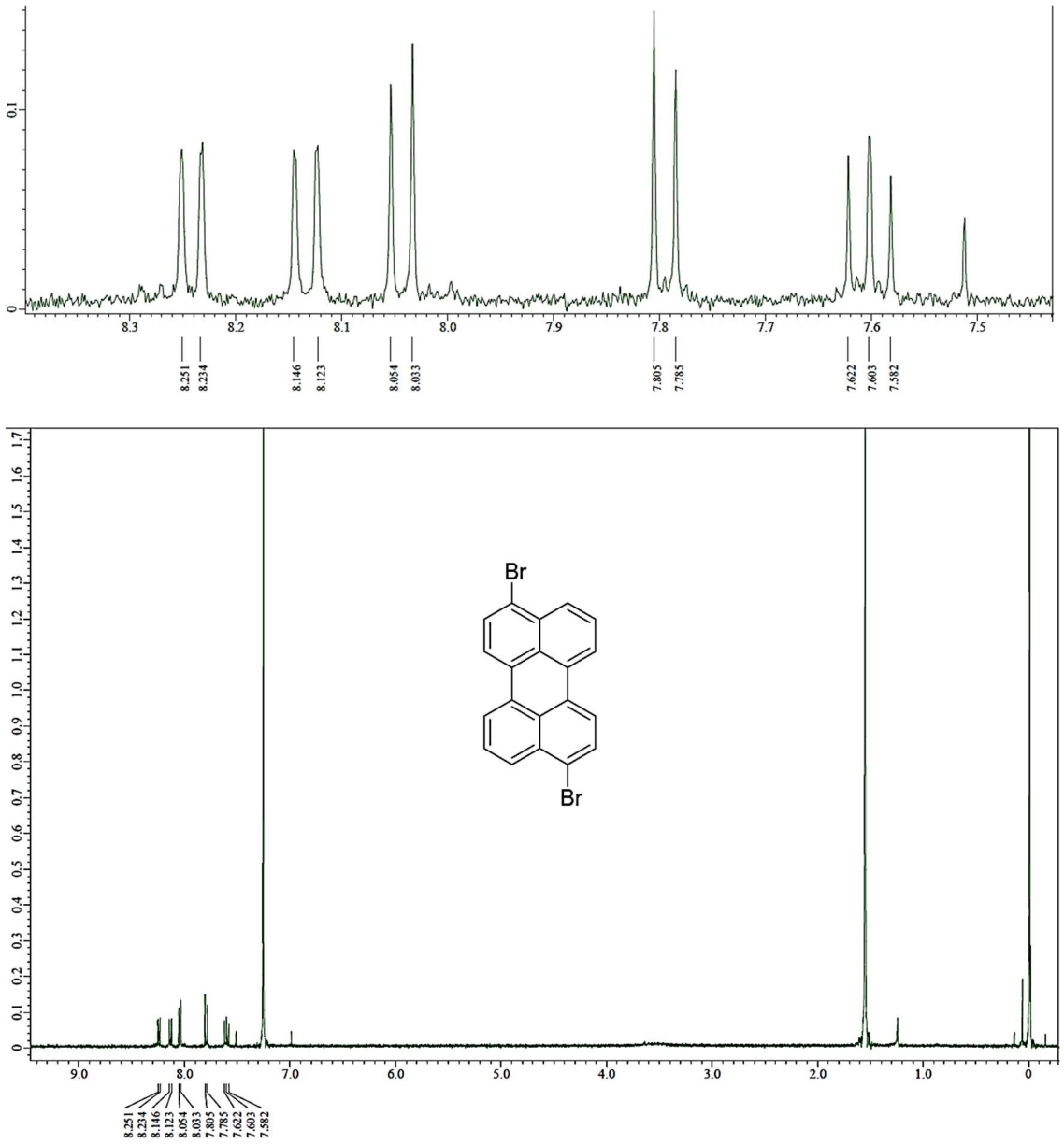

S2.2 ^{1}H NMR (400 MHz) of compound **34** in $CDCl_3$

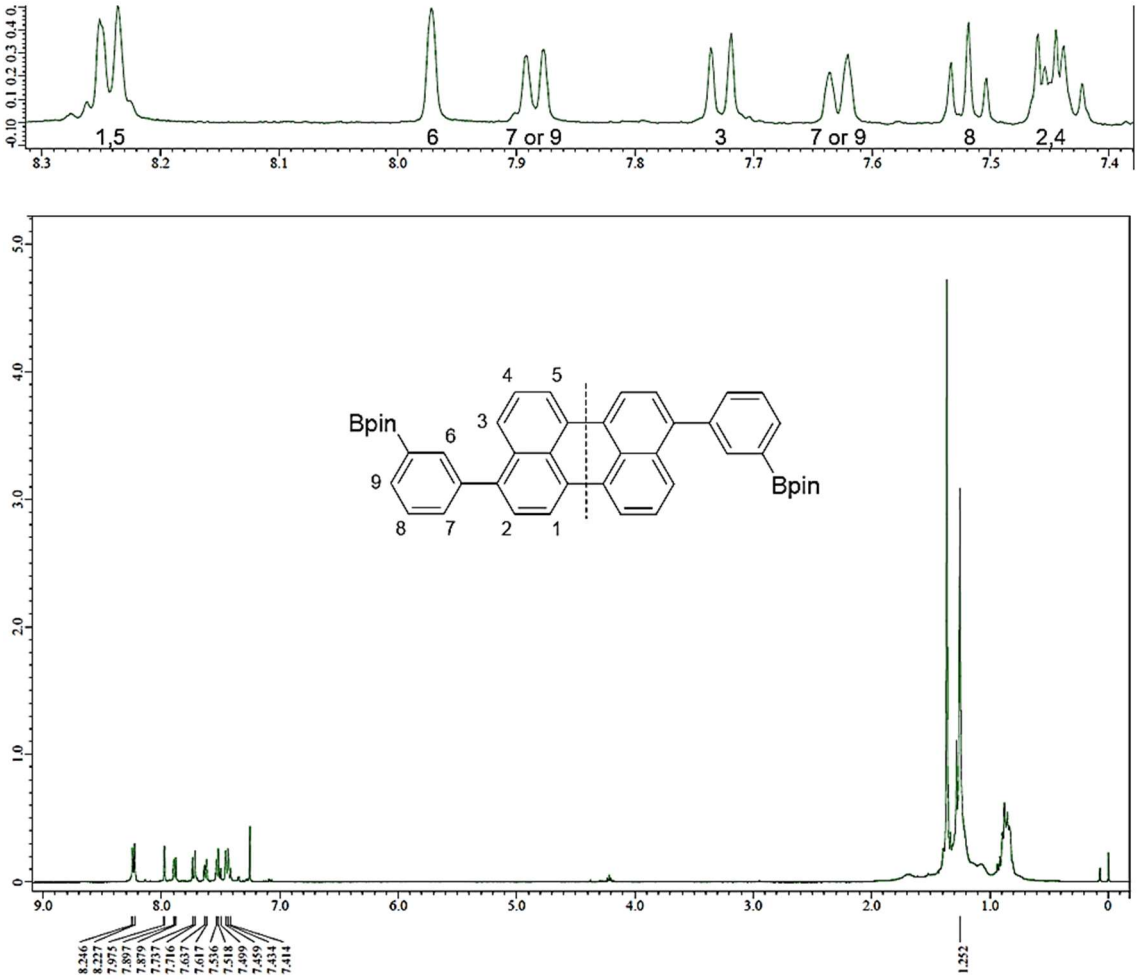

S2.3 ^{1}H NMR (500 MHz) compound **35** in $CDCl_3$

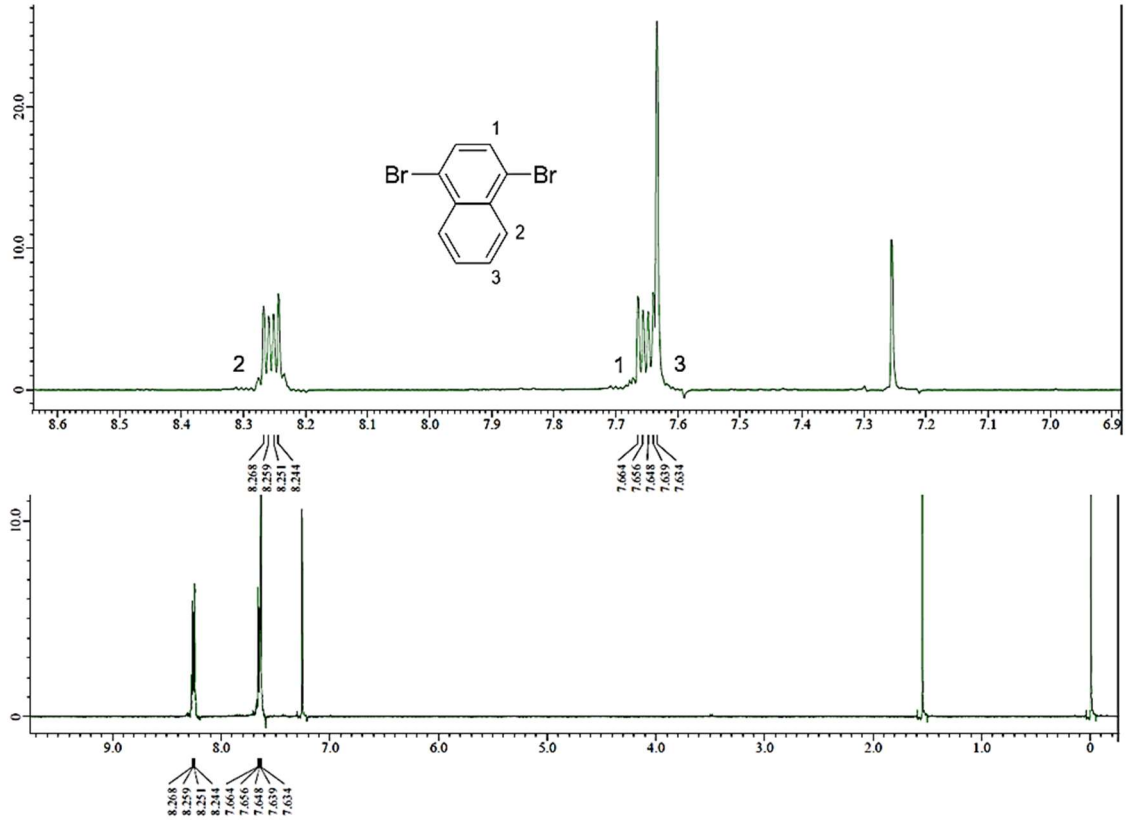

S2.4 ^{1}H NMR (400 MHz) of 1,4-dibromonaphthalene in $CDCl_3$

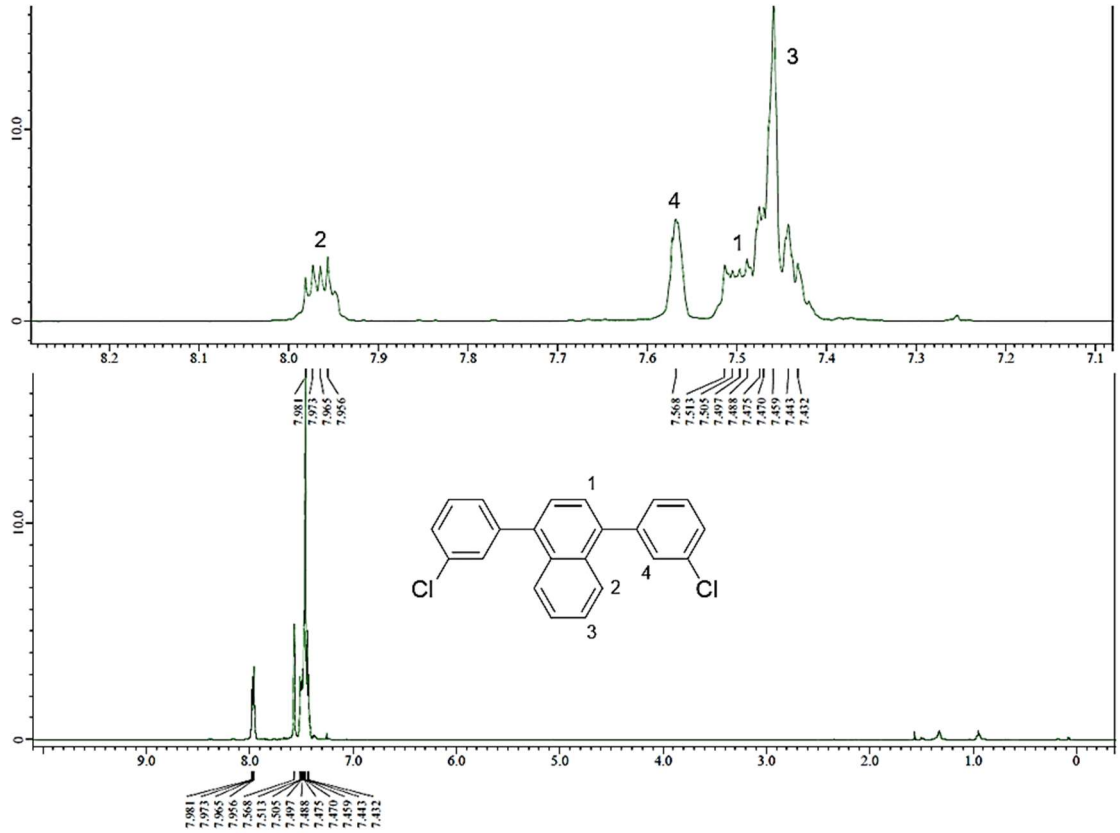

S2.5 ^{1}H NMR (400 MHz) of compound **DCPN** in $CDCl_3$

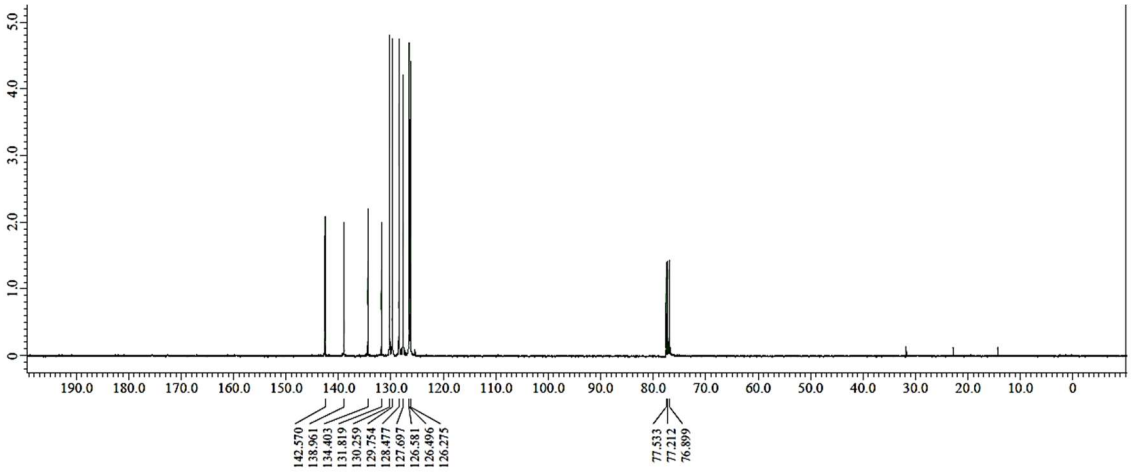

S2.6 ^{13}C NMR (400 MHz) of compound **DCPN** in $CDCl_3$

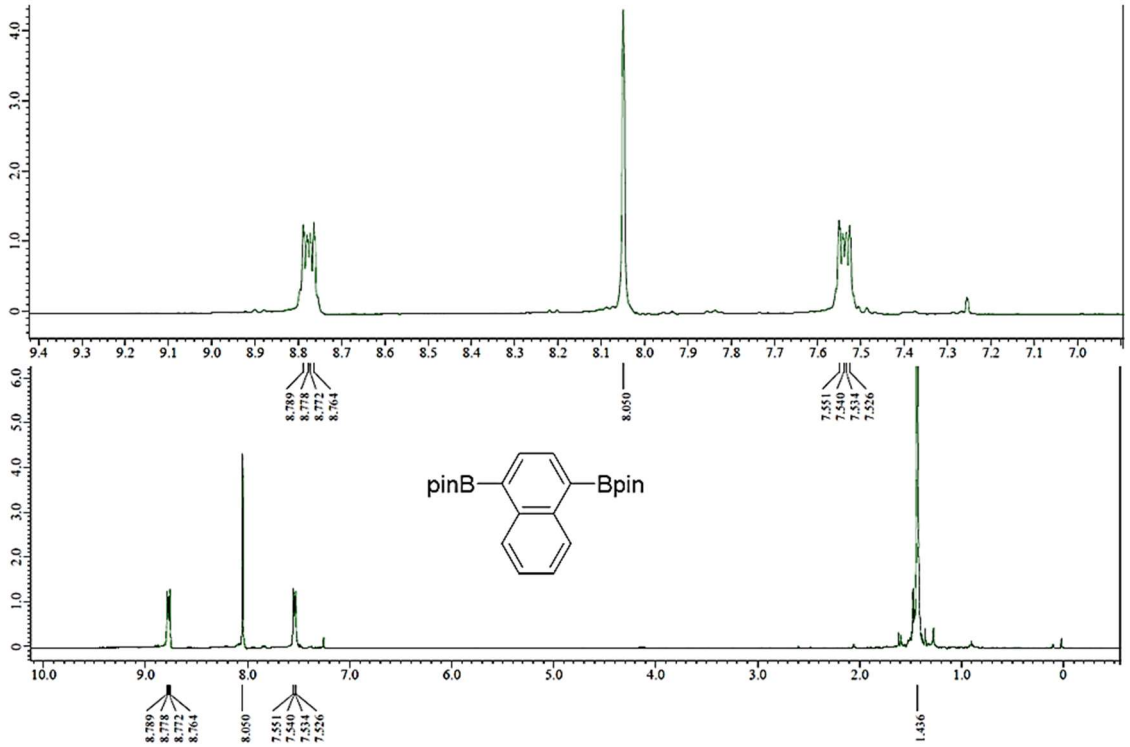

S2.7 ^{1}H NMR (400 MHz) of compound **DBN** in $CDCl_3$

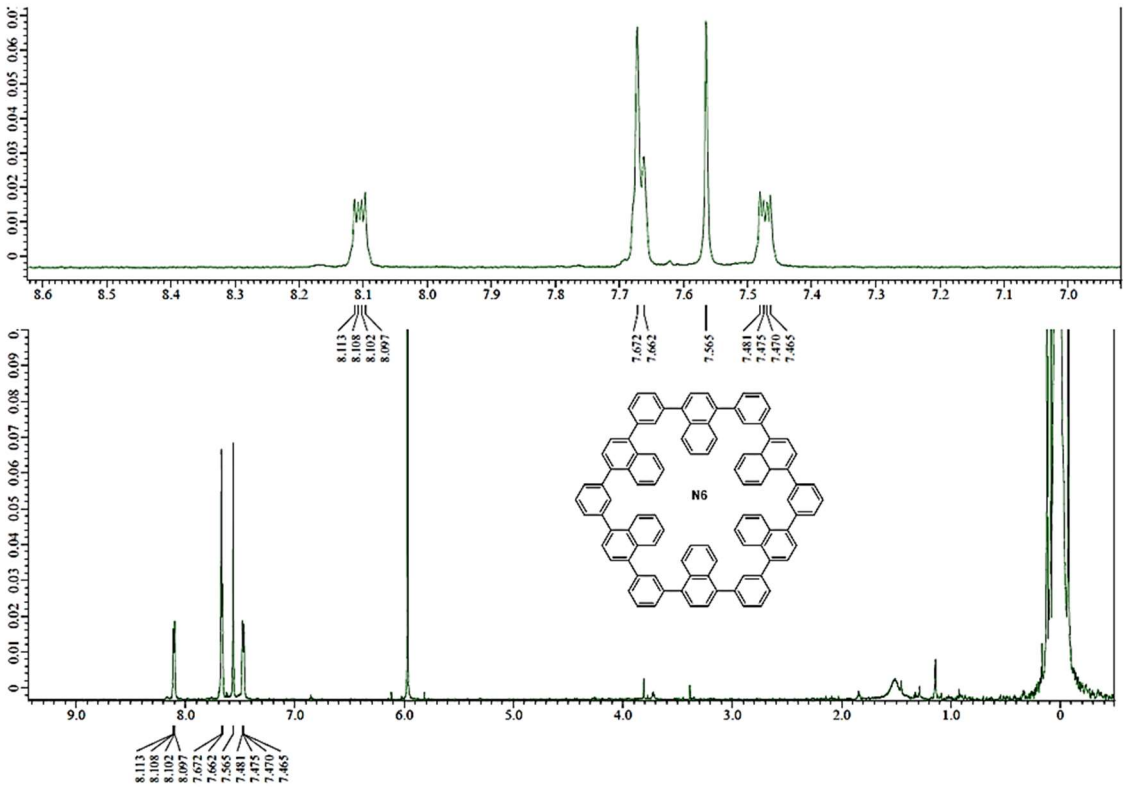

S2.8 ^{1}H NMR (600MHz, 60℃) of **N6** in $C_2D_2Cl_4$

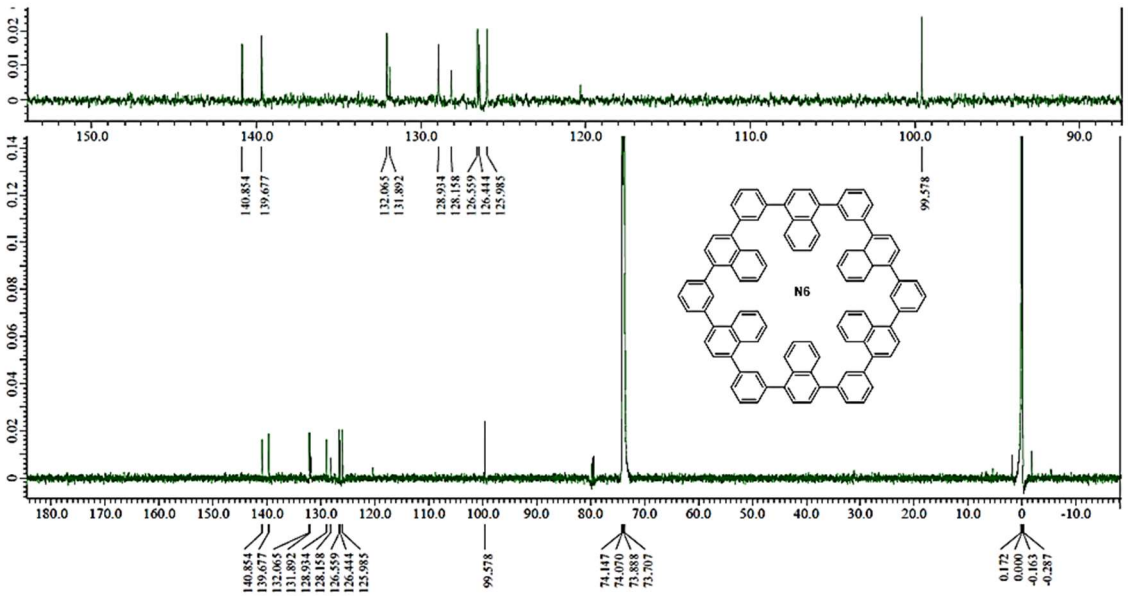

S2.9 ^{13}C NMR spectrum (600MHz, 60℃) of **N6** in $C_2D_2Cl_4$

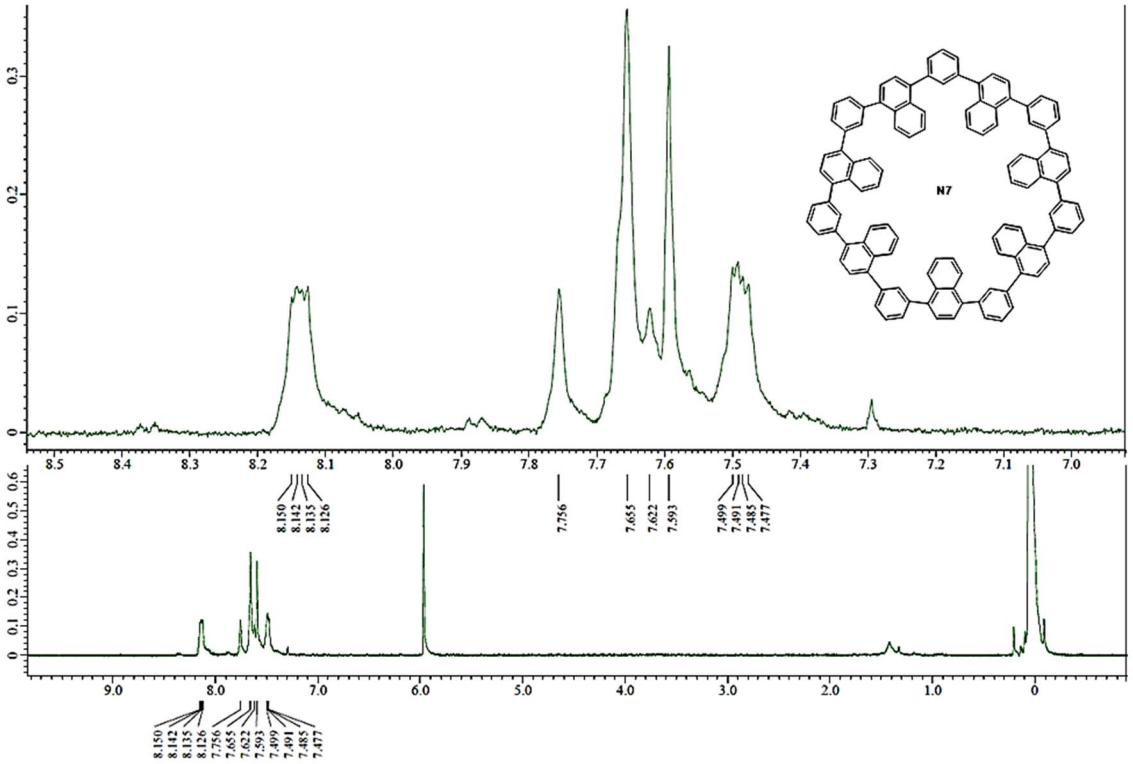

S2.10 ^{1}H NMR spectrum (400MHz, 120℃) of **N7** in $C_2D_2Cl_4$

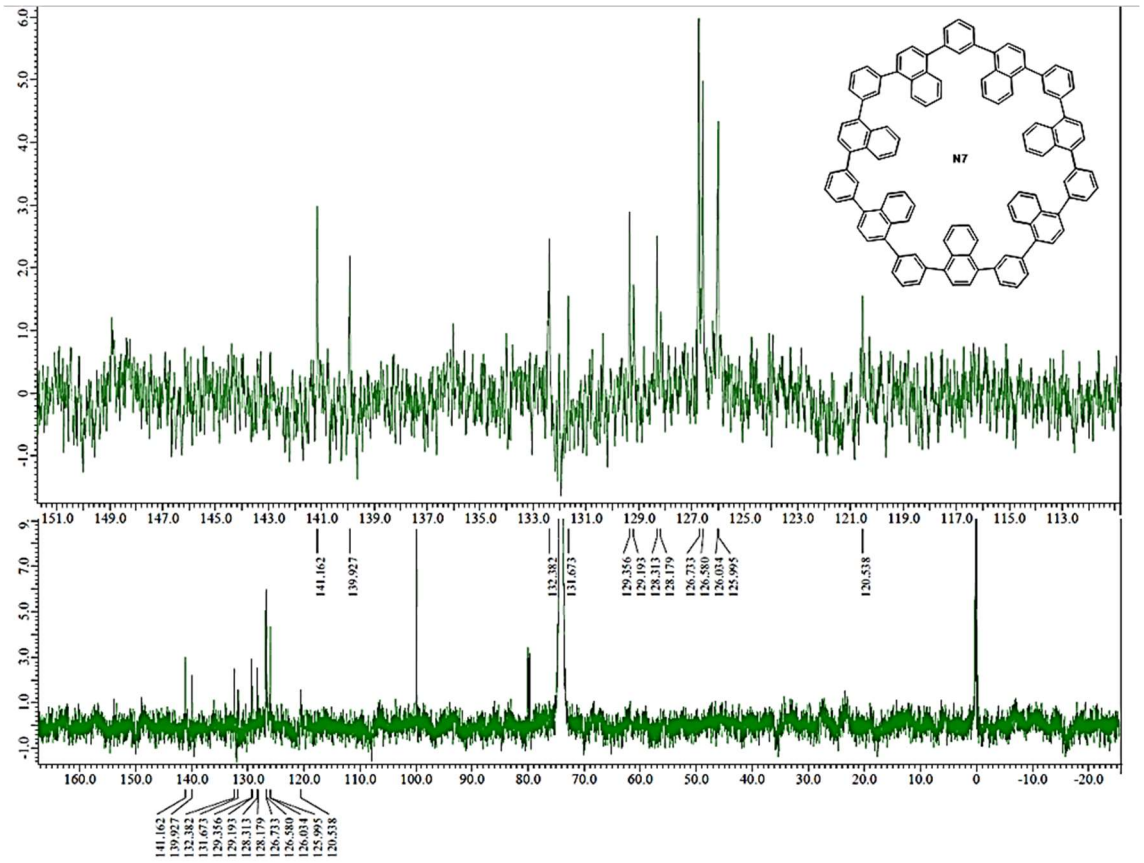

S2.11 ^{13}C NMR spectrum (400MHz, 120℃) of **N7** in $C_2D_2Cl_4$

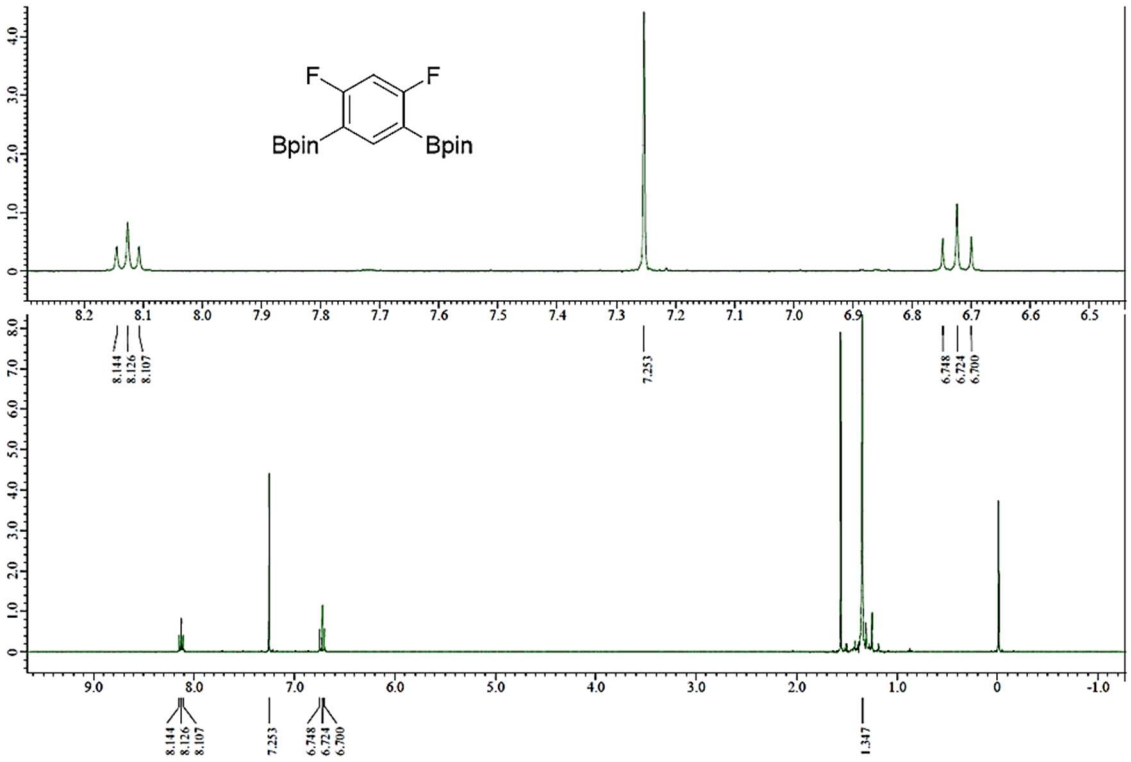

S2.12 ^{1}H NMR spectrum (400MHz) of compound **27** in $CDCl_3$

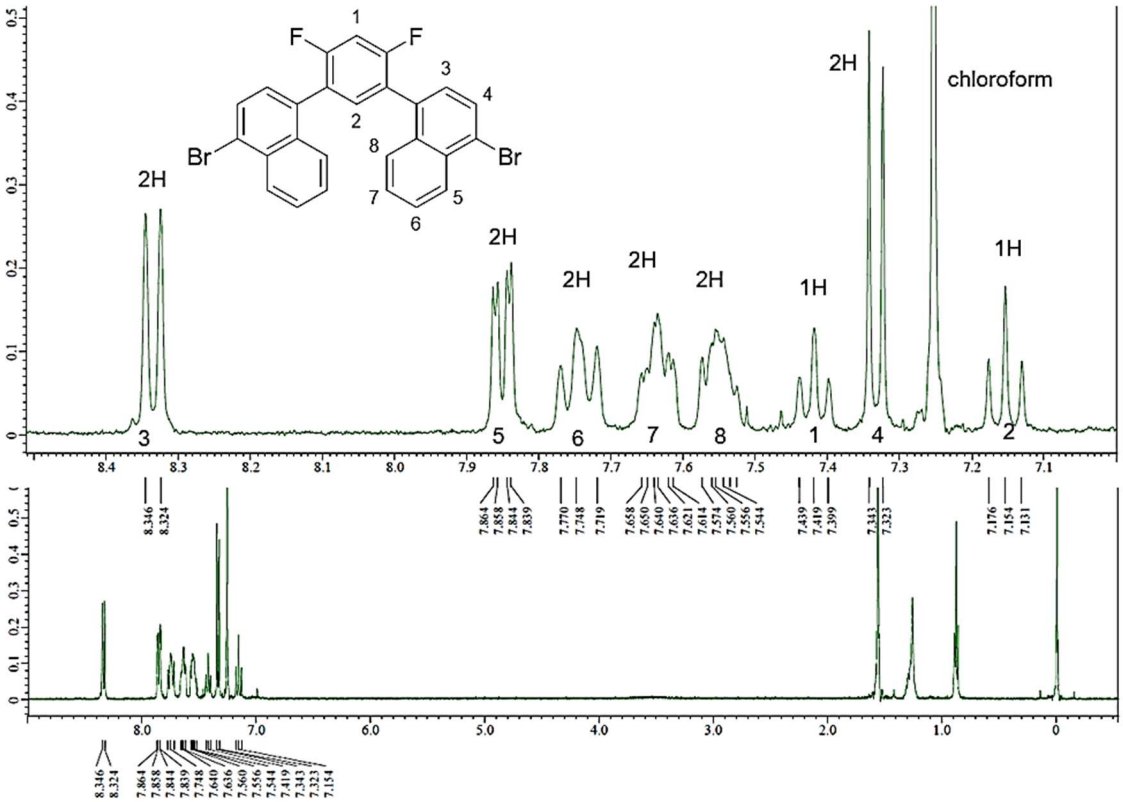

S2.13 ^{1}H NMR spectrum (400MHz, 120℃) of **N7** in $C_2D_2Cl_4$

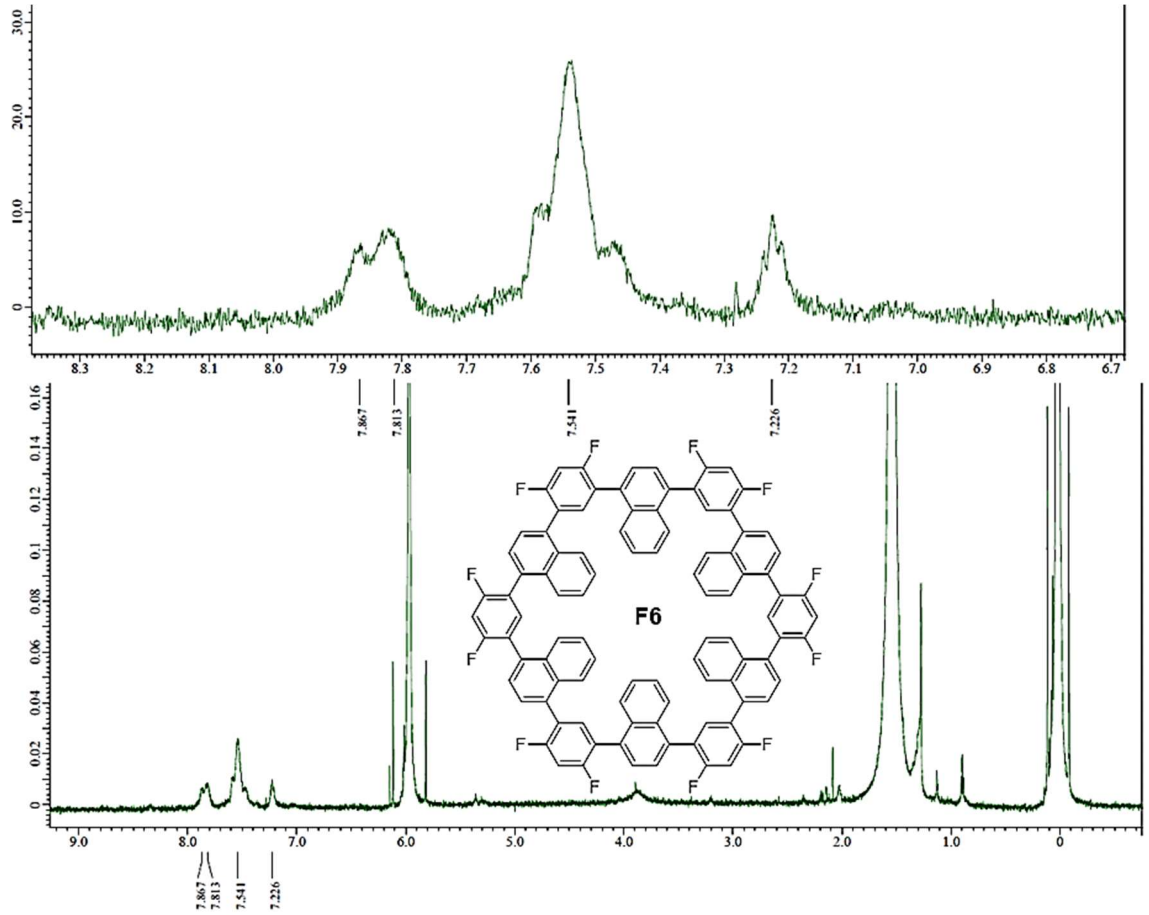

S2.14 ^{1}H NMR spectrum (600MHz, 70℃) of **F6** in $C_2D_2Cl_4$

Crystallography

Empirical Formula	$C_{96}H_{60}$
Formula Weight	1213.53
Crystal Color, Habit	colorless, prism
Crystal Dimensions	0.120 × 0.030 × 0.020 mm
Crystal System	monoclinic
Lattice Type	Primitive
Lattice Parameters	a = 20.4724(6) Å
	b = 15.7890(5) Å
	c = 24.9750(8) Å
	β = 91.270(6)°
	V = 8070.9(4) Å^3
Space Group	$P2_1/c$ (#14)
Z value	4
Dcalc	0.999 g/cm^3
F_{000}	2544.00
μ(MoKα)	0.565 cm^{-1}

S2.15 Crystallographic data for **N6**

(two manners of n6 c60)

Empirical formula	$C_{180}H_{80}Cl_4$
Formula weight	2384.24
Temperature	90 K
Wavelength	0.71073 Å
Crystal system	Triclinic
Space group	*P*-1
Unit cell dimensions	a = 11.110(5) Å α= 94.214(7)°
	b = 14.775(6) Å β= 94.286(7)°
	c = 17.361(7) Å γ= 101.721(7)°
Volume	2771(2) Å^3
Z	1
Density (calculated)	1.429 Mg/m^3
Absorption coefficient	0.174 mm^{-1}
F(000)	1228
Crystal size	0.200 x 0.100 x 0.010 mm^3
Theta range for data collection	1.758 to 25.000°.
Index ranges	$-13 \le h \le 10$, $-14 \le k \le 17$,
	$-20 \le l \le 20$
Reflections collected	14425
Independent reflections	9669 [R(int) = 0.0439]
Completeness to theta = 25.000°	99.0 %
Absorption correction	Semi-empirical from equivalents
Max. and min. transmission	0.998 and 0.781
Refinement method	Full-matrix least-squares on F^2
Data / restraints / parameters	9669 / 238 / 853
Goodness-of-fit on F^2	1.011
Final R indices [$I>2\sigma(I)$]	R_1 = 0.0889, wR_2 = 0.1959
R indices (all data)	R_1 = 0.1605, wR_2 = 0.2486
Extinction coefficient	n/a
Largest diff. peak and hole	1.629 and -0.683 e.Å^{-3}

S2.16 Crystallographic data for C_{60}@**N6**

Empirical formula	$C_{172}H_{65}Cl$
Formula weight	2166.69
Temperature	103 K
Wavelength	0.71073 Å
Crystal system	Triclinic
Space group	*P*-1 (#2)
Unit cell dimensions	a = 11.75(4) Å α= 106.46(3)°
	b = 14.98(5) Å β= 101.62(3)°
	c = 15.88(5) Å γ= 98.45(3)°
Volume	2563(14) Å^3
Z	1
Density (calculated)	1.404 Mg/m^3
Absorption coefficient	0.105 mm^{-1}
F(000)	1114
Crystal size	0.100 x 0.050 x 0.020 mm^3
Theta range for data collection	1.651 to 19.995°.
Index ranges	$-10 \le h \le 11$, $-14 \le k \le 13$,
	$-15 \le l \le 11$
Reflections collected	5549
Independent reflections	4553 [R(int) = 0.2291]
Completeness to theta = 19.995°	95.1 %
Absorption correction	Semi-empirical from equivalents
Max. and min. transmission	0.998 and 0.642
Refinement method	Full-matrix least-squares on F^2
Data / restraints / parameters	4553 / 1029 / 1114
Goodness-of-fit on F^2	1.084
Final R indices [I>2σ(I)]	R_1 = 0.1092, wR_2 = 0.2259
R indices (all data)	R_1 = 0.4092, wR_2 = 0.4205
Extinction coefficient	n/a
Largest diff. peak and hole	0.255 and -0.332 e.Å^{-3}

S2.17 Crystallographic data for C_{70}@**N6**

Others

DFT calculations

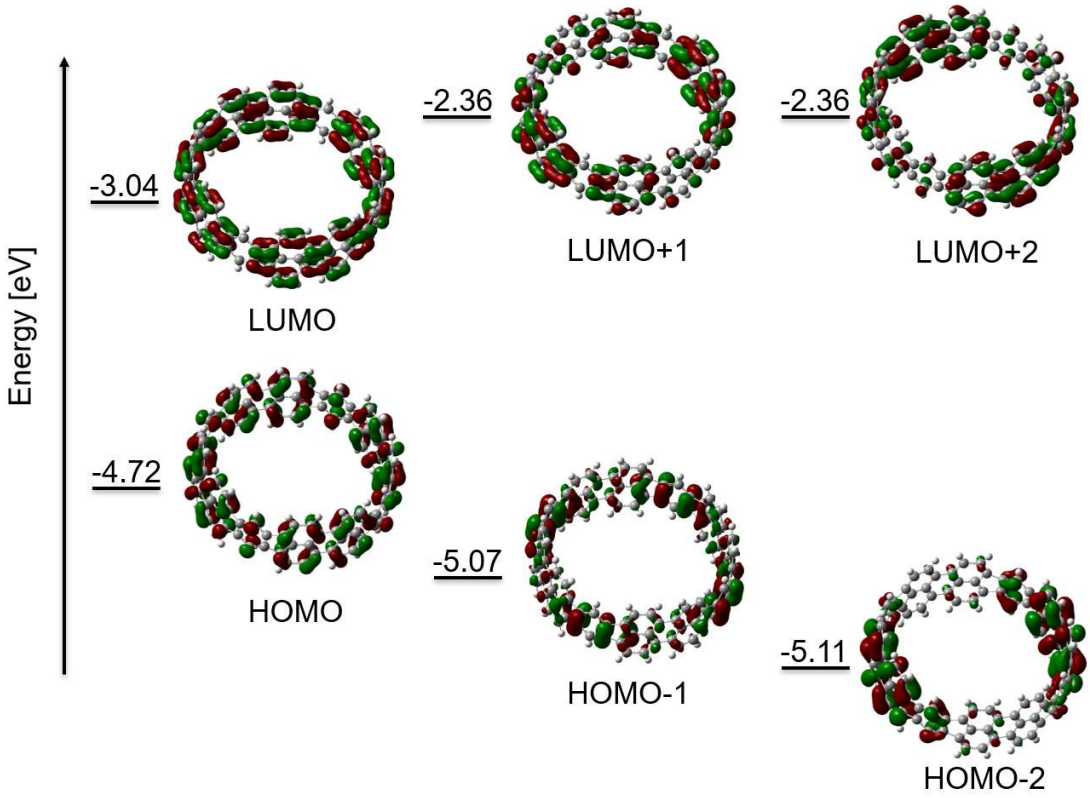

S2.18 DFT calculation of fused 4PP B3LYP/6-31G*

Frag.1-Frag.2	**N6**-**N6**(0-a)	**N6**-**N6**(0-bc)	**N6**-**N6**(0-abc)
V_{hole}/meV	1.8	19.7	1.6
$V_{electron}$/meV	42.2	25.3	20.0

S2.19 Charge transfer integrals of **N6**

(ADF calculation based on the date of **N6**'s single crystal)

Fusion byproduct

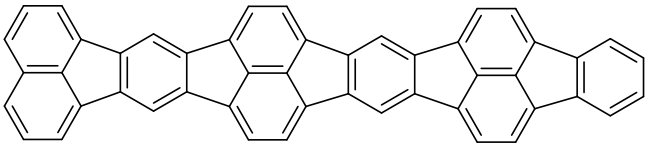

F3
(Speculated structure)

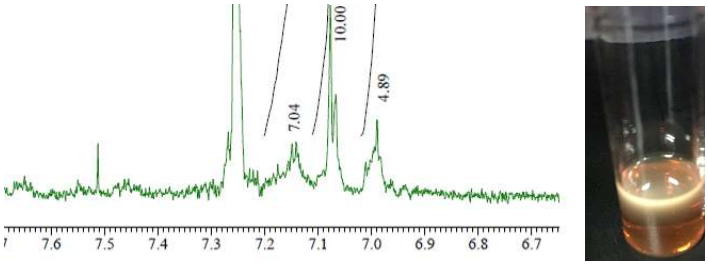

S2.20 ^{1}H NMR spectrum of compound **F3** (400MHz) in $CDCl_3$

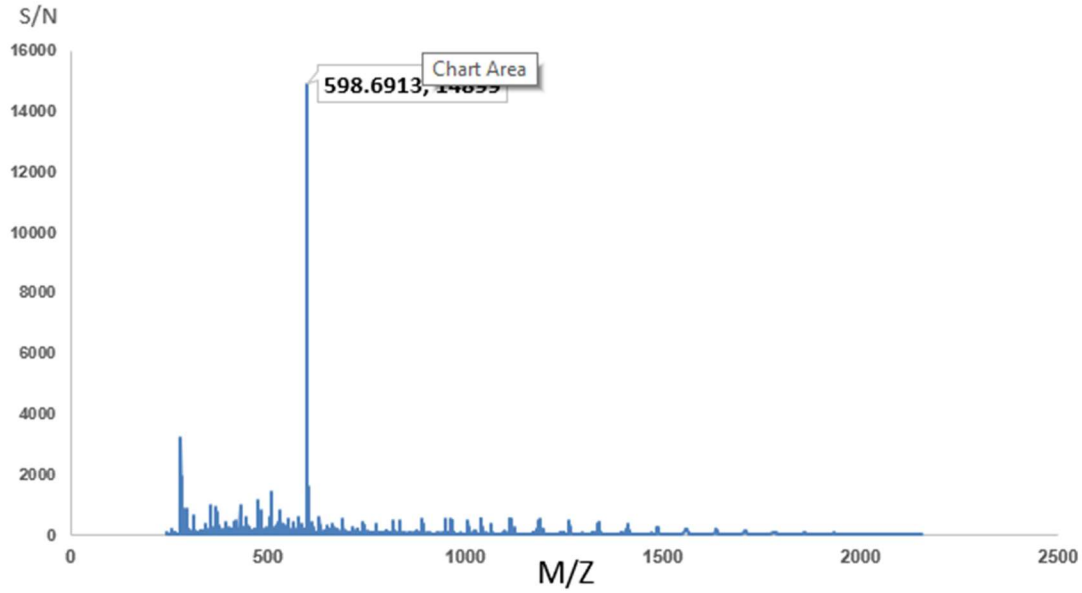

S**2.21** APCI MS of compound **F3** (positive/low)

References

[39] V. Hensel, K. Lützow, J. Jakob, K. Gessler, W. Saenger and A. D. Schlüter, *Angew. Chem. Int. Ed. Engl*, **1997**, *36*, 2654–2656; V. Hensel and A. D. Schlüter, *Chem.–Eur. J*, **1999**, *5*, 421–429.

[40] H. A. Staab and F. Binnig, *Tetrahedron Lett*, **1964**, *5*, 319–321.

[41] J. Y. Xue, K. Ikemoto, N. Takahashi, T. Izumi, H. Taka, H. Kita, S. Sato and H. Isobe, *J. Org. Chem*, **2014**, *79*, 9735–9739 and the references are therein.

[42] (a) H.–W. Jiang, S. Ham, N. Aratani, D. Kim and A. Osuka, *Chem.–Eur. J*, **2013**, *19*, 13328–13336; (b) Y. Nakamura, N. Aratani and A. Osuka, *Chem. Soc. Rev*, **2007**, *36*, 831–845.

[43] H. Sugita, M. Nojima, Y. Ohta and T. Yokozawa, *Chem. Commun*, **2017**, *53*, 396–399.

[44] (a) M. Kasha, *Rad. Res*, **1963**, *20*, 55–70; (b) A. Osuka and K. Maruyama, J. *Am. Chem. Soc*, **1988**, *110*, 4454–4456.

[45] G. F. Woods, F. T. Reed, T. E. Arthur and H. Ezekiel, *J. Am. Chem. Soc*, **1951**, *73*, 3854–3856.

[46] M. J. Frisch, G. W. Trucks, H. B. Schlegel, G. E. Scuseria, M. A. Robb, J. R. Cheeseman, G. Scalmani, V. Barone, B. Mennucci, G. A. Petersson, H. Nakatsuji, M. Caricato, X. Li, H. P. Hratchian, A. F. Izmaylov, J. Bloino, G. Zheng, J. L. Sonnenberg, M. Hada, M. Ehara, K. Toyota, R. Fukuda, J. Hasegawa, M. Ishida, T. Nakajima, Y. Honda, O. Kitao, H. Nakai, T. Vreven, J. A. Montgomery Jr, J. E. Peralta, F. Ogliaro, M. Bearpark, J. J. Heyd, E. Brothers, K. N. Kudin, V. N. Staroverov, R. Kobayashi, J. Normand, K. Raghavachari, A. Rendell, J. C. Burant, S. S. Iyengar, J. Tomasi, M. Cossi, N. Rega, J. M. Millam, M. Klene, J. E. Knox, J. B. Cross, V. Bakken, C. Adamo, J. Jaramillo, R. Gomperts, R. E. Stratmann, O.

Yazyev, A. J. Austin, R. Cammi, C. Pomelli, J. W. Ochterski, R. L. Martin, K. Morokuma, V. G. Zakrzewski, G. A. Voth, P. Salvador, J. J. Dannenberg, S. Dapprich, A. D. Daniels, O. Farkas, J. B. Foresman, J. V. Ortiz, J. Cioslowski and D. J. Fox, *Gaussian 09, Revision A.1, Gaussian, Inc, Wallingford CT*, **2009**.

[47] (a) B. W. Smith, M. Monthioux and D. E. Luzzi, *Nature*, **1998**, *396*, 323; (b) S. Bandow, M. Takizawa, H. Kato, T. Okazaki, H. Shinohara and S. Iijima, *Chem. Phys. Lett*, **2001**, *347*, 23.

[48] http://supramolecular.org/

[49] (a) K. S. Troche, V. R. Coluci, S. F. Braga, D. D. Chinellato, F. Sato, S. B. Legoas, R. Rurali, and D. S. Galvão, *Nano Letters*, **2005**, *5*(2), 349–355; (b) M. Ortiz, S. Cho, J. Niklas, S. Kim, O. G. Poluektov, W. Zhang, G. Rumbles and J. Park, *J. Am. Chem. Soc*, **2017**, *139* (12), 4286–4289

[50] T. P. Nguyen, J. H. Shim, and J. Y. Lee, *J. Phys. Chem. C*, **2015**, *119(21)*, 11301−11310.

[51] (a) G. te Velde, F.M. Bickelhaupt, E.J. Baerends, C. Fonseca Guerra, S.J.A. van Gisbergen, J.G. Snijders and T. Ziegler, J. Comput. Chem. **2001**, *22*, 931; (b) ADF 2021.1, SCM, Theoretical Chemistry, Vrije Universiteit, Amsterdam, The Netherlands, http://www.scm.com.

[52] (a) T. J. Savenije, J. E. Kroeze, M. M. Wienk, J. M., Kroon and J. M. Warman, *Phys. Rev. B*, **2004**, 69(15), 155205. (b)A. Saeki, M. Tsuji, and S. Seki, *Adv. Energy Mater.* **2011**, *1*(4), 661-669.

[53] D. Lorbach, M. Wagner, M. Baumgarten and K. Müllen, *Chem. Commun*. **2013**, *49*, 10578–10580.

[54] A. Matsumoto, M. Suzuki, D. Kuzuhara, H. Hayashi, N. Aratani and H. Yamada, *Angew. Chem. Int. Ed*. **2015**, *127*(28), 8293-8296.

[55] M. Daigel, A. P. Lafod, E. Soligo and J. F. Morin, *Angew. Chem. Int. Ed*, **2016**, *55*, 2042−2047

[56] (a) K. Y. Amsharov and P. Merz, *J. Org. Chem*, **2012**, *77*(12), 5445−5448; (b) A.K. Steiner and K. Y. Amsharov, *Angew. Chem. Int. Ed*, **2017**, *56*(46), 14732-14736; (c) O. Papaianina, V. A. Akhmetov, A. A. Goryunkov, F. Hampel, F. W. Heinemann and K. Y. Amsharov, *Angew. Chem. Int. Ed*, **2017**, *56*, 4834−4838

[57] G. M. Sheldrick, Acta Crystallogr, *Sect. A: Found. Adv*, **2015**, *A71*, 3–8.

[58] G. M. Sheldrick, Acta Crystallogr, *Sect. C: Struct. Chem*, **2015**, *C71*, 3–8.

[59] 16 (a) Squeeze-Platon and A. L. Spek, *PLATON, A Multipurpose Crystallographic Tool, Utrecht, The Netherlands*, **2005**; (b) P. van der Sluis and A. L. Spek, *Acta Crystallogr, Sect. A: Found. Crystallogr*, **1990**, *46*, 194–201.

[60] F. S. Han, M. Higuchi and D.G. Kurth, *Org. Lett*, **2007**, *9*(4), 559-562.

[61] J. H. Kim, H. U. Kim, D. Mi, S. H. Jin, W. S. Shin, S. C. Yoon, I. N. Kang and D.H. Hwang, *Macromolecules*, **2012**, *45(5)*, 2367-2376.

[62] D. Alezi, Y. Belmabkhout, M. Suyetin, P. M. Bhatt, Ł. J. Weseliński, V. Solovyeva, K. Adil, I. Spanopoulos, P. N. Trikalitis, A.-H. Emwas and M. Eddaoudi, *J. Am. Chem. Soc*, **2015**, *137*(41), 13308-13318.

[63] L. Murphy, P. Brulatti, V. Fattori, M. Cocchi and J. G. Williams, *Chem. Comm*, **2012**, *48*(47), 5817-5819.

[64] T. Ishiyama, M. Murata and N. Miyaura, *J. Org. Chem*, **1995**, *60*, 7508-7510.

Chapter 3. Facile synthesis and supramolecular investigation of cyclic pyrene oligomers

3.1 Introduction

Pyrene is an important PAH among those building units for larger cycloarylenes because of its highly emissive property and large π-surface.[65] The synthesis of cyclic pyrene oligomers has been challenging, which has led to the exploring of many synthetic strategies. In previous works, Müllen's group reported the stepwise synthesis of [6]cyclo-1,3-pyrenylene,[66] and Isobe's group independently performed a one-pot nickel-mediated homo-coupling of 1,3-dibromopyrene[67] (**Scheme 16**).

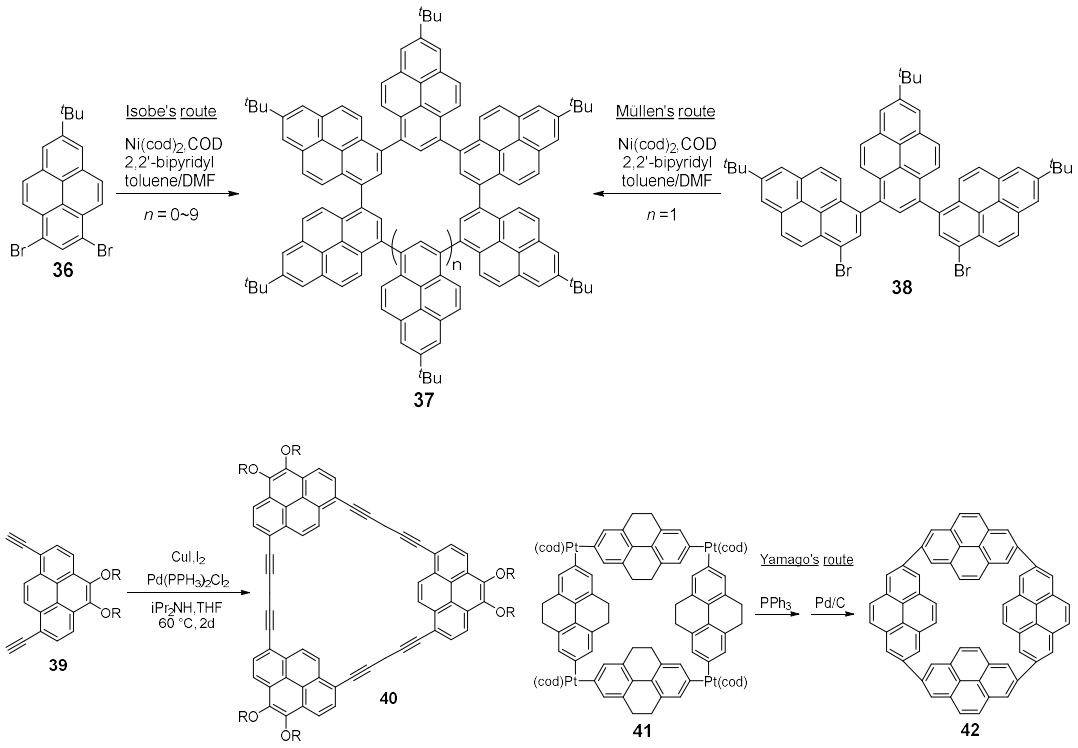

Scheme 16. Synthesis of cyclic pyrene oligomers[66]

Bodwell's group synthesized the [3] and [4]cyclo-1,8-pyrenylene-ethynylene by the self Sonogashira-coupling reaction (**Scheme 16**).[68] Yamago and coworkers synthesized [4]cyclo-2,7-pyrenylene by their platinum-mediated assembly method.[69] The reason for the formation of the tetramer, in this case, is that the platinum complex intermediate has a bonding angle of approximately 90°. These single substrate reactions[70] worked well to give cyclic pyrene oligomers[71] and effectively shorten the reaction route, but the cross-coupling reaction with multiple substrates is also a powerful technique,[72] especially when we want to selectively synthesize heptameric[73] and octameric[74] compounds (**Scheme 17**).

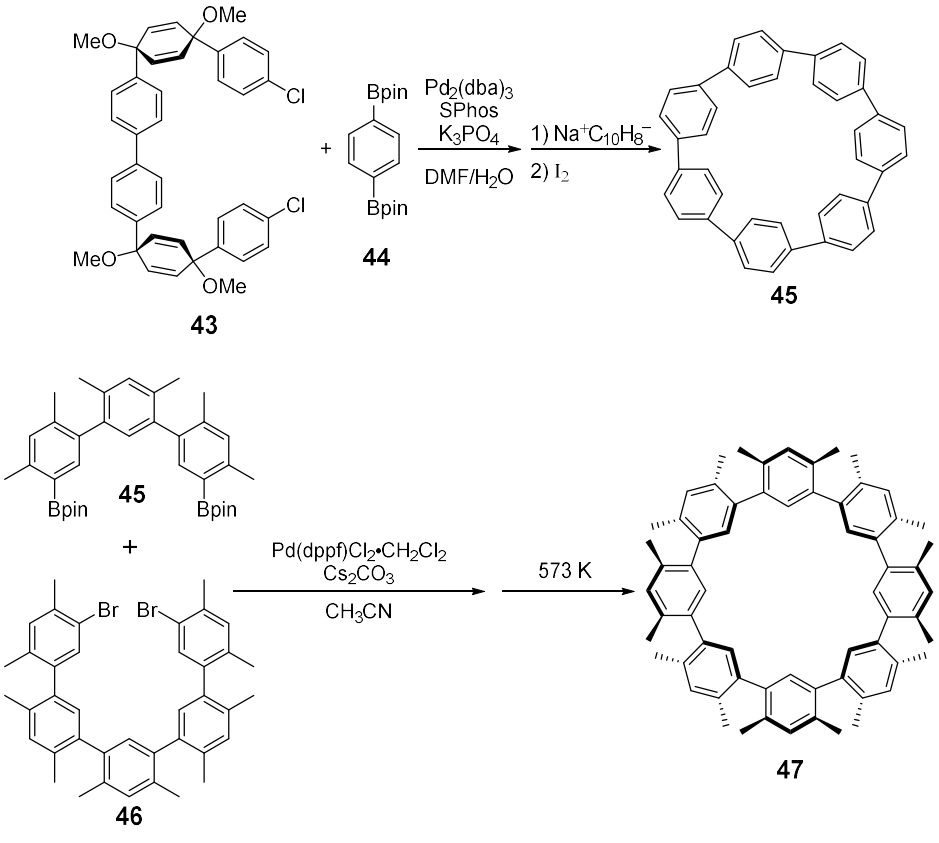

Scheme 17. Synthesis of heptameric and octameric carbon nanorings[73][74]

In the case of 1,3-cyclopyrenexlenens, pentamer and hexamer were the main products. Therefore, we were curious about the case of 1,4'-3,9'-pyrenlenene.

In this work, the synthesis of 3 kinds of 1,3-pyrene oligomers (**CP, CBP, CMP**) was explored by the Suzuki-Miyaura cross-coupling reaction *via* a one-step reaction between diiodopyrene and bis-borylated species.

3.2 2,2'-*tert*-Butyl-5,9-6',8'-cyclo-octameric pyrenylene [8]CP

3.2.1 Molecular design and synthesis

To prepare 6,8-diborylated pyrene **51**, *tert*-butyl group was introduced at the 2-position of pyrene to block the 1,3-positions followed by the bromination then borylation.[75] This compound serves as a versatile platform in the synthesis of disubstituted pyrenes. Slow vapor diffusion of methanol into a chloroform solution of **51** afforded crystals suitable for X-ray diffraction analysis. 2-*tert*-Butyl-5,9-diiodopyrene **60** was obtained through an indirect synthetic route reported by Müllen and coworkers.[76]

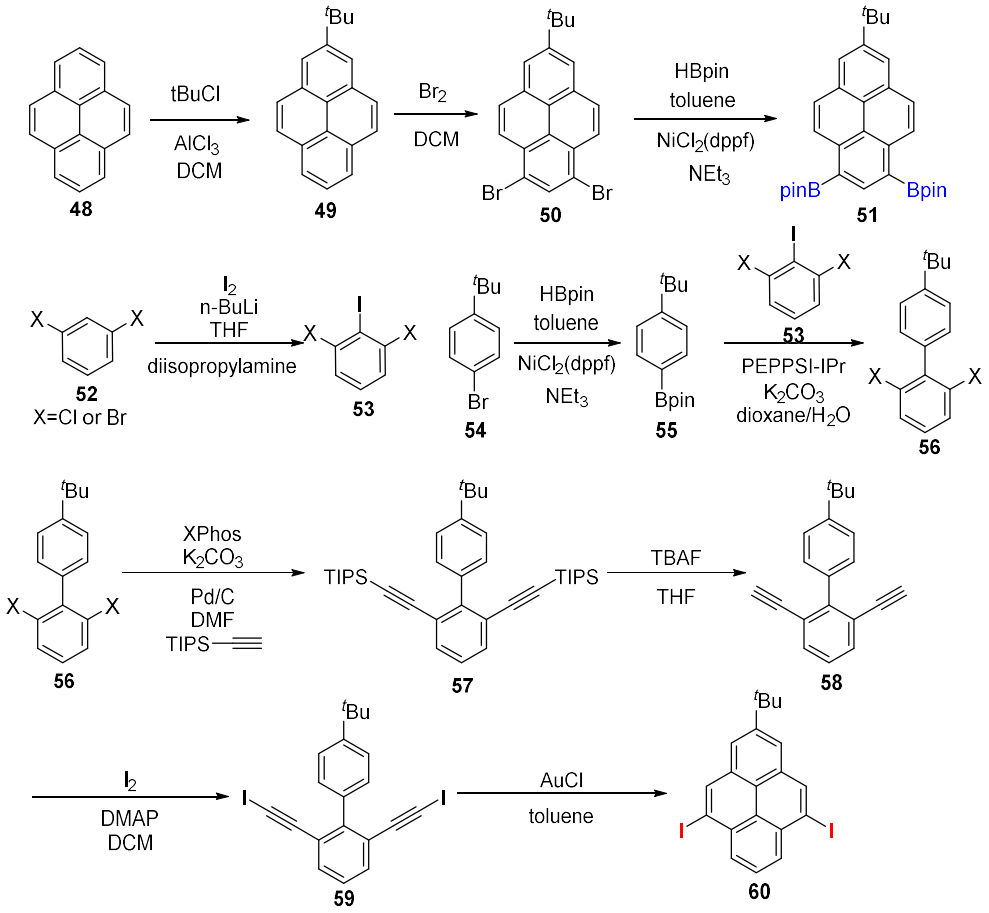

Scheme 18. Synthetic route of compounds **51** and **60**

The synthesis of **[8]CP** stared from the previous member in our lab. After optimization of reaction conditions. (**Scheme 19**) **[8]CP** was then synthesized by the Suzuki-Miyaura cross coupling reaction of **51** and **60** [75][76] (**Scheme 19**). 2.5 mg of **[8]CP** was obtained in 2.8% yield as the main product.

The coupling between the peri-positions would limit the steric angle and predominantly gave the octamer, the selective formation of which is unusual as a one-step synthesis of oligomers. Totally eight equivalent carbon-carbon bonds were formed by this cross-coupling, which means that the reaction yield per one bond is going on at 64%. The success of the synthesis here is closely related to the inspiration during the

synthesis of **N6**. Especially, the temperature controlling. And it was confirmed that temperature affected the reaction much and lower temperature benefits the formation of cyclic molecules.

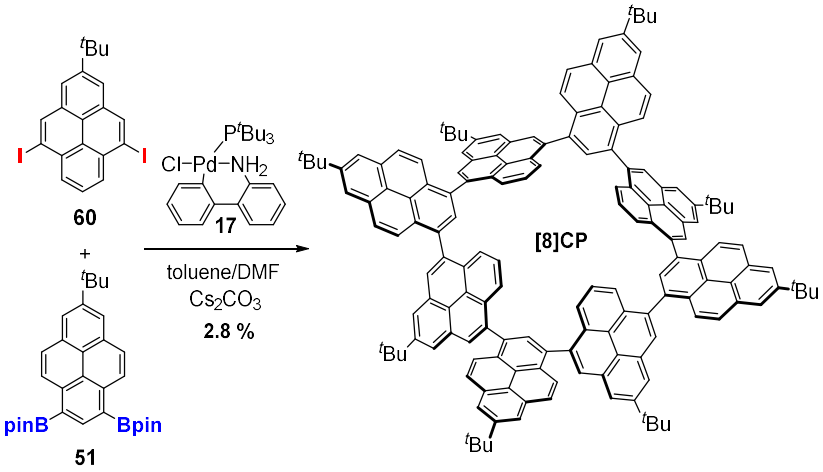

Scheme 19. One-pot reaction to the synthesis of **[8]CP**

Entry	Catalyst amount	Base	Solvent	Temp./time	Result
1*	0.10	CsF	THF/H_2O	r.t for 3 days	linear oligomers
2	0.25	Cs_2CO_3	Toluene/DMF	100ºC for 23 h	linear oligomers
3	0.25	Cs_2CO_3	Toluene/DMF	r.t for 6 h + 100ºC for 19h	**[8]CP** obtained

Table 2. Optimization of the reaction conditions
(*carried out by Dr. Matsumoto)

3.2.2 ^{1}H NMR and HR-MALDI-TOF mass of [8]CP

The compound has been characterized by ^{1}H NMR spectroscopy and HR-MALDI-TOF mass spectrometry. HR MALDI-TOF-MS detected a parent ion peak at *m*/*z* = 2049.0026 (calcd. for $C_{160}H_{128}$ = 2049.0011 $[M]^+$) for **[8]CP**. The ^{1}H NMR spectrum of **[8]CP** in 1,1,2,2-tetrachloroethane-d_2 reveals two sets of signals that consist of four singlet peaks at 8.36, 8.34, 8.26 and 8.08 ppm, three doublet peaks at 8.10, 8.04 and 7.72 ppm, and one triplet peak at 7.61 ppm for aromatic protons, indicating the highly symmetric cyclic structure.

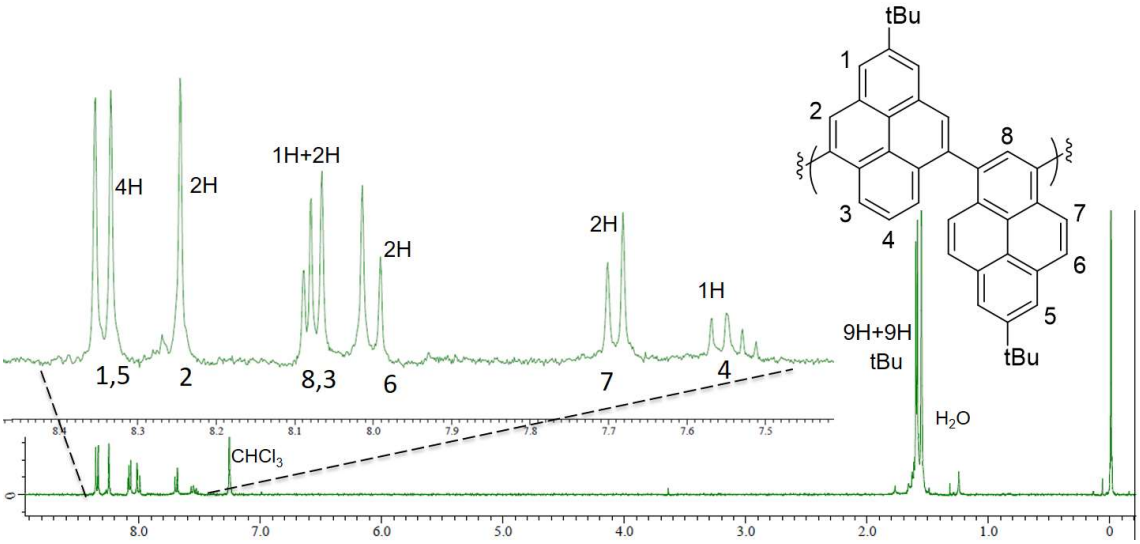

Figure 27. ^{1}H NMR spectrum of **[8]CP**.

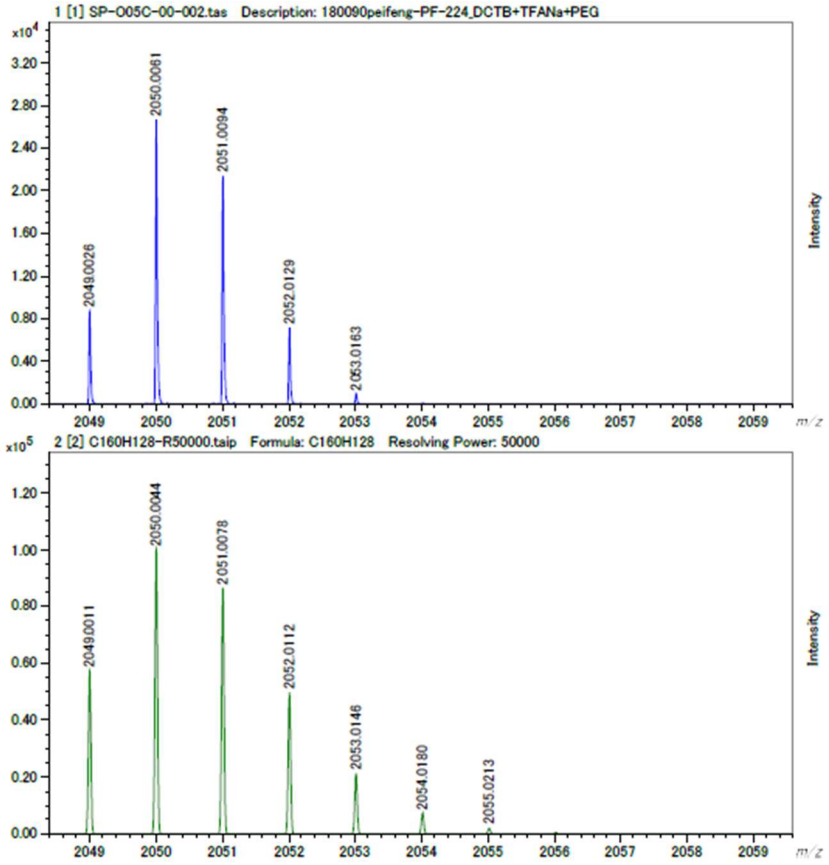

Figure 28. HR-MALDI-TOF-MS of **[8]CP**.

3.2.3 Single crystal X-ray analysis of [8]CP

The cyclic structure of **[8]CP** was determined by single crystal X-ray diffraction analysis (**Figure 29**). Slow vapor diffusion of methanol into a chloroform solution of **[8]CP** afforded crystals suitable for X-ray diffraction analysis. In the solid state, the dihedral angles between pyrene units are 72.5-88.4°, expecting that the small π-conjugation between pyrene units.

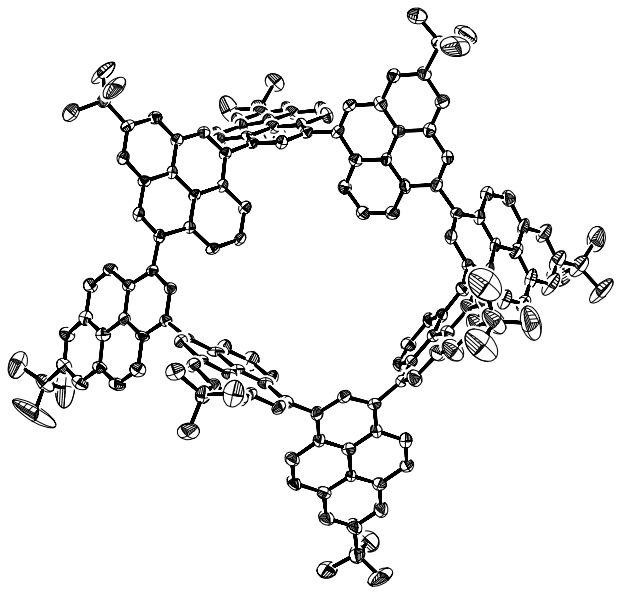

Figure 29. X-ray single crystal structure of **[8]CP**

3.2.4 Attempts to make CNB from [8]CP

After getting the cyclic molecule **[8]CP**, I run the oxidation reaction to make **CNB10**. The method was reported by Mullen to make fused pyrene dimer and trimer, in 2013.[53] Unfortunately, the reaction didn't work to give the CNB target. This may because of the low reactivity of the 5,9-position of pyrene.

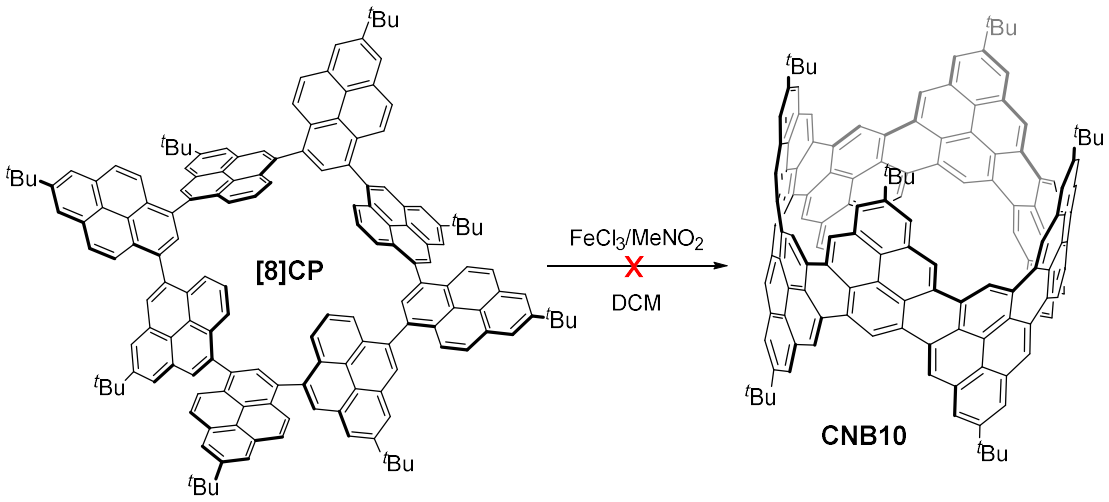

Scheme 20. Fusion of **[8]CP** via an oxidation reaction

3.3 Synthesis of [*n*]CBPs

3.3.1 Molecular design

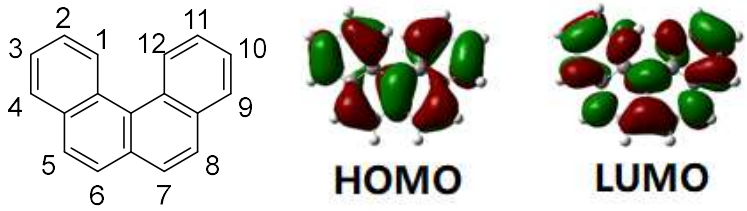

Figure 30. MO (Molecular orbital) of benzo[*c*]phenanthrene

Since the oxidation of **[8]CP** didn't work, considering the low reactivity of the 4,9-positions of pyrene, we changed half of the pyrene units to benzo[*c*]phenanthrene. Because the 4,9- positions of this unit have higher HOMO coefficients.

3.3.2 Synthesis of 5,8-bis(4,4,5,5-tetramethyl-1,3,2-dioxaborolan-2-yl)benzo[*c*]phenanthrene

The synthesis of compounds **61** to **68** can be carried out smoothly according to the method provided in the literature. Then **66** is selectively brominated. Although the purification process of **67** was reported, in this research here, compound **67** was not successfully isolated due to solubility problems in the synthesis process of this study. Instead of it, compound **67** was used in the state of mixture to synthesize **68**. The problem of low solubility of compound **67** is improved by introducing the Bpin groups. Thus compound **68** has been successfully separated. The two steps of reactions gave a total yield of 11%. As far as I know, it should be the first synthesis of compound **68**. As the solubility increases, compared to compound **67**, compound **68** should be able to provide a key intermediate for the construction of many syntheses containing benzo[*c*]phenanthrene units.

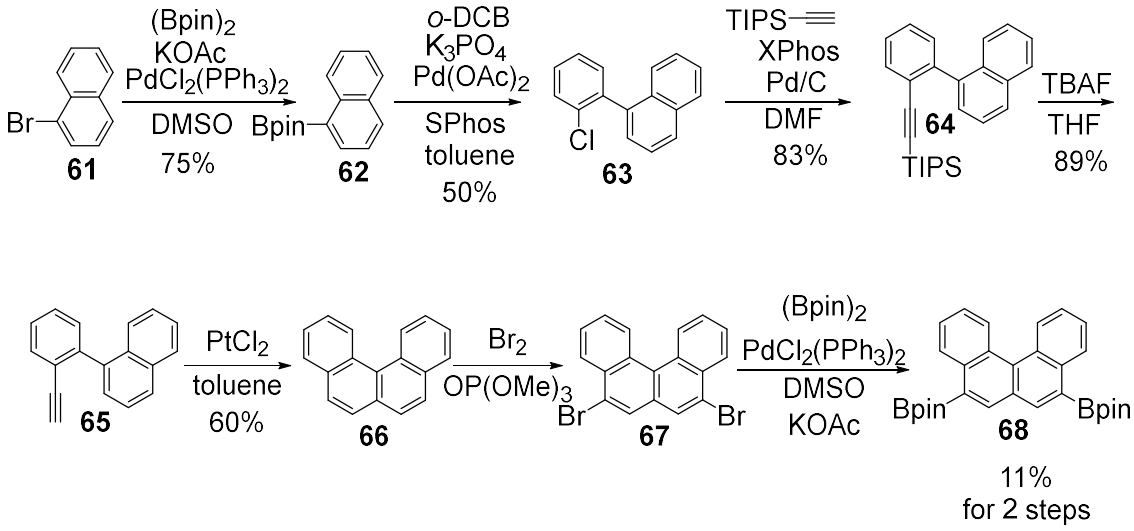

Scheme 21. Synthesis of compound **68**

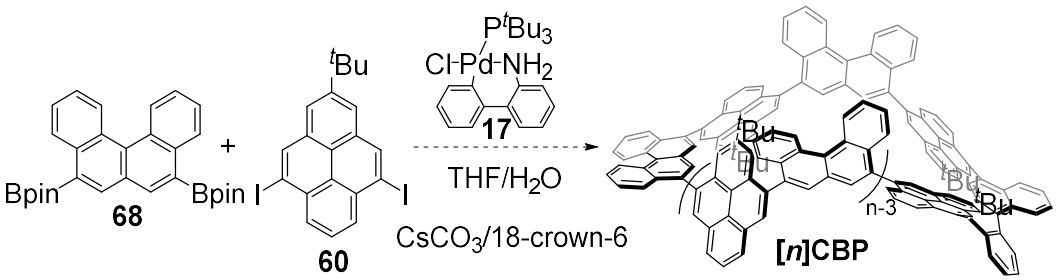

Scheme 22. Synthesis of compound **[*n*]CBP**

3.3.3 Synthesis towards [*n*]CBPs

The similar cyclization by one-pot Suzuki coupling reaction was carried out after obtaining the diboride **68**. After being purified by a preparative GPC, Oligomers with **n=2-5** could be obtained. After separation on GPC, fractions with **n= 3 and 4** was gathered and checked by HR-MALDI-TOF-MS. However, no fractions were confirmed to contain the oligomer of **n= 2 and 5**. The separated compounds (~2 mg for each) were confirmed to contain only very little amount of desired cyclic molecules. (n=3,4) Unable to separate (n=2,5)

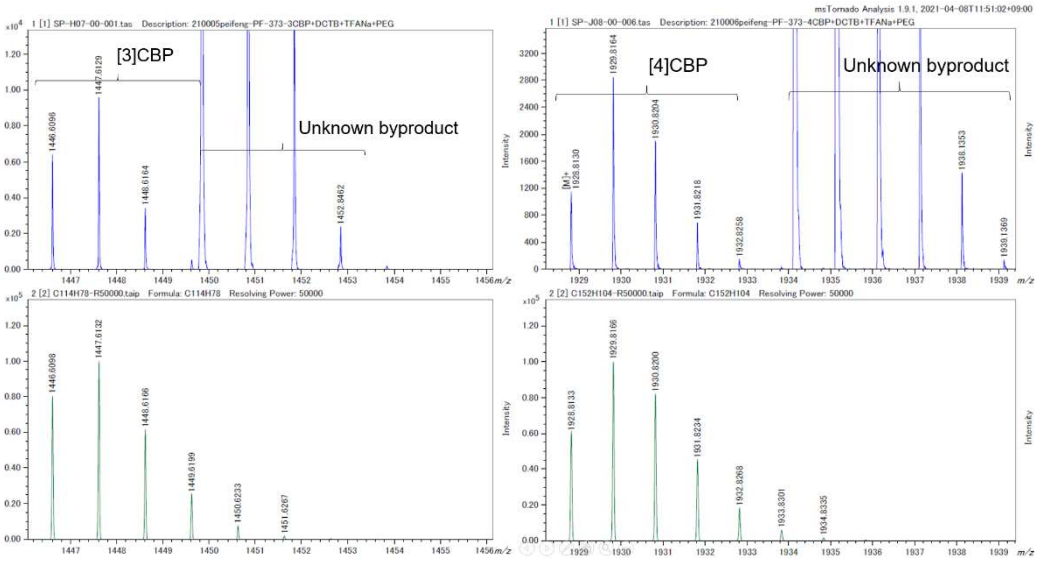

Figure 30. HR-MALDI-TOF-MS of the fractions of **[3]CBP** and **[4]CBP**

3.4 Synthesis of [*n*]CMPs

3.4.1 Molecular design

Since it was hard to obtain **[*n*]CBPs**, the next plan was to change the bigger benzophenanthrene units to the smaller anisole unit. The 2,6-positions of anisole have the higher HOMO coefficients as well.

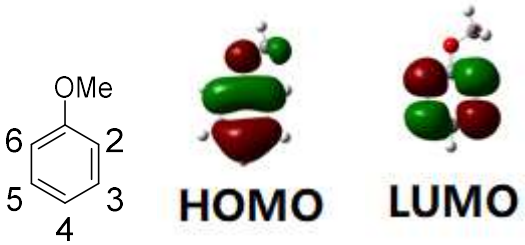

Figure 30. MO of anisole

3.4.2 Synthesis of [*n*]CMPs

The cyclization of anisole units was carried out. Fortunately, the reaction worked well in this case. **Table 3** showed the separation result of the cyclic oligomers. Tetramer and pentamer can be continuously synthesized from repeated reactions with a yield of 3-

4%. Interestingly, as the largest cyclic molecule isolated. The decamer was also confirmed by NMR. Even though the yield looks not that high. The efficiency to form CC bonds is incredibly high. Up to 80% for each bond. Is really amazing that a one-pot reaction can form 20 C-C bonds just in 24h. And to afford a cyclic molecule with 20 PAH units.

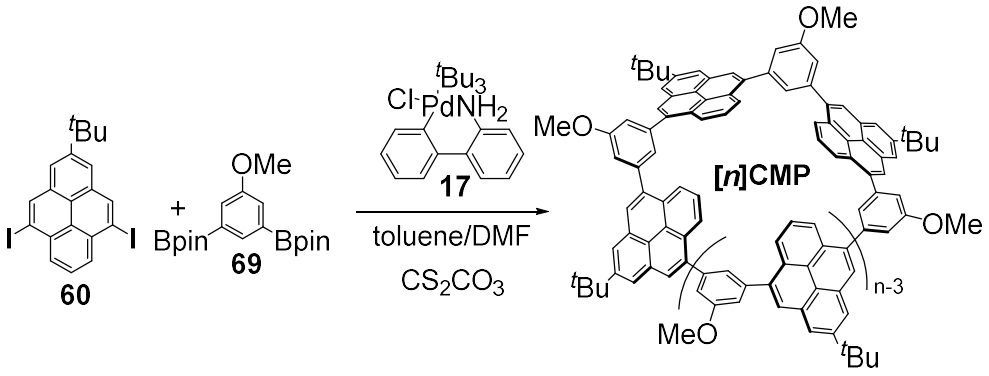

Scheme 23. Synthesis of **[*n*]CMP**

n	3	4	5	6	7	8	9	10	Sum
Entry1/mg		5.3	3.5		2.2	1.7			
Yield		7.5%	4.9%		3.1%	2.4%			17.9%
Entry2/mg	2.2	5.2	4.4	3.9		3.2	0.4	2.4	
Yield	1.6%	3.7%	3.1%	2.8%		2.3%	0.3%	1.7%	15.5%

Table 3. Distributions of products (Entry 2 represents a repeating reaction starting from 190 mg of compound **60**.)

3.4.3 Fusion reaction of [*n*]CMPs

After obtaining the cycle oligomers. The similar fusion reaction was carried out to make carbon Nanohorn. The fusion of the small sized oligomers didn't work. But for larger ones, it's still hopeful. More fusion attempts are still on the way.

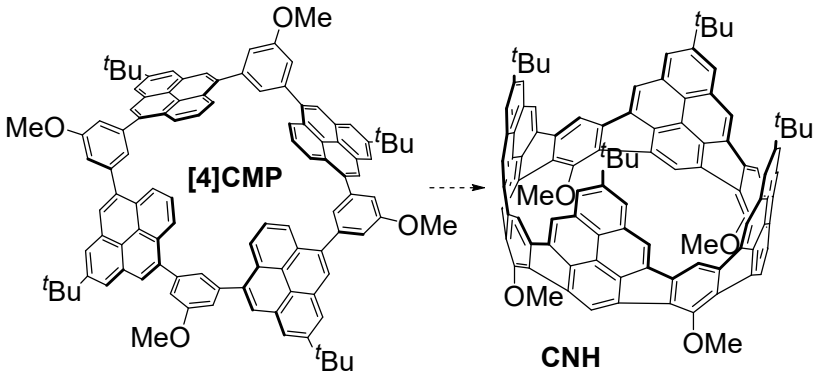

Scheme 23. Synthesis of **CNH**

Entry	n	Oxidant/reagent	Time	Solvent	Temperature	Result
1st	5	DDQ/$Sc(OTf)_3$	18 h	toluene	up to 110°C	No reaction
2nd	5	DDQ/TfOH	1 h	toluene	r.t	Decomposed
3rd	5	$FeCl_3$	12 h	toluene/$MeNO_2$	up to 70°C	Insert of [O]s
4th	4	$FeCl_3$*	12 h	DCM/$MeNO_2$	-15°C to r.t	Decomposed
5th	6	$FeCl_3$*	12 h	DCM/$MeNO_2$	-15°C to r.t	Decomposed

Table 4. Fusion reaction conditions

3.5 Conclusion

In summary, 2,2'-*tert*-butyl-5,9-6',8'-cyclo-octameric pyrenylene **[8]CP** was synthesized by the one-step Suzuki-Miyaura cross coupling reaction from two kinds of monomers. The octameric molecular structure was revealed by X-ray diffraction analysis. To the best of our knowledge, this is the largest pyrene oligomer for which a single crystal structure has been obtained. Recently, we presented pyrene-based homoditopic molecular host, which has back-to-back arranged binding cavities.[77] Taking advantage of the unique structural feature, **[8]CP** also can bind the spherical fullerenes owing to concave-convex complementarity. The directly-linked pyrene octamer would demonstrate a new potential of the planar cyclic pyrene oligomers. Examination of the photophysical properties of these complexes is active in progress.

Supporting Information

Materials and instrumentation

^{1}H NMR (500 MHz) spectra were recorded with a JEOL JNM-ECX500 spectrometer by using tetramethylsilane as an internal standard. HR-MALDI-TOF-MS was measured on a JEOL SpiralTOF/JMS-S3000 spectrometer. X-ray crystallographic data were recorded at 90 K using a BRUKER-APEXII X-Ray diffractometer using Mo-Kα radiation equipped with a large area CCD detector. TLC and gravity column chromatography were performed on Art. 5554 (Merck KGaA) plates and silica gel 60N (Kanto Chemical), respectively. All solvents and chemicals were reagent-grade quality, obtained commercially and used without further purification. For spectral measurements, spectral-grade toluene was purchased from Nacalai Tesque.

Single-crystal X-ray diagram: crystals of **57** were grown by slow diffusion of methanol into a solution of **57** in $CHCl_3$ to yield colorless prisms. Crystals of **[8]CP** were grown by slow diffusion of methanol into a solution of **[8]CP** in $CHCl_3$ to yield colorless prisms. The contributions to the scattering arising from the presence of disordered solvents in the crystal of **[8]CP** were removed by use of the utility SQUEEZE in the PLATON software package.[78] CCDC 2023859 (**57**) and 2023860 ([8]CP) contain the supplementary crystallographic data for this paper. These data can be obtained free of charge from The Cambridge Crystallographic Data Centre via www.ccdc.cam.ac.uk/getstructures.

Experimental section

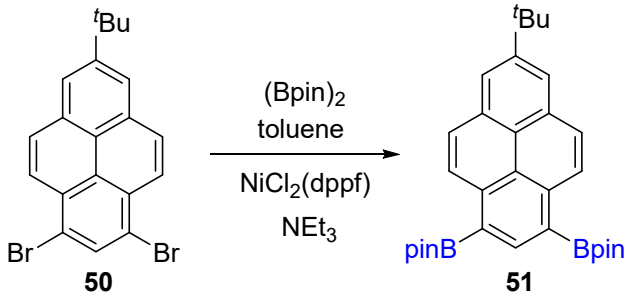

Compound 51: In a 200 mL 3-necked flask, compound **50** (6.20 g, 14.9 mmol) was dissolved by toluene (100 mL). Then, triethylamine (10.5 mL) and bispinacolatodiboron (5.20 g, 40.2 mmol) was added. After argon bubbling for 30 min, $NiCl_2$(dppp) was added under argon flow. The mixture was heated under 110°C for 48 h. After cooling to room temperature, the mixture was extracted with dichloromethane, washed with water and brine. The organic layer was gathered and evaporated. Reprecipitation gave 5.70 g of compound **51** with yield 75%.^{1}H NMR (400 MHz, $CDCl_3$) δ = 9.02 (d, J = 9.2Hz, 2H), 8.95 (s, 1H), 8.23(s, 2H), 8.13 (d, J = 9.2Hz, 2H), 1.59 (s, 9H), 1.50 (s, 24H) ppm.

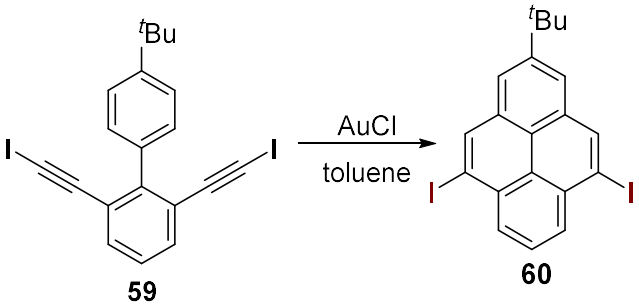

Compound 60: To a solution of 210 mg 4'-(*tert*-butyl)-2,6-bis(iodoethynyl)-1,1'-biphenyl (041 mmol, 1equiv.) in 15 mL anhydrous toluene 38 mg Au(I)Cl (0.16 mmol, 0.4 equiv.) was added and the mixture was degassed with argon for 30 min. After stirring at 60°C for 16 h the reaction mixture was concentrated under reduced pressure. Purification by column chromatography (hexane) followed by GPC, reprecipitation (CH_2Cl_2/methanol) afforded 520 mg of 5 in 32% yield as yellow needle crystals.

[8]CP: Compound **51** (90 mg, 0.176 mmol), 2-*tert*-butyl-5,9-diiodopyrene **60** (90 mg, 0.176 mmol), Cs_2CO_3 (288 mg, 0.882 mmol), dry toluene (3 mL) and dry DMF (1.2 mL) was added to a 25 mL Schlenk flask. After degassing with three freeze-pump-thaw cycles, the Pd catalyst **17** (24 mg, 0.046 mmol) was quickly added. After degassing again, the solution was stirred at room temperature for 8 h and then 100°C for 16 h. The MALDI-TOF-MS of the reaction mixture indicates the formation of oligomers. After cooling, the mixture was extracted with dichloromethane and washed with water and brine. After being concentrated by a rotary evaporator, the mixture was roughly separated on a silica gel column (dichloromethane). Then, separation on gel-permeation chromatography (GPC) gave 2.5 mg of **[8]CP** in 2.8% yield as the main product. ^{1}H NMR (tetrachloroethane-d_2, 400 MHz): δ = 8.36 (s, 8H), 8.34 (s, 8H), 8.26 (s, 8H), 8.10 (d, J = 9.6 Hz, 8H), 8.08 (s, 4H), 8.04 (d, J = 9.6 Hz, 8H), 7.72 (d, J = 7.6 Hz, 8H), 7.61 (t, J = 7.6 Hz, 4H), 1.58 (s, 36H) and 1.57 (s, 36H) ppm. HR-MALDI-TOF-MS: m/z $[M]^+$ calcd for $C_{160}H_{128}$: 2049.0011; found: 2049.0026.

Fusion reaction of [8]CP: The pyrene octamer **[8]CP** (~2 mg, 8.4×10^{-4} mmol) was dissolved in 1 mL distilled DCM. Then Argon flow was inlet for 15 min. After that a solution of $FeCl_3$ in $MeNO_3$ (~1.3 mg, ~0.0042 mL, 300 mg/mL) was added drop-wise. The Argon flow was kept for 20min while stirring. Then the tube was sealed and the solution was stirred for 1.5 h. 3 mL MeOH was added first and the mixture was poured

into an aqueous $NaHSO_3$ solution. Then it was extracted with DCM and washed with water and brine. The organic layer was dried over Na_2SO_4 and then evaporated. Then it was purified through a silica gel column (DCM). The target compound was not detected by MALDI-TOF-MS.

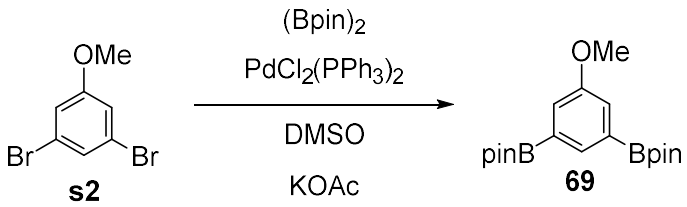

Compound 69: To a 24 mL DMSO solution of compound **s2** (1.33 g, 5.00 mmol) was added bispinacolatodiboron (2.80 g, 11.0 mmol), KOAc (2.45 g, 25.0 mmol) and $PdCl_2(PPh_3)_2$ (176 mg, 0.250 mmol), and the solution was stirred at 80℃ for 24 h. After the reaction mixture was cooled to room temperature, the mixture was extracted with ether for three times and washed with water and brine. The organic layer was dried over Na_2SO_4, filtered, concentrated and purified by column chromatography on silica gel (Hexane: EtOAc = 15:1 to 6:1) to give compound **69** as a white solid (1.72 g, 95%).^{1}H NMR (chloroform-*d*, 400 MHz): δ = 7.86 (s, 1H), 7.42 (d, J = 0.9 Hz, 2H), 3.83 (s, 3H) and 1.33 (s, 24H) ppm.

[*n*]CBPs: 5,8-bis(4,4,5,5-tetramethyl-1,3,2-dioxaborolan-2-yl)benzo[c]phenanthrene (20 mg, 0.042 mmol), 1,4-dibromonaphthalene (21 mg, 0.042 mmol), Cs_2CO_3 (68 mg, 0.021 mmol), dry toluene (1 mL) and dry DMF (0.5 mL) were added into a 25 mL 2-neck flask. After degassing, chloro[(tri-*tert*-butylphosphine)-2-(2-aminobiphenyl)] palladium (II) (7.7 mg, 0.015 mmol) was quickly added under flowing argon. After degassing again, the solution was stirred for 16 h at 100℃. The mixture was extracted with

dichloromethane and washed with water and brine. Then it was purified by chromatography on silica gel (dichloromethane).

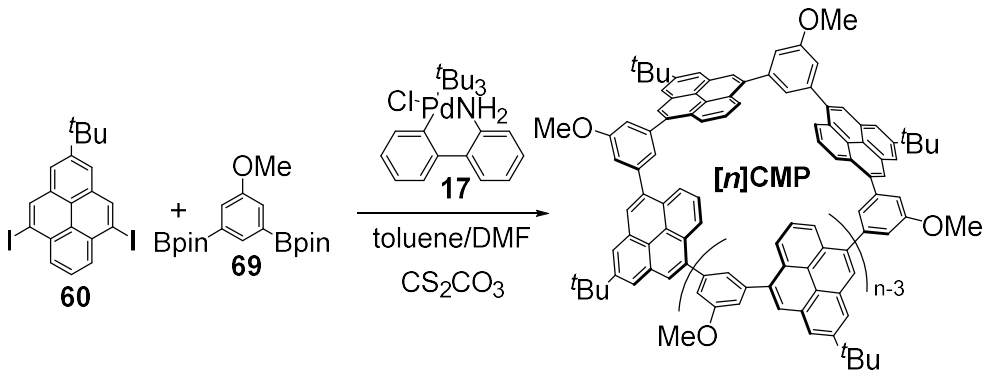

Compound **61**[17] (14 mg, 0.039 mmol), 2-*tert*-butyl-5,9-diiodopyrene (**69**)[18] (20 mg, 0.039 mmol), Cs_2CO_3 (64 mg, 0.20 mmol), dry toluene (1 mL) and dry DMF (0.3 mL) was added to a 25 mL Schlenk flask. After degassing with three freeze-pump-thaw cycles, the Pd catalyst **17** (5.3 mg, 0.010 mmol) was quickly added. After degassing again, the solution was stirred at room temperature for 11 h and then 100℃ for 15 h. After cooling, the mixture was extracted with dichloromethane and washed with water and brine. After being concentrated by a rotary evaporator, the mixture was roughly separated on a silica gel column (dichloromethane). Then, separation on gel-permeation chromatography (GPC) gave a serial of oligomers as in **Table 3**.

Fusion reaction of CMPs: [*n*]CMP (~2 mg, 8.4×10^{-4} mmol) was dissolved in 1 mL distilled DCM. Then Ar flow was inlet for 15 min. After that a solution of $FeCl_3$ in $MeNO_3$ (~1.3 mg, ~0.0042 mL, 300 mg/mL) was added drop-wise. The Ar flow was kept for 20 min while stirring. Then the tube was sealed and the solution was stirred for 1.5 h. 3 mL MeOH was added first and the mixture was poured into an aqueous $NaHSO_3$ solution. Then it was extracted with DCM and washed with water and brine. The organic layer was dried over Na_2SO_4 and then evaporated. Then it was purified through a silica gel column (DCM). The target compound was not detected by MALDI-TOF-MS.

NMR

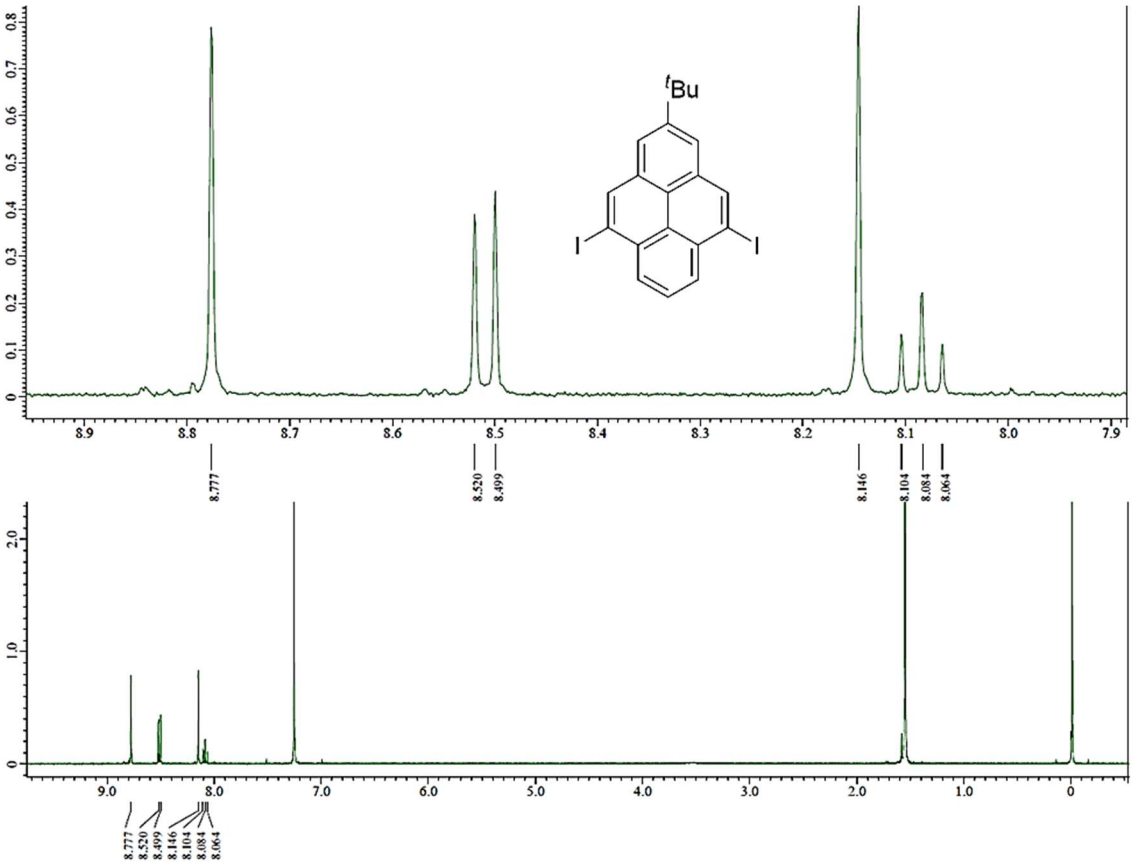

S3.1 ^{1}H NMR spectrum (400MHz) of **compound 60** in $CDCl_3$

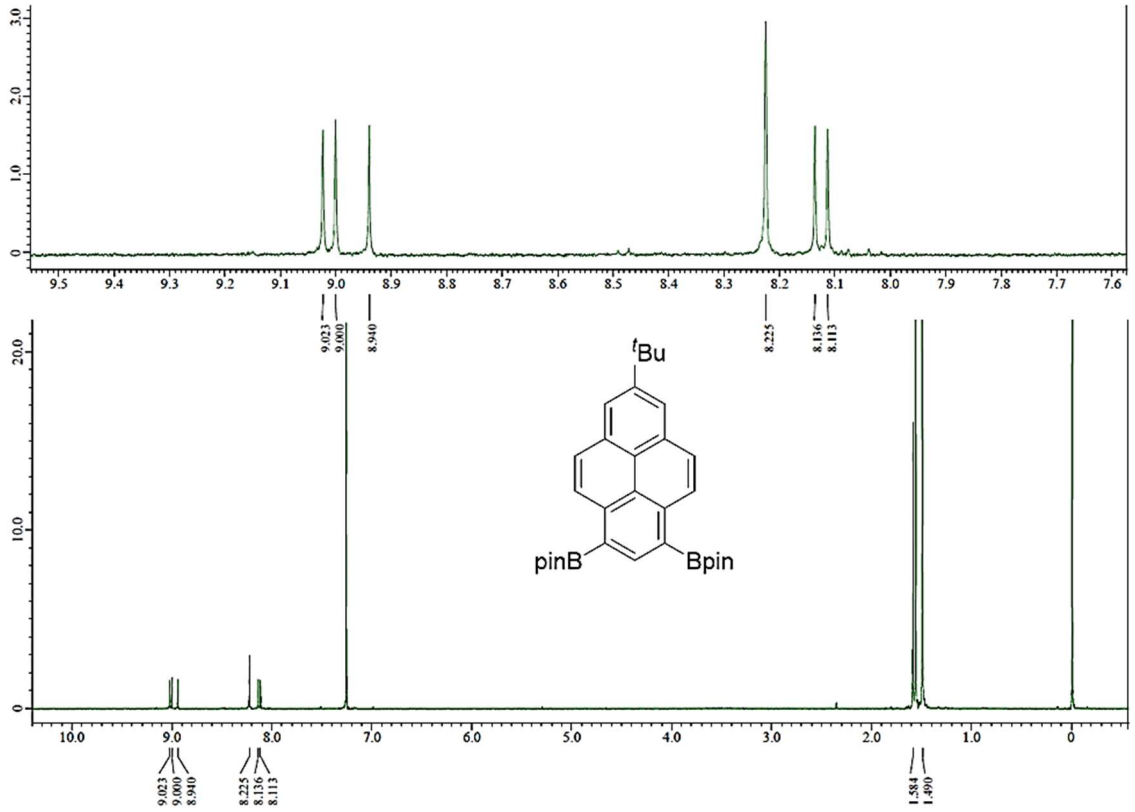

S3.2 ^{1}H NMR spectrum (400MHz) of **compound 69** in $CDCl_3$

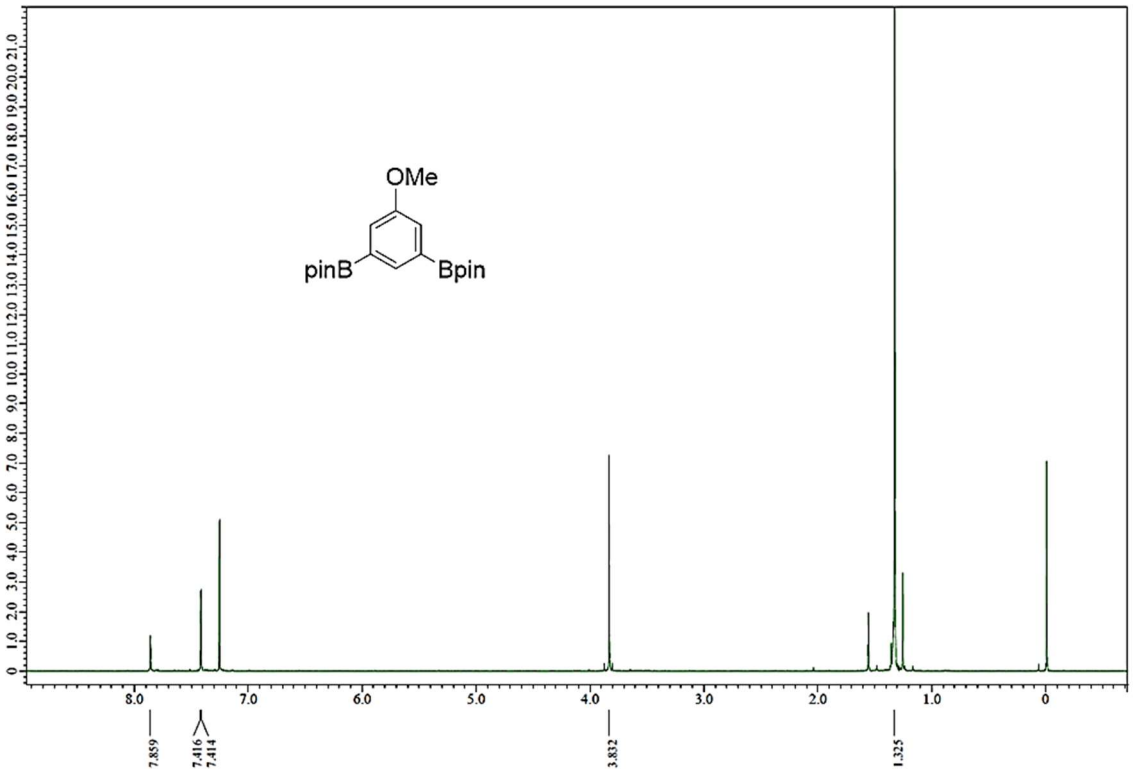

S3.3 ^{1}H NMR spectrum (400MHz) of **compound 69** in $CDCl_3$

MS and HR-MS

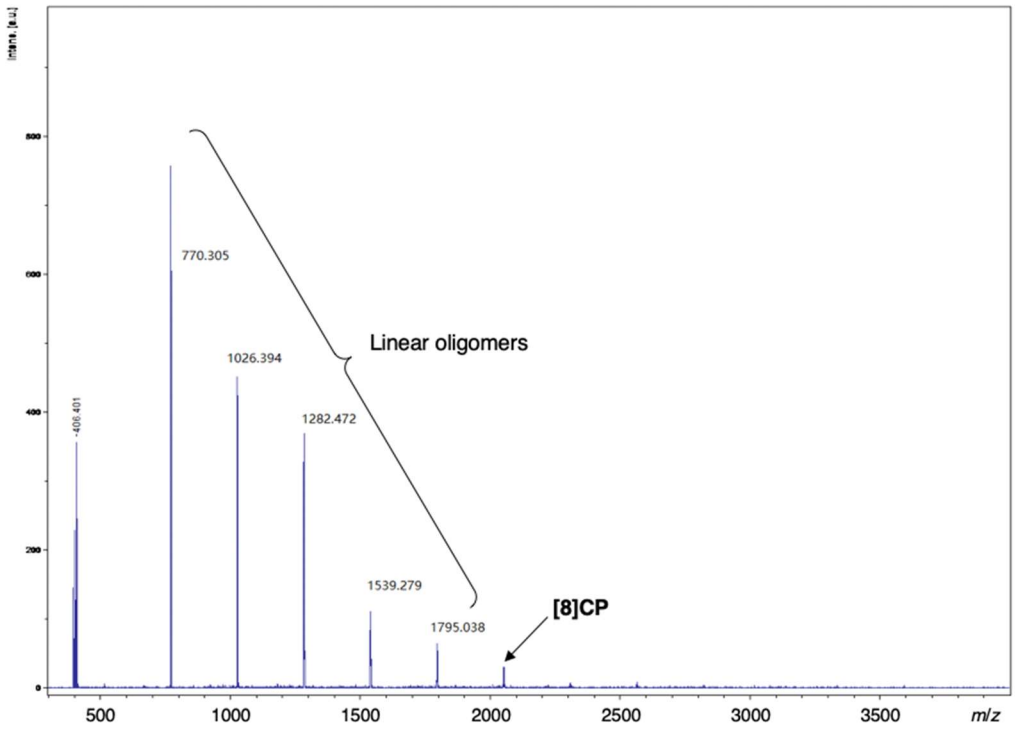

S3.1 MALDI-TOF-MS of the reaction mixture of **[8]CP**.

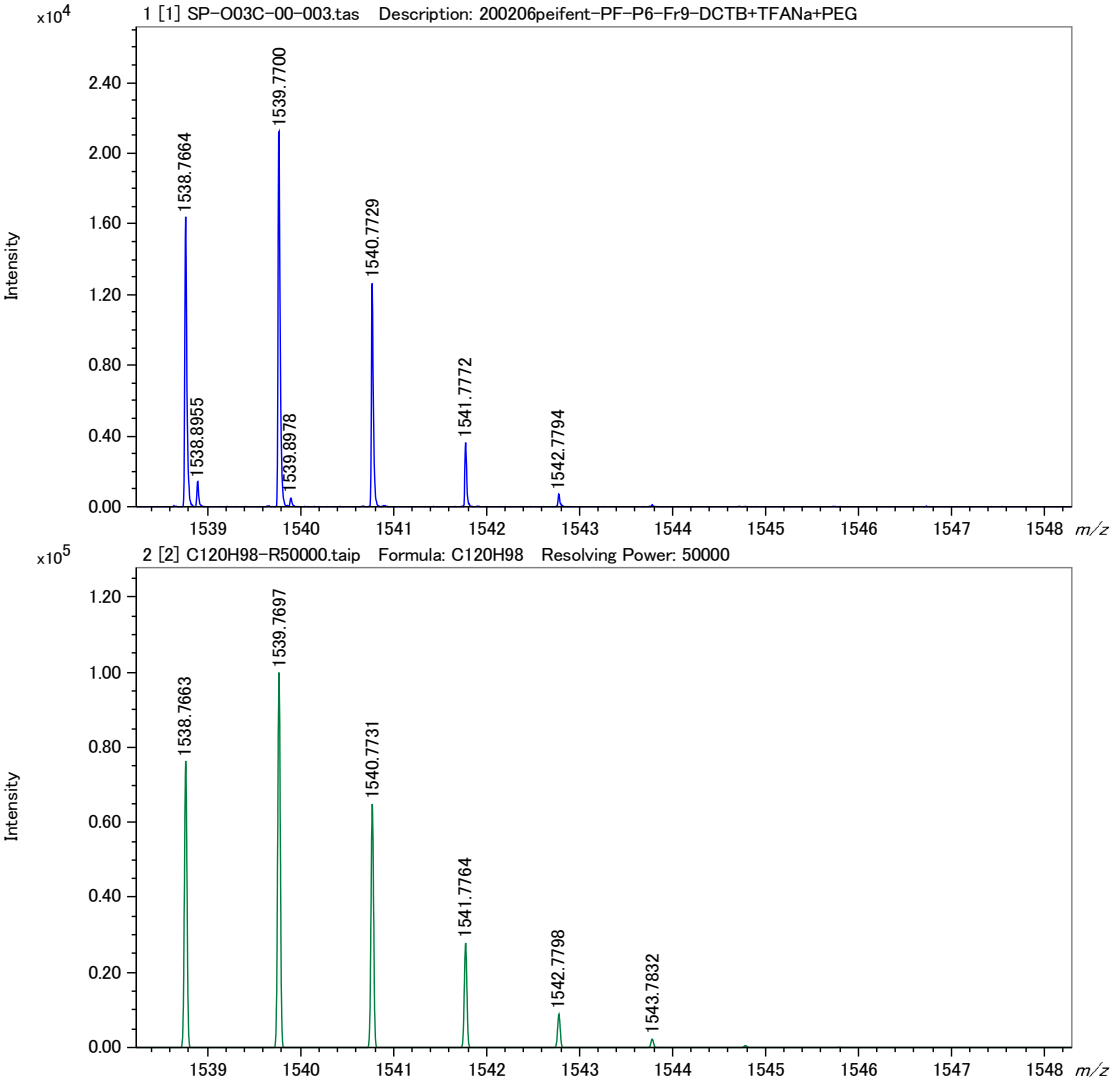

S3.2 HR-MALDI-TOF-MS of linear pyrene hexamer.

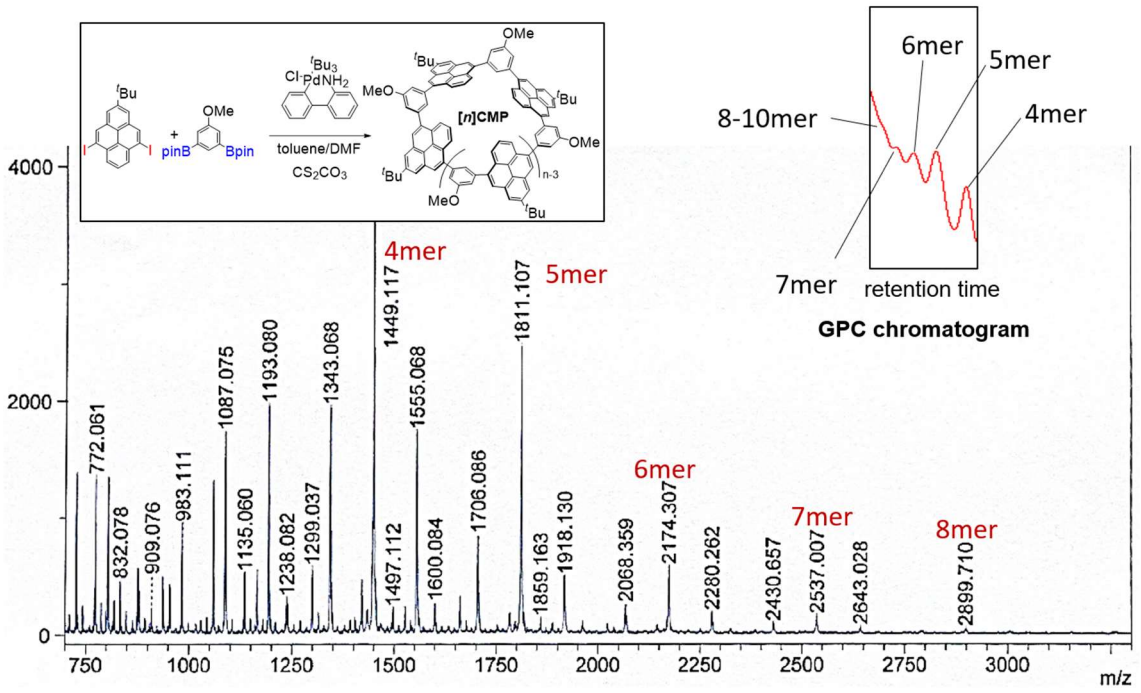

S3.3 MALDI-TOF-MS (linear/positive) and GPC chromatogram of the reaction mixture

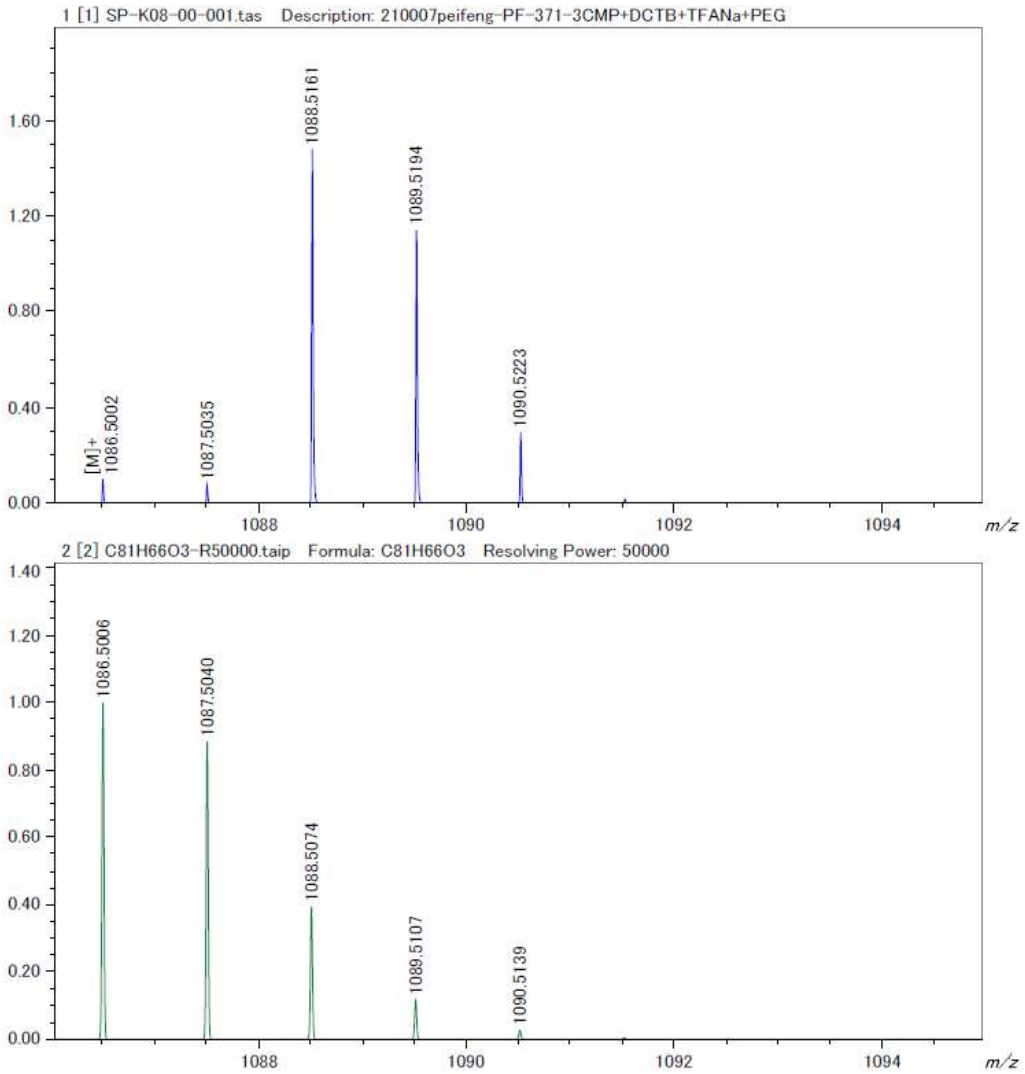

S3.3 HR-MALDI-TOF-MS of a fraction suspected to be **3CMP** (confirming not to be **3CMP**)

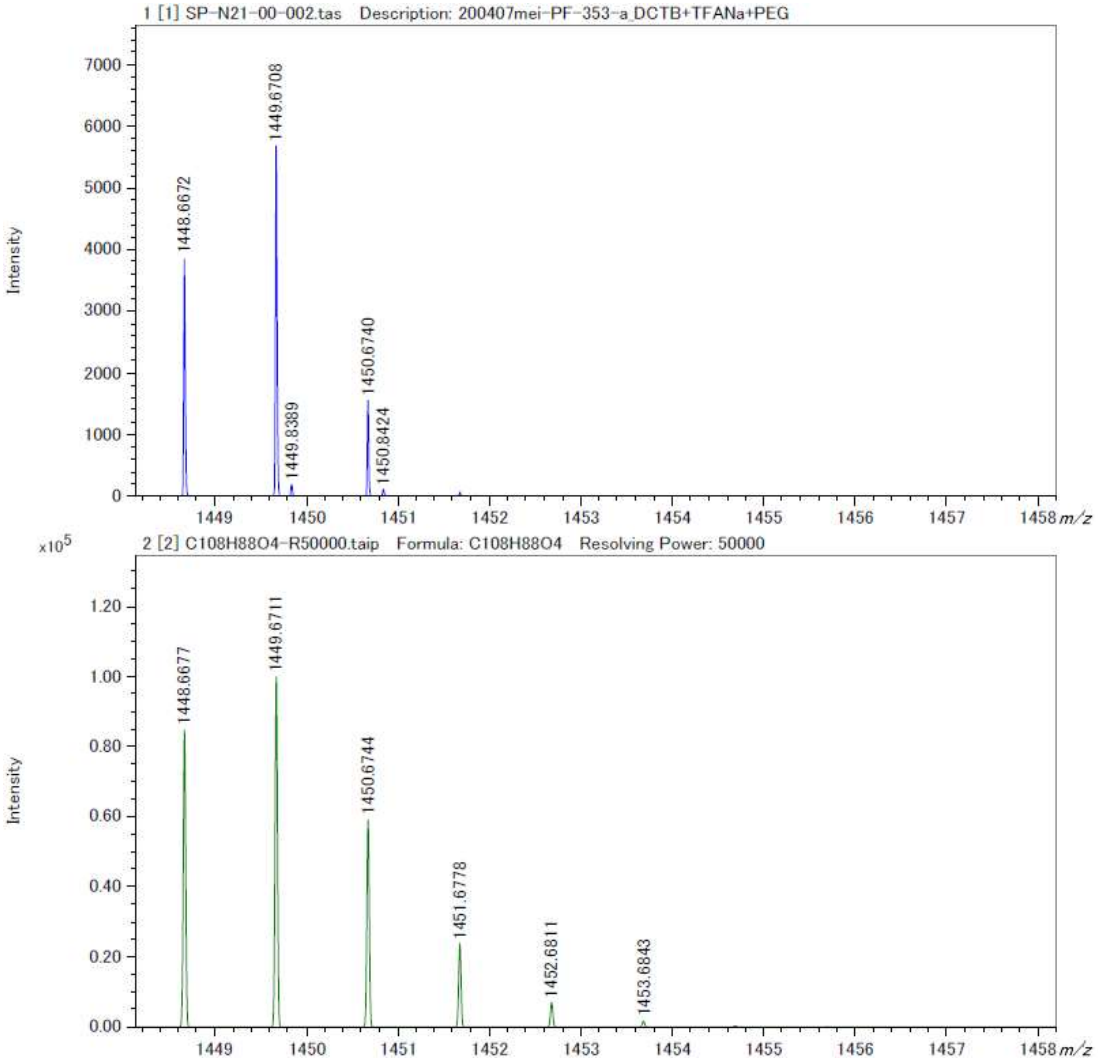

S3.4 HR-MALDI-TOF-MS of **4CMP**

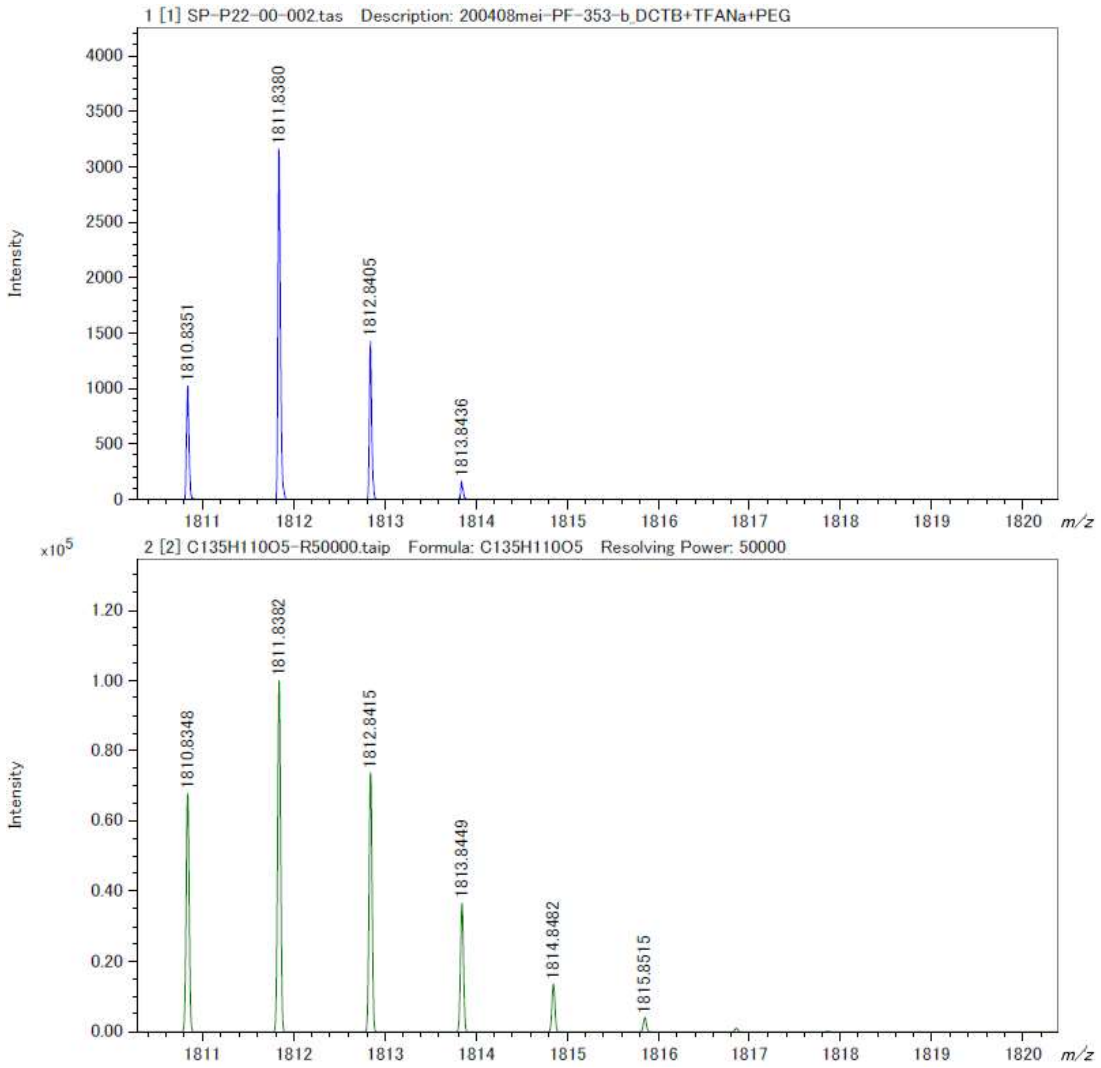

S3.5 HR-MALDI-TOF-MS of **5CMP**

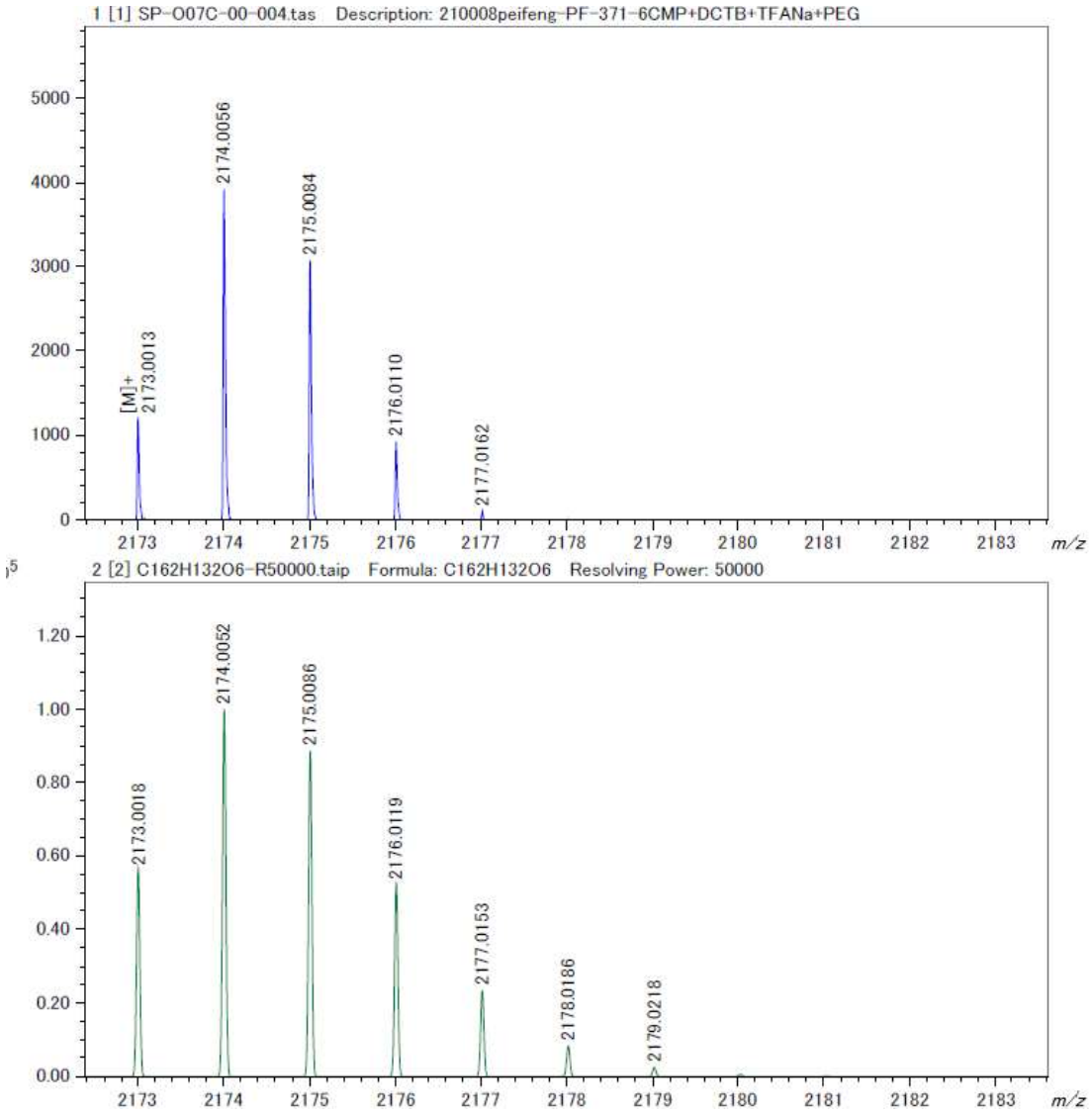

S3.6 HR-MALDI-TOF-MS of **6CMP**

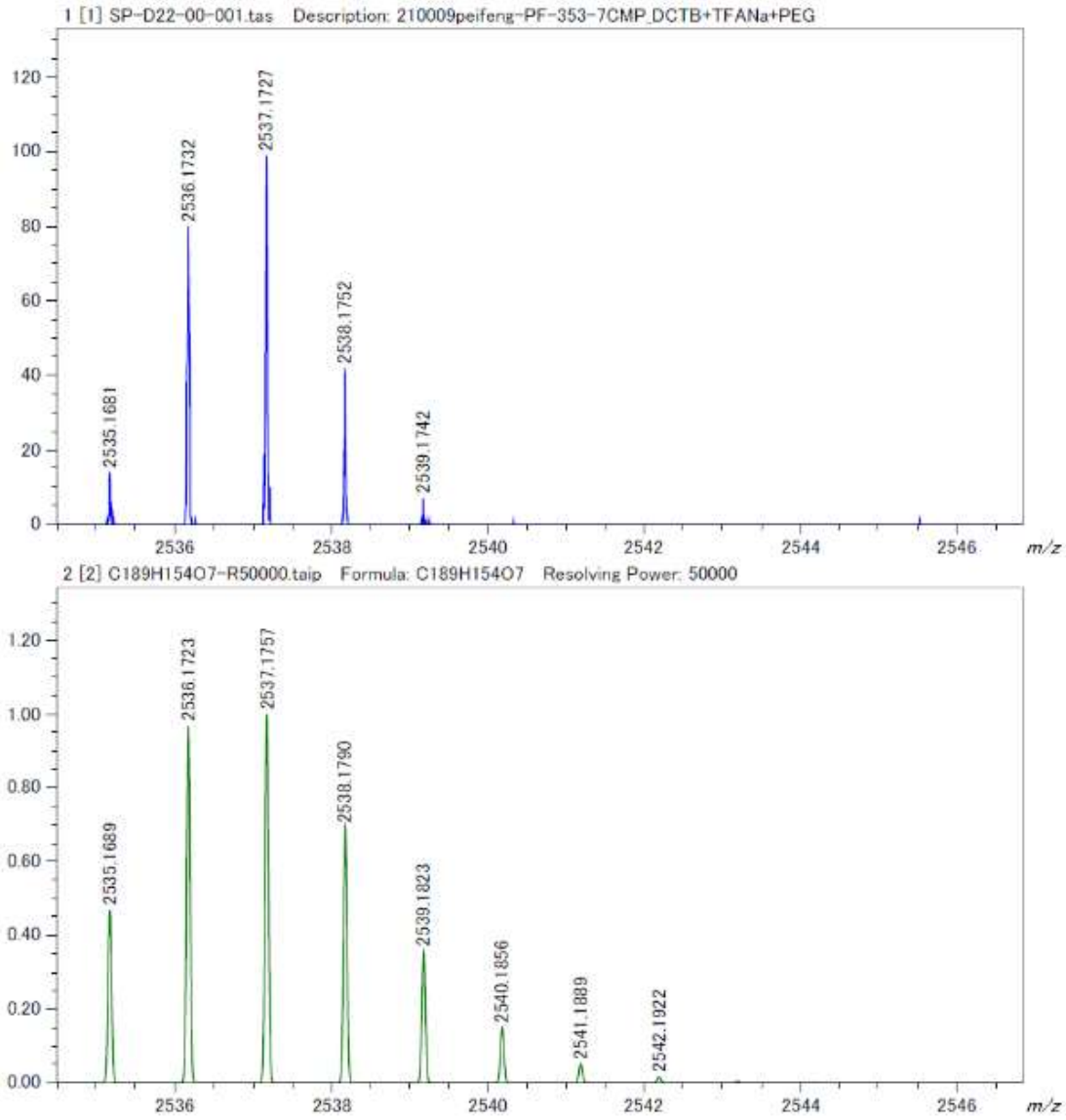

S3.7 HR-MALDI-TOF-MS of **7CMP**

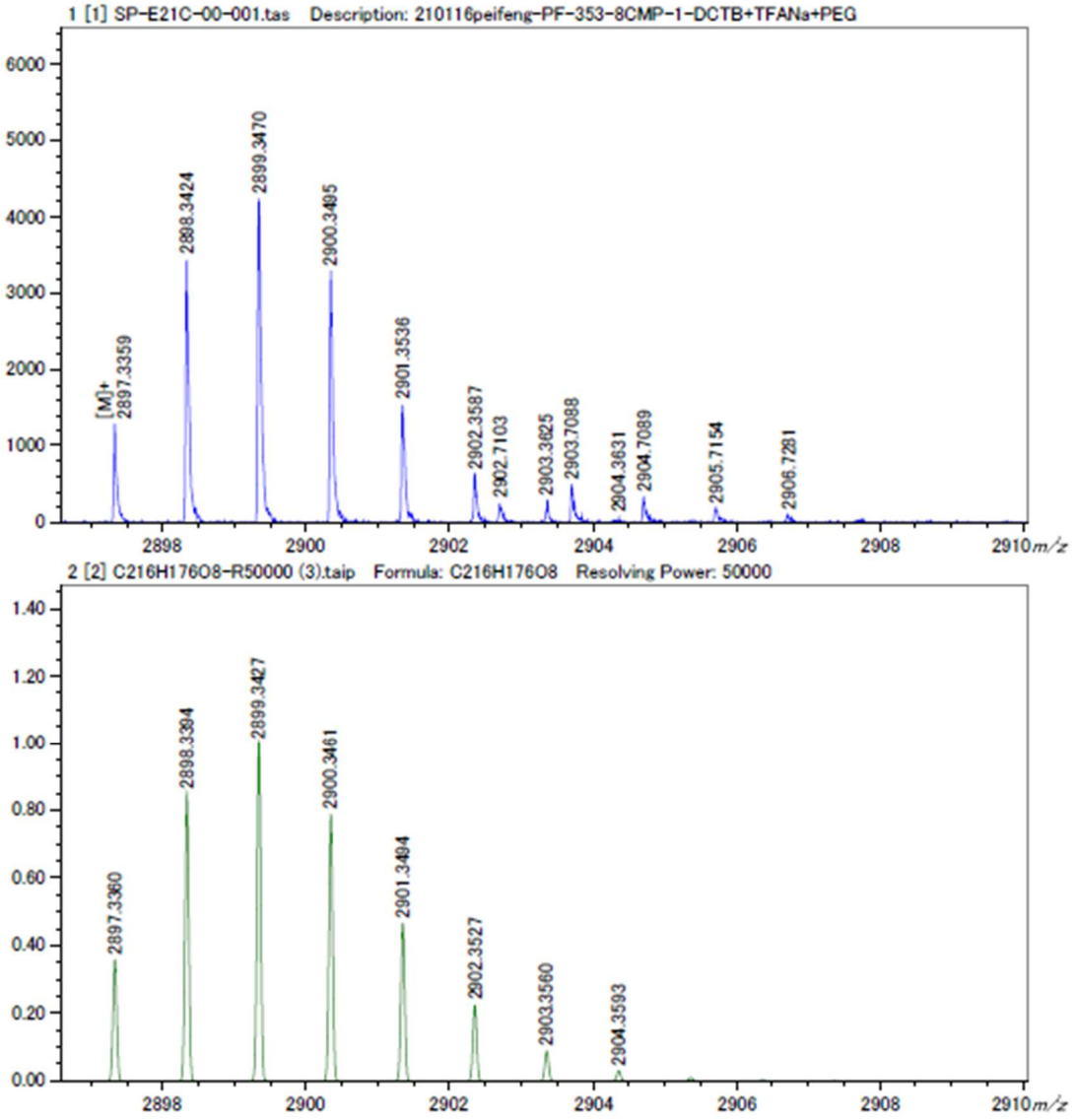

S3.8 HR-MALDI-TOF-MS of **8CMP**

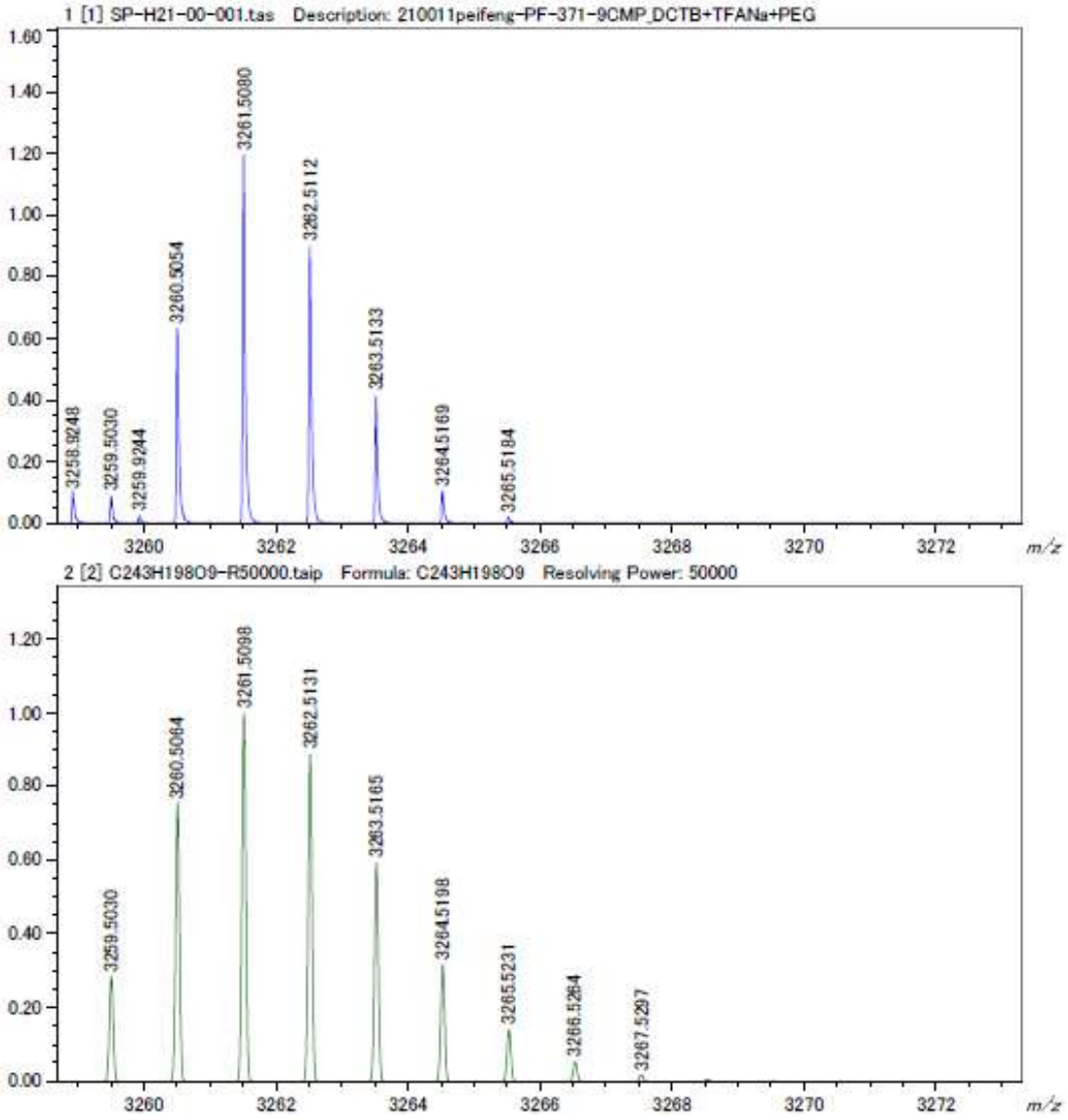

S3.9 HR-MALDI-TOF-MS of **9CMP**

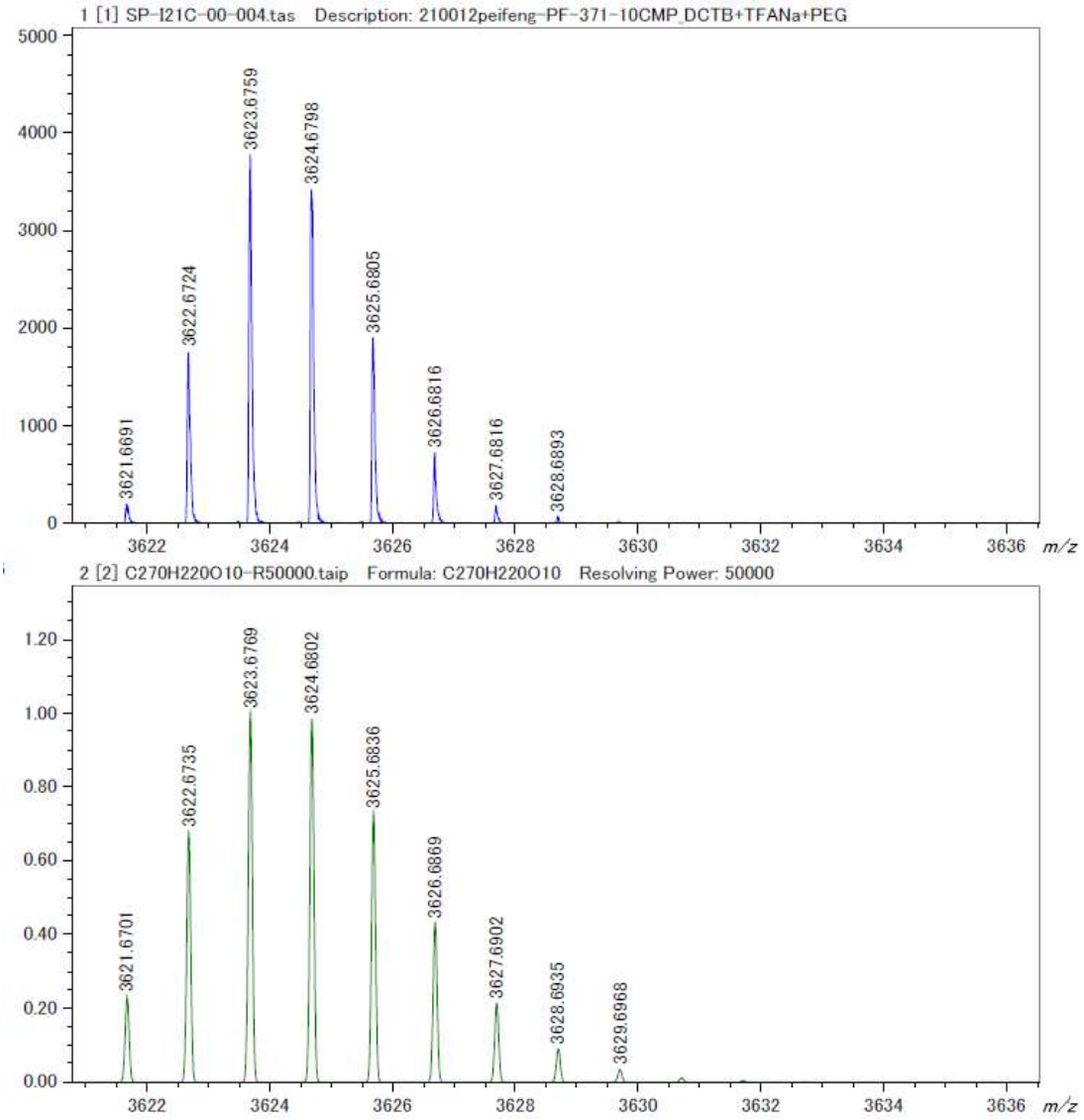

S3.10 HR-MALDI-TOF-MS of **10CMP**

Crystallography

Empirical formula	$C_{160}H_{128}$	
Formula weight	2050.62	
Temperature	90(2) K	
Wavelength	0.71073 Å	
Crystal system	triclinic	
Space group	*P*-1	
Unit cell dimensions	a = 17.391(3) Å	α = 82.806(3)°
	b = 19.361(3) Å	β = 77.912(3)°
	c = 26.681(4) Å	γ = 72.488(2)°
Volume	8359(2) Å^3	
Z	2	
Density (calculated)	0.815 g/cm^3	
Absorption coefficient	0.046 mm^{-1}	
F(000)	2176	
Crystal size	0.300 x 0.100 x 0.050 mm^3	
Theta range for data collection	0.782 to 25.000°	
Index ranges	$-20 \le h \le 20$, $-16 \le k \le 23$, $-27 \le l \le 31$	
Reflections collected	44855	
Independent reflections	29215 [R(int) = 0.0585]	
Completeness to theta	= 25.000° 99.3%	
Max. and min. transmission	0.998 and 0.808	
Refinement method	Full-matrix least-squares on F^2	
Data / restraints / parameters	29215 / 24 / 1464	
Goodness-of-fit on F^2	1.005	
Final R indices [$I > 2\sigma(I)$]	R_1 = 0.0853, wR_2 = 0.1786	
R indices (all data)	R_1 = 0.1871, wR_2 = 0.1990	
Largest diff. peak and hole	0.438 and –0.278 e.Å^{-3}	

S3.11 Crystal data and structure refinement for **[8]CP**.

References

[65] T. M. Figueira-Duarte and K. Müllen, *Chem. Rev*. **2011**, *111*, 7260–7314.

[66] D. Lorbach, A. Keerthi, M. T. Figueira-Duarte, M. Baumgarten, M. Wagner, K. Müllen, *Angew. Chem. Int. Ed*. **2016**, *55*, 418–421

[67] K. Ikemoto, S. Sato and H. Isobe, *Chem. Lett*. **2016**, *45*, 217–219.

[68] G. Venkataramana, P. Dongare, L. N. Dawe, D. W. Thompson, Y. Zhao and G. J. Bodwell, *Org. Lett*. **2011**, 13, 2240–2243.

[69] T. Iwamoto, E. Kayahara, N. Yasuda, T. Suzuki and S. Yamago. *Angew. Chem. Int. Ed*. **2014**, *53*, 6430–6434.

[70] M. A. Majewski and M. Stępień, M, *Angew. Chem. Int. Ed*. **2019**, *58*, 86.

[71] R. Kurosaki, M. Suzuki, H. Hayashi, M Fujiki, N. Aratani and H. Yamada, *Chem. Commun*. **2019**, *55*, 9618.

[72] H. Sugita, M. Nojima, Y. Ohta and T. Yokozawa, *Chem. Commun*. **2017**, *53*, 396–399.

[73] T. J. Sisto, M. R. Golder, E. S. Hirst and R. Jasti, *J. Am. Chem. Soc*. **2011**, *133*, 15800–15802.

[74] Y. D. Yang and H. Y. Gong, *Chem. Commun*. **2019**, *55*, 3701–3704.

[75] M. A. Zwijnenburg, G. Cheng, T. O. McDonald, K. E. Jelfs, J. X. Jiang, S. Ren, T. Hasell, F. Blanc, A. I. Cooper and D. J. Adams, D. J. *Macromolecules,* **2013**, *46*, 7696–7704.

[76] D. Lorbach, M. Wagner, M. Baumgarten and K. Müllen, *Chem. Commun*. **2013**, *49*, 10578–10580.

[77] R. Kurosaki, K. Matsuo, H. Hayashi, H. Yamada and A. Aratani, *Chem. Lett*. **2020**, *49*, 892–895.

[78] For the SQUEEZE-Platon program: P. van der Sluis and A. L. Spek, *Acta Crystallogr, Sect. A: Found. Crystallogr*, **1990**, *46*, 194–201.

Chapter 4. Summary

General conclusion

The focus of this thesis is to utilize the one-pot Suzuki reaction to carry out conjugated aromatic macrocyclic compounds and to try to synthesize CNBs. The synthesis of **N6**, **[8]CP**, and **[*n*]CMP** was successful. Preliminary verification has been achieved of the versatility of the one-pot Suzuki reaction for different reaction substrates. The reactivity of **N6**, **[8]CP**, and **[*n*]CMP** as the precursors to synthesize CNBs was verified. In Chapter 2, the supramolecular binding properties of **N6** as a host molecule for C_{60} and C_{70} are deeply studied. The property as the semiconductor material of the 1:1 complex **C_{70}@N6** was checked. A fusion attempt of **N6** was carried out to construct fully fused CNB molecules. In Chapter 3, by fine-tuning the one-pot reaction, the ring **[8]CP** and **[*n*]CMP** containing larger pyrene groups were synthesized. The one-step Suzuki reaction in this work was confirmed to well form multiple c-c bonds. In the future, it can be used as an important candidate for the construction of macrocyclic 3D nanocarbon structures and even bigger nanocarbon structures.

The exploration of one-step reactions can help reduce the cost of synthesis. This will facilitate large-scale reactions of cyclic compounds and then building a sturdy foundation for the in-depth research. The synthesis of **N6** and **[8]CP** provide rare examples of carbon nanorings with larger building unit than benzene rings, especially **[8]CP** as an example of large ring size (octameric) with large building units (pyrene).

The study on **N6**-fullerene complexes opens a new window to the development of nanoring-fullerene complex in electronics. The **N6**-C_{60} and **N6**-C_{70} complexes are promising to have high charge transfer mobility. With further molecular designs to tune the intermolecular interactions, the value of mobility will have even bigger room for improvement.

Research achievement

First author papers

[1] **Peifeng Mei**, Ryo Kurosaki, Akinobu Matsumoto, Hiroko Yamada, Naoki Aratani, One-Pot "Synthesis of a cyclic pyrene octamer from two bifunctionalized pyrene monomers", *Synthesis*, **2021**, *53*,344–347

[2] **Peifeng Mei**, Akinobu Matsumoto, Hironobu Hayashi, Mitsuharu Suzuki, Naoki Aratani and Hiroko Yamada "1,3-Phenylene-bridged naphthalene wheels synthesized by one-pot Suzuki-Miyaura coupling and the complex of hexamer with C_{60}" *RSC Advances,* **2018**, *8*, 20872–20876.

Other publications

[1] Keiji Uehara, **Peifeng Mei**, Toshihisa Murayama, Fumito Tani, Hironobu Hayashi, Mitsuharu Suzuki, Naoki Aratani and Hiroko Yamada "An anomalous antiaromaticity that arises from the cycloheptatrienyl anion equivalent" *European Journal of Organic Chemistry,* **2018**, *2018*, 4508–4511.

[2] Keiji Uehara, **Peifeng Mei**, Tomohisa Murayama, Fumito Tani, Hironobu Hayashi, Mitsuharu Suzuki, Naoki Aratani and Hiroko Yamada, Response to "The seven-membered ring in bis-azuleno-naphthalene is non-aromatic", *European Journal of Organic Chemistry*, **2019**, *4*, 860–861.

International conferences

○Keiji Uehara, **Peifeng Mei**, Tomohisa Murayama, Naoki Aratani, and Hiroko Yamada, "An anomalous antiaromaticity that arises from the cycloheptatrienyl anion equivalent", 14th International Workshop on Supramolecular Nanoscience of Chemically Programmed Pigments (SNCPP18), Ritsumeikan Univ. (Kusatsu), 15-17 June, 2018

○**Peifeng Mei**, Naoki Aratani, and Hiroko Yamada, "Facile synthesis of cyclic π-conjugated compounds by Suzuki-Miyaura cross-coupling reaction", 18th International Symposium on Novel Aromatic Compounds (ISNA18), Sapporo Convention Center, Sapporo, Hokkaido, JAPAN, 21–26 July, 2019

Domestic conferences

[1]○**メイ ペイフェン**・荒谷直樹・山田容子 「鈴木-宮浦クロスカップリングによる簡便な環状π共役系化合物の合成」 第 15 回ホスト–ゲスト・超分子化学シンポジウム, 立命館大学 (滋賀), 2017 年 6 月

[2]○**Peifeng Mei**、Akinobu Matsumoto、Naoki Aratani、Hiroko Yamada「Facile synthesis of cyclic π-conjugated compounds by Suzuki-Miyaura cross coupling」 第 28 回基礎有機化学討論会, 九州大学 (福岡), 2017 年 9 月

[3]○**Peifeng Mei**、Naoki Aratani、Hiroko Yamada「Synthesis and photophysical properties of a hexabenzohexacene」 第 29 回基礎有機化学討論会, 東京工業大学 (東京), 2018 年 9 月

Acknowledgment

This dissertation deals with the studies accomplished by the author under the direction of Prof. Hiroko Yamada at Nara Institute of Science and Technology (NAIST).

First of all, I would like to appreciate to Prof. Hiroko Yamada and Prof. Naoki Aratani in NAIST for excellent guidance and constant encouragement for my study during these past five years. I thank my supervisors, Prof. Hironari Kamikubo and Prof. Tsumoru Morimoto for giving me important suggestions and useful advice for this study. I also appreciate very much Prof. Mitsuharu Suzuki who used to be in NAIST, Prof. Hironobu Hayashi, Prof. Kyohei Matsuo at NAIST for useful advice and encouragement. I would like to thank Ms. Yoshiko Nishikawa and Mr. Fumio Asanoma in NAIST for measuring and analyzing samples. I would also like to thank former members of Prof. Yamada's group, especially, Dr. Akinobu Mastumoto and Dr. Songlin Xue, for guiding me in my initial research life. Furthermore, I am greatly indebted to my lab mates in this doctoral course, especially Ms. Juanjuan Zhu, Mr. Keiji Uehara, Ms. Ryo Kurosaki for helping me in experiments and sharing their vast knowledge during our daily discussions.

This work was partly supported by the Nara Institute of Science and Technology (NAIST) Special Fund. I would like to thank JASSO Honor Scholarship for supporting me for living in Japan.

Lastly, I would like to thank my family for all their love and encouragement.